DISS. ETH NO. 20638

Phosphorus losses from grassland dominated catchments: modeling and experimental validation

A dissertation submitted to

ETH ZURICH

for the degree of

DOCTOR OF SCIENCES

presented by

CLAUDIA HAHN
Dipl. Geoökologin, Technische Universität Bergakademie Freiberg
born 31st March 1982
German

accepted on the recommendation of

Prof. Dr. Rainer Schulin, examiner

Dr. Volker Prasuhn, co-examiner

Dr. Christian Stamm, co-examiner

Dr. Jean-Marcel Dorioz, co-examiner

2012

Contents

Summary

In many regions of the world, diffuse phosphorus (P) losses from agricultural land cause eutrophication of surface waters, leading to a loss of their ecosystem functions. In Switzerland, severe eutrophication problems occur in some lakes on the Swiss Plateau, such as Lake Sempach and Lake Baldegg. A reduction of diffuse P losses is needed to enhance the water quality of these lakes. Various international studies reported that P found in runoff of a catchment outlet originated from a small fraction of the catchment only. Directing mitigation options to those critical source areas (CSA) is considered to be the most cost-effective and efficient way to reduce diffuse P losses. Therefore, tools that enable reliable predictions of CSAs, preferably on the basis of easily available data, are needed to guide the implementation of mitigation measures. The main objective of this study was to assess and enhance the predictive capabilities of the parsimonious Rainfall-Runoff-Phosphorus (RRP) model, which determines CSAs using a low amount of input data. The model was developed for catchments dominated by grassland with low permeability subsoils. We improved the model and tested the reliability of its predictions, applying it to the Stägbach catchment which delivers high P loads to Lake Baldegg and was not used for calibration.

In the first step, we carried out artificial rainfall experiments on two Swiss grassland sites to expand the database of the RRP model and assess the model concepts. In particular, we investigated the role of soil-P status, band-applied manure and rainfall intensity on P losses. On each plot, medium intensity rainfall was applied by means of a sprinkler device. Thereafter, a watering can was used to simulate a highly intensive rain burst. For both modes of irrigation a linear relationship between water soluble P (WSP) concentration in soil and dissolved reactive P (DRP) concentration in runoff was observed. The differences in extraction coefficients (0.085 kg L^{-1} for the sprinkler experiments and 0.017 kg L^{-1} for the watering can experiments) indicate that P losses with runoff were more sensitive to soil P stocks for medium intensity rainfall than for highly intensive storm events. Also when P losses increased after manure application, the underlying soil P signal was clearly visible. This highlights the importance of soil P stocks for P losses. P concentrations in runoff decreased with increasing time between manure application and the rainfall event. Manure application did not significantly affect runoff generation. The experiments indicated that the processes implemented in the P sub-model are sufficient to estimate DRP losses and that the

additive approach to account for soil P and manure P sources is appropriate. The WSP-DRP relationship determined by the sprinkler experiments was implemented in the RRP model, substituting the original relationship.

In the second step, we re-calibrated the RRP model and applied it to the Stägbach catchment. While this catchment was not used for calibration, it showed similar characteristics as the calibration catchments. We compared model predictions with discharge and DRP measurements at the catchment outlet and with measurements of soil moisture, ground water level and overland flow that were collected in 2010 at different locations in the catchment. Furthermore, we assessed the sensitivity of the model predictions on the assignment of soils to the two drainage classes distinguished by the model. This assignment is left to the user. The model predictions were in good agreement with discharge and DRP measurements at the outlet of the Stägbach catchment and a sub-catchment for both classifications of drainage classes employed. Comparing spatial hydrological predictions with distributed field measurements of soil moisture, ground water level and overland flow indicated reasonably good spatial model performance, suggesting that the underlying assumptions of the model are valid and that the RRP model can be used to predict CSAs in grassland dominated hilly catchments. According to the model more than 50% of the total DRP losses originated from only 10% of the area, and ‘legacy’ soil P was the dominant source.

In the last step, we compared the RRP model with two other, even simpler tools that based hydrological predictions either solely on soil and geological data or topography. The Dominant Runoff Processes (DoRP) model is a GIS based approach that uses soil and geological data to identify a dominant runoff process (DoRP) for each location within a catchment. Based on estimates of soil water storage capacity for these DoRP, a simple “bucket approach” is used to predict storm flow discharge. The Sensitive Catchment Integrated Modelling Analysis Platform (SCIMAP), on the other hand, solely uses topographic data to derive maps of relative runoff risk. In combination with soil P data, these can be converted into relative DRP loss risks. All three models were applied to the Lippenrütibach catchment, one of the catchments used to calibrate the RRP model, and the Stägbach catchment. Predictions were compared among the three models and with the spatial validation data from the Stägbach catchment. Although in some locations only the available soil information explained the differences in their hydrological responses, the DoRP scheme alone was not sufficient to identify runoff risk areas. Most differences in runoff behavior between sites could be explained by their topographic position, indicating that runoff risks were mainly controlled by topography. Limitations in topographic connectivity did not seem to play a major role in our catchments. Overall, the RRP model performed well for our study

catchments, where soils are generally of low permeability and usually connected to streams via surface pathways or artificial drainage.

As we applied the model only to one validation catchment showing similar characteristics as the calibration catchments, we do not know how far its range of validity extends to different environments. Based on the model structure, we assume that the model will not deliver satisfactory results in regions with a large extent of highly permeable soils, for very dry conditions, and for areas where mainly infiltration excess runoff (IER) occurs. While the need for soil P data vastly restricts the application of the P sub-model, the hydrological sub-model is based on readily available data and can therefore be widely used to determine hydrological risk areas.

In conclusion, our field experiments and model calculations illustrate that soil P stocks are a major source for P losses and confirm concerns that P enriched soils located on hydrologically active areas pose a high risk for surface water quality. Despite its limitations, the RRP model proved to be valid as a predictor of runoff and P losses in the study catchments. It was thus found to be a promising tool to delineate CSAs and guide the implementation of mitigation measures to reduce these risks in hilly grassland dominated catchments where hydrological responses to rainfall events are primarily governed by topography.

Zusammenfassung

Weltweit verursachen diffuse Phosphorverluste aus landwirtschaftlichen Gebieten die Eutrophierung von Gewässern, was zu einem Verlust ihrer Ökosystemfunktionen führt. In der Schweiz treten derartige Eutrophierungsprobleme in einigen Seen des Schweizer Mittellandes auf, wie zum Beispiel dem Sempachersee und dem Baldeggersee. Eine Reduzierung des Phosphorverlustes ist nötig, um die Gewässerqualität in diesen Seen zu verbessern. Verschiedene internationale Studien berichten, dass Phosphor (P) im Gebietsabfluss häufig nur aus einem kleinen Teil des Einzugsgebietes stammt. Es wird angenommen, dass die Implementierung von Massnahmen in diesen beitragenden Gebieten (critical source areas CSA) die kostengünstigste und effizienteste Methode ist, um P Einträge in Gewässern zu verringern. Um derartige gezielte Massnahmen zu ermöglichen, braucht es Werkzeuge, die zuverlässige Vorhersagen von CSAs ermöglichen, vorzugsweise auf der Grundlage von verfügbaren Daten. Das Ziel dieser Arbeit war es, die Vorhersagefähigkeit des Niederschlags-Abfluss-Phosphor Modells RRP (Rainfall-Runoff-Phosphorus Model), welches nur wenig Eingangsdaten benötigt, zu bewerten und zu verbessern. Das Modell wurde für Einzugsgebiete entwickelt, in denen Graslandflächen und schlecht drainierte Böden dominieren. Wir verbesserten das Modell und testeten die Zuverlässigkeit der Modellvorhersagen, indem wir das Modell auf das Stägbach Einzugsgebiet, welches hohe P-Frachten in den Baldeggersee liefert und nicht für die Kalibration verwendet wurde, anwendeten.

Im ersten Arbeitsschritt wurden an zwei Standorten im Schweizer Mittelland Beregnungsexperimente durchgeführt, um die Datengrundlage für das Modell zu verbessern und die zugrundeliegenden Konzepte zu beurteilen. Im Speziellen untersuchten wir, welche Rolle Boden-P-Gehalte, in Bändern applizierte Gülle (Schleppschlauchsimulation) und verschiedene Niederschlagsintensitäten für den P-Verlust spielen. Jede Versuchsfläche wurde zuerst mittels einer Beregnungsanlage (Sprinkler) mit einer mittleren Intensität beregnet. Danach wurde eine Gießkanne verwendet, um einen kurzen, extrem intensiven Niederschlag zu simulieren. Für beide Beregnungsmethoden wurde ein linearer Zusammenhang zwischen wasserlöslicher P-Konzentration im Boden (WSP) und gelöstem P im Abfluss (DRP) beobachtet. Die unterschiedlichen Extraktionskoeffizienten (0.085 kg L^{-1} für Experimente mit der Beregnungsanlage und 0.017 kg L^{-1} für die

Giesskannenexperimente) deuten darauf hin, dass P-Gehalte im Abfluss für mittlere Niederschlagsereignisse sensitiver auf den P-Gehalt im Boden reagieren als für extreme Niederschlagsereignisse. Obwohl sich die P-Verluste nach dem Aufbringen von Gülle erhöhten, blieb der Einfluss des Boden-P Gehaltes klar ersichtlich. Dies betont die Bedeutung von Boden-P-Gehalten für P-Verluste. Die P-Konzentrationen im Abfluss verringerten sich mit zunehmendem Zeitabstand zwischen der Aufbringung der Gülle und dem Niederschlagsereignis. Die Aufbringung der Gülle hatte keinen signifikanten Einfluss auf die Abflussbildung. Die Experimente weisen darauf hin, dass die Mechanismen im P-Teilmodell ausreichen um die DRP Verluste abzuschätzen und dass der additive Ansatz zur Erfassung der Boden-P und Gülle-P Quellen angemessen ist. Die Beziehung zwischen WSP und DRP, welche aus den Sprinkler Experimenten abgeleitet wurde, wurde anstelle der ursprünglichen Beziehung in das RRP Modell implementiert.

Im zweiten Arbeitsschritt wurde das RRP Modell neu kalibriert und auf das Stägbach Einzugsgebiet angewendet. Das Einzugsgebiet wurde nicht zur Kalibration benutzt, wies aber vergleichbare Eigenschafen wie die zur Kalibrierung genutzten Einzugsgebiete auf. Die Modellvorhersagen wurden mit Abfluss- und DRP-Messungen am Gebietsauslauf sowie mit räumlich verteilten Messungen der Bodenfeuchte, des Grundwasserstandes und des Oberflächenabflusses, welche 2010 durchgeführt wurden, verglichen. Des Weiteren wurde die Sensitivität der Modellvorhersagen bezüglich der Zuordnung der Böden zu den zwei Drainage-Klassen des Modells untersucht. Diese Zuordnung ist dem Benutzer überlassen. Die Modellvorhersagen für zwei verschiedene Bodenklassifikationen zeigten eine gute Übereinstimmung mit den Abfluss- und DRP-Messungen am Auslauf des Stägbach Einzugsgebietes sowie am Auslauf eines Teileinzugsgebietes. Der Vergleich der räumlichen hydrologischen Vorhersagen mit den im Einzugsgebiet verteilten Feldmessungen der Bodenfeuchte, des Grundwasserstandes und des Oberflächenabflusses belegte eine hinreichend gute räumlichen Vorhersage des Modelles. Dies deutet darauf hin, dass die dem Modell zugrundeliegenden Annahmen gültig sind und das RRP Modell verwendet werden kann, um CSAs in Grasland dominierten hügeligen Einzugsgebieten vorherzusagen. Laut Modellvorhersagen stammen mehr als 50% der gesamten DRP Verluste aus nur 10% des Gebietes, und im Boden vorhandenes P von früheren Einträgen (‚legacy P‘) war die dominante P-Quelle.

Im letzten Teil der Arbeit verglichen wir das RRP Modell mit zwei weiteren noch einfacheren Modellen, welche hydrologische Vorhersagen lediglich auf Grundlage von Boden- und geologischen Daten oder der Topographie liefern. Das “Dominant Runoff Processes” Modell (DoRP) ist ein GIS-basierter Ansatz, welcher anhand von Boden- und geologischen Daten die dominanten Abflussprozesse für jeden Standort innerhalb eines

Einzugsgebietes vorhersagt. Basierend auf Abschätzungen der Bodenwasser-speicherkapazität für jede DoRP-Kategorie wurde ein einfacher „Bucket-Ansatz“ genutzt, um Abflüsse bei Niederschlagsereignissen vorherzusagen. Demgegenüber steht das “Sensitive Catchment Integrated Modelling Analysis Platform” (SCIMAP) Modell, welches lediglich topographische Daten verwendet, um Karten von relativen Abflussrisiken zu erstellen. Zusammen mit Boden-P-Daten können diese in relative-DRP Verluste umgerechnet werden. Alle drei Modelle wurden auf das Lippenrütibach Einzugsgebiet, eines der zur Kalibration genutzten Einzugsgebiete, und auf das Stägbach Einzugsgebiet angewandt. Die Vorhersagen der drei Modelle wurden untereinander und mit den räumlichen Validierungsdaten aus dem Stägbach Einzugsgebiet verglichen. Obwohl in einigen Gebieten nur mit Hilfe der Bodeninformationen Unterschiede im hydrologischen Verhalten erklärt werden konnten, war das DoRP-Modell allein nicht ausreichend, um hydrologische Risikogebiete im Einzugsgebiet zu identifizieren. Die meisten Unterschiede im Abflussverhalten verschiedener Gebiete konnten mithilfe ihrer topografischen Position erklärt werden. Dies deutet darauf hin, dass das Abflussverhalten hauptsächlich von der topographischen Lage bestimmt wird. Einschränkungen in der topografischen Konnektivität schienen keine große Rolle in den untersuchten Einzugsgebieten zu spielen. Insgesamt lieferte das RRP Modell gute Vorhersagen für die betrachteten Einzugsgebiete, welche überwiegend schlecht durchlässige Böden aufweisen, die meist oberirdisch oder über künstlichen Drainagen mit dem Gewässernetz verbunden sind.

Es ist uns nicht möglich, den Gültigkeitsbereich des Modells für andere Umgebungsbedingungen abzuschätzen, da das Modell zur Validierung nur auf ein Einzugsgebiet angewandt wurde, welches ähnliche Eigenschaften aufweist wie die zur Kalibrierung verwendeten Gebiete. Basierend auf der Struktur des Modelles nehmen wir an, dass das Modell in Regionen mit stark durchlässigen Böden, sowie für sehr trockene Bedingungen und für Gebiete in denen „Infiltration Excess Runoff” (IER) dominiert, keine zufriedenstellenden Ergebnisse liefert. Der Bedarf an hochaufgelösten Boden-P-Daten beschränkt die Anwendbarkeit des P-Teilmodells. Das hydrologische Teilmodell nutzt lediglich leicht verfügbare Daten und kann deshalb weithin dazu verwendet werden hydrologische Risikogebiete zu bestimmen.

Die Feldexperimente sowie die Modellrechnungen haben gezeigt, dass die P-Vorräte im Boden ein hohes Risiko für P-Verluste darstellen. Dies bestätigt Befürchtungen, dass die mit P angereicherten Böden in hydrologisch aktiven Gebieten ein hohes Risiko für die Gewässerqualität darstellen. Trotz aller Einschränkungen konnte gezeigt werden, dass das RRP Modell ein geeignetes Vorhersageinstrument für Abfluss und P-Verluste in den betrachteten Einzugsgebieten ist. Somit kann das RRP Modell als vielversprechendes

Werkzeug zur Bestimmung von CSAs genutzt werden und die Implementierung von Maßnahmen zur Verminderung der P-Verluste in hügeligen, von Grasland dominierten Einzugsgebieten, deren hydrologisches Verhalten hauptsächlich von der Topographie bestimmt wird, unterstützen.

1
Introduction

Phosphorus (P) is an essential nutrient element and as such important for agricultural productivity. Minable P is a limited resource, which is predominantly used in agriculture (Van Vuuren et al., 2010). At the same time, P is a major pollutant of aquatic ecosystems, causing eutrophication of freshwater bodies and coastal ecosystems world-wide (Carpenter et al., 1998; Smith et al., 2006). Consequences of eutrophication are e.g. algal blooms, oxygen shortage, fish death and loss of water bodies for recreation and as freshwater resource.

In Switzerland, eutrophication is most prominent in some lakes of the Swiss Plateau region, where high livestock production and excessive manure applications on permanent grassland in the past led to elevated P stocks in soils of generally low permeability and to severe water quality problems (Gächter, 1987; Herzog, 2005; Prasuhn and Lazzarotto, 2005). Particularly well documented is the P pollution problem for Lake Sempach and Lake Baldegg. The two lakes are artificially oxygenated since 1983 (Lake Baldegg) and 1984 (Lake Sempach), but this did not solve the eutrophication problem (Gächter, 1987).

In many regions P losses from point sources, which can be determined and targeted rather easily, were considerably reduced within the last decades (Dubrovsky et al., 2010; Herzog, 2005; Prasuhn and Sieber, 2005). While losses from point sources are still pre-dominant in areas enclosing big cities and industry (Prasuhn and Sieber, 2005), diffuse P losses from agriculture are now the dominant source for eutrophication of water bodies in rural areas (Carpenter et al., 1998; Sharpley et al., 1994).

This applies also for Switzerland. The construction of waste water treatment plants and the ban of P-containing detergents (1986) substantially reduced P inputs into surface waters, but were often not enough to sufficiently enhance water quality (Lehmann et al., 1998). In the case of Lake Baldegg, these measures reduced P inputs into the lake, but was not sufficient to reach the target concentrations of 30 mg P m^{-3} (Gächter, 1987; Stadelmann et al., 2002). In 2002 more than 85% of the total P loads into Lake Baldegg were attributed to diffuse P losses from agricultural land (Stadelmann et al., 2002), which increased dramatically with the intensification of agriculture in Switzerland after 1950 (Spiess, 2011).

Based on national nutrient balances, Spiess (2011) showed that the average P surplus in Swiss agriculture reached a maximum of 27 kg ha^{-1} in 1980, and then decreased again, reaching 5 kg P ha^{-1} in 2008. “The majority of the surplus generally accumulates in the soil, while the remainder is lost through erosion, surface runoff and leaching” (Spiess, 2011). A revision of Swiss agricultural policy in 1993 aiming to enhance the environmental performance of agriculture, introduced direct payment to farmers in order to motivate environmentally friendly agricultural practices (Spiess, 2011). Art. 62a of the Swiss law for water protection, added in 1998, enabled further subsidies for farmers. Based on Art. 62a, intensive mitigation programs were introduced in the Lake Baldegg and Lake Sempach catchments. Farmers who agree to specific measures such as reduced P inputs, obligatory soil analysis and restrictions on the timing of manure application, are entitled to receive subsidies. The mitigation programs were based on and accompanied by intensive research in this region, e.g. on P availability in soils and fertilizer strategies (Frossard et al., 2005), and P losses with runoff and its development with time (Braun et al., 2001; Braun et al., 1998; Lazzarotto et al., 2005; Prasuhn and Lazzarotto, 2005; Stadelmann et al., 2002).

In Europe the Water Framework Directive (WFD), which was implemented in the year 2000, provides a framework for the protection of water bodies, and requires a “good ecological status” of water bodies possibly till 2015, but latest by 2027 (Hering et al., 2010). Within the framework of the COST Action 869 various mitigation options were proposed and discussed (Schoumans et al., 2011). Some aim to reduce the transport of nutrients from fields to surface waters by reducing runoff or flow velocity, e.g. through buffer strips (Roberts et al., 2012; Stutter et al., 2012). Others aim to immobilize P sources in soil and manure by applying P sorbing materials (Buda et al., 2012). The placement of such measures needs to be considered carefully in order to maximize their efficiency and minimize economic losses.

Various studies reported that the P found in runoff at the catchment outlet mostly originated from rather small parts of the catchment (Gburek and Sharpley, 1998; Pionke et al., 2000; Pionke et al., 1997). Targeting those critical source areas (CSAs) when implementing mitigation measures is expected to be the most efficient and cost-effective approach (Doody et al., 2012; Gitau et al., 2004; Heathwaite et al., 2003; Rodriguez et al., 2011). Critical source areas are characterized by the exposure of available P sources to transport processes that deliver P to a water body (Gburek and Sharpley, 1998).

Kleinman et al. (2011b) provided a comprehensive overview about P sources and transport processes. Sources of P include (1) soils that are enriched with P due to excessive fertilizer application in the past (Kleinman et al., 2011a; Vadas et al., 2005), also called ‘legacy’ P, (2) freshly applied manure and other fertilizers (Shigaki et al., 2007; Smith et al.,

2001; Vadas et al., 2011), and - to a much smaller extent - (3) plants that are freshly grazed, trampled or in process of decay (Kleinman et al., 2011b). While erosion and surface runoff were considered the only relevant transport processes in earlier studies (Gburek and Sharpley, 1998), now it is accepted that also subsurface flow (Kleinman et al., 2009), including tile drain flow (Kleinman et al., 2007; Stamm et al., 1998; Vadas et al., 2007), can transport substantial amounts of P to surface waters (Doody et al., 2012; Kleinman et al., 2011b).

Despite much research, the process understanding regarding the effects of P enrichment in soils and of recently applied manure on DRP losses is still rather limited. It is widely accepted that the DRP concentration in runoff depends on the P concentration in the soil from which runoff is generated. In many cases DRP in runoff increased linearly with the concentration of water soluble P (WSP) in the soil. Vadas et al. (2005) compared the results of various studies and suggested to use a single relationship to describe this dependency. Other scientists emphasized the need to differentiate between different runoff types (Leh and Chaubey, 2009; Lindenschmidt et al., 2004; McDowell and Srinivasan, 2009; Radcliffe et al., 2009; Sanchez and Boll, 2005). Application of manure is known to temporarily elevate available P and thereby increase the risk of DRP losses. Contradictory reports exist regarding the role of manure in runoff generation. Manure application could lead to soil sealing and thus to more surface runoff, as reported by Burkhardt et al. (2005) and Smith et al. (2001). On the other hand, Srinivasan et al. (2007) observed that on dry sites manure absorbed rainwater and thus delayed runoff generation.

Runoff from locations with high soil P concentrations or freshly applied manure can entail high risks for P export. Also sites with relatively low soil P concentrations can possess a high risk for P losses, if runoff volumes are large (Buda et al., 2009). Because of the complexity and interaction of the processes involved in diffuse P losses, the prediction of CSAs is a challenging task (Doody et al., 2012; Kleinman et al., 2011a; Kleinman et al., 2011b). On the catchment scale, which is the scale of operation defined in the WFD, models are needed to delineate CSAs and to quantify their contribution to P losses (White et al., 2009). A variety of tools that can be used to identify CSAs exist (Radcliffe et al., 2009; Schoumans et al., 2009; Sharpley et al., 2003). There are static site assessment tools such as the P-Index (Weld and Sharpley, 2007) as well as process-based dynamic models such as SWAT (Arnold et al., 1998), INCA-P (Wade et al., 2002), and ANSWERS-2000 (Beasley et al., 1980). In contrast to static models, spatially distributed dynamic models are able to account for the temporal variability of runoff and P losses. However, they are often over-parameterized (Radcliffe et al., 2009) and require input data that are not widely available. As

pointed out by Radcliffe (2009) and Heathwaite et al. (2007), parsimonious models that can be used to determine the spatial distribution of P export risks in a catchment are needed.

A parsimonious Rainfall Runoff Phosphorus (RRP) model, developed by Lazzarotto (2005), delivered promising results regarding the spatial prediction of CSAs in small grassland dominated catchments located on the Swiss Plateau. It simulates the variation of discharge and DRP loads over time at catchment outlets, as well as CSAs. The RRP model focuses on dissolved reactive P (DRP) transport, because this form is immediately available for algal uptake (Sharpley, 1993; Sharpley et al., 1994) and therefore has a large effect on eutrophication (Kleinman et al., 2011b). The development of the model was based on an extensive study about discharge and P export dynamics of two catchments draining into Lake Sempach (Lazzarotto et al., 2005). It consists of a hydrological and a P sub-model. The P sub-model describes the P losses from soil and manure sources with runoff calculated by the hydrological sub-model. The hydrological sub-model was calibrated using discharge data from four catchments draining into Lake Sempach. Discharge and DRP loads at the catchment outlets from the same catchments but for a different time period were used for model validation. Questions that remained open were in particular concerning the risks of P export associated with the application of manure on grasslands; the WSP-DRP relationship for highly P enriched soils; the applicability of the model to catchments for which it is not specifically calibrated; and the validity of the model in general in predicting the spatial distribution of runoff and P export, i.e. CSAs.

Objectives and contents of the thesis

The main objective of this thesis was to validate and improve the predictive capabilities of the parsimonious Rainfall Runoff Phosphorus model in order to enable reliable predictions of CSAs on the basis of readily available data. The main questions addressed are:

1) How do P enriched soils and recently applied manure affect P losses with runoff?
2) Is the RRP model transferable to catchments not used for calibration?
3) How reliable are spatial model predictions?

The validation of hydrological catchment and P export models is often limited to discharge and load measurements at catchment outlets, as it is much more difficult to obtain useful validation data relating to the spatial distribution of processes. A major problem for spatial validation of P export predictions is the high spatial and temporal variation of

processes controlling P export. A relatively large number of measurement locations and rather long monitoring periods are therefore needed to quantify spatio-temporal variations of pollutant loads (White et al., 2009). In this study we used spatially distributed measurements, field plot experiments with artificial rainfall application on manured vs. unmanured grassland; and comparisons with other models to assess the RRP model performance, the spatial predictions and the level of detail in soil and topographic data needed to make reliable predictions of CSAs.

Chapter 2 describes artificial-rainfall experiments that were carried out in 2008 on grassland plots in the catchment area of Lake Baldegg in order to extend the data base of the model with regard to highly P enriched grassland soils, and in particular to gain information on the role of recently applied manure on runoff generation, on the amounts of incidental P losses and their dependence on soil P status and timing after manure application.

In Chapter 3 we investigate the predictive capabilities of the RRP model and its sensitivity on the binary classification of soils by drainage behaviour. To test whether the RRP model is transferable to non-calibration catchments, it was applied to the Stägbach catchment, which drains into Lake Baldegg, whereas the catchments used for calibration drain into Lake Sempach. The spatial performance of the model was assessed using field data on soil moisture, ground water level, runoff and P load measurements acquired in 2010.

In Chapter 4 we compare the capability of the RRP model with those of two other models that have been proposed to delineate risk areas: (i) the Dominant Runoff Processes (DoRP) model proposed by Schmocker-Fackel et al. (2007) and (ii) the Sensitive Catchment Integrated Modelling Analysis Platform (SCIMAP) developed by Reaney et al. (2011). In contrast to the binary classification of soils used in the RRP model, the DoRP model can make use of all relevant spatial information available in a soil map and also accounts for the parent material on basis of geological maps. SCIMAP, on the other hand, is solely based on topographic and soil P data, but in contrast to RRP and DoRP accounts for connectivity. Comparing the three models revealed the relative importance of topographic and soil data for CSA determination.

References

Arnold, J.G., Srinivasan, R., Muttiah, R.S., Williams, J.R., 1998. Large area hydrologic modeling and assessment - Part 1: Model development. J. Am. Water Resour. Assoc. 34, 73-89.

Beasley, D.B., Huggins, L.F., Monke, E.J., 1980. ANSWERS - a model for watershed planning. T. Asae 23, 938-944.

Braun, M., Aschwanden, N., Wüthrich-Steiner, C., 2001. Abschwemmung von Phosphor. AGRARForschung 8, 36-41.

Braun, M., Wüthrich-Steiner, C., Spiess, E., Stauffer, W., Prasuhn, V., 1998. Wirkungskontrolle der Öko-Massnahmen im Gewässerschutz. Agrarforschung 5, 129-132.

Buda, A.R., Koopmans, G.F., Bryant, R.B., Chardon, W.J., 2012. Emerging technologies for removing nonpoint phosphorus from surface water and groundwater: introduction. J. Environ. Qual. 41, 621-627.

Buda, A.R., Kleinman, P.J.A., Srinivasan, M.S., Bryant, R.B., Feyereisen, G.W., 2009. Effects of hydrology and field management on phosphorus transport in surface runoff. J. Environ. Qual. 38, 2273-2284.

Burkhardt, M., Stamm, C., Waul, C., Singer, H., Muller, S., 2005. Surface runoff and transport of sulfonamide antibiotics and tracers on manured grassland. J. Environ. Qual. 34, 1363-1371.

Carpenter, S.R., Caraco, N.F., Correll, D.L., Howarth, R.W., Sharpley, A.N., Smith, V.H., 1998. Nonpoint pollution of surface waters with phosphorus and nitrogen. Ecol. Appl. 8, 559-568.

Doody, D.G., Archbold, M., Foy, R.N., Flynn, R., 2012. Approaches to the implementation of the Water Framework Directive: Targeting mitigation measures at critical source areas of diffuse phosphorus in Irish catchments. J. Environ. Manage. 93, 225-234.

Dubrovsky, N.M., Burow, K.R., Clark, G.M., Gronberg, J.M., P.A., H., Hitt, K.J., Mueller, D.K., Munn, M.D., Nolan, B.T., Puckett, L.J., Rupert, M.G., Short, T.M., Spahr, N.E., Sprague, L.A., Wilber, W.G. 2010. The quality of our Nation's waters—Nutrients in the Nation's streams and groundwater, 1994 - 2004, http://water.usgs.gov/nawqa/nutrients/pubs/circ1350.

Frossard, E., Bolomey, S., T., F., Sinaj, S. 2005. Phosphor im Boden und Düngestrategie - Der Fall Baldeggersee. Bundesamt für Umwelt, Wald und Landschaft, Bern.

Gächter, R., 1987. Lake restoration - Why oxygenation and artificial mixing cannot substitute for a decrease in the external phosphorus loading. Schweizerische Zeitschrift Fur Hydrologie-Swiss Journal of Hydrology 49, 170-185.

Gburek, W.J., Sharpley, A.N., 1998. Hydrologic controls on phosphorus loss from upland agricultural watersheds. J. Environ. Qual. 27, 267-277.

Gitau, M.W., Veith, T.L., Gburek, W.J., 2004. Farm-level optimization of BMP placement for cost-effective pollution reduction. T. Asae 47, 1923-1931.

Heathwaite, A.L., Reaney, S., Lane, S. 2007. Understanding spatial signals in catchments: linking critical areas, identifying connection and evaluating response Diffuse phosphorus loss: risk assessment, mitigation options and ecological effects in river basins. the 5th International Phosphorus Workshop (IPW5), Silkeborg, Denmark.

Heathwaite, L., Sharpley, A., Bechmann, M., 2003. The conceptual basis for a decision support framework to assess the risk of phosphorus loss at the field scale across Europe. J. Plant Nutr. Soil Sc. 166, 447-458.

Hering, D., Borja, A., Carstensen, J., Carvalho, L., Elliott, M., Feld, C.K., Heiskanen, A.-S., Johnson, R.K., Moe, J., Pont, D., Solheim, A.L., van de Bund, W., 2010. The European Water Framework Directive at the age of 10: A critical review of the achievements with recommendations for the future. Sci. Total Environ. 408, 4007-4019.

Herzog, P. 2005. Sanierung des Baldegger Sees, Auswertung der Zufluss-Untersuchungen 2000 bis 2004. (In German.) Luzern.

Kleinman, P.J.A., Sharpley, A.N., Saporito, L.S., Buda, A.R., Bryant, R.B., 2009. Application of manure to no-till soils: phosphorus losses by sub-surface and surface pathways. Nutr. Cycl. Agroecosys. 84, 215-227.

Kleinman, P.J.A., Sharpley, A.N., Buda, A.R., McDowell, R.W., Allen, A.L., 2011a. Soil controls of phosphorus in runoff: Management barriers and opportunities. Can. J. Soil Sci. 91, 329-338.

Kleinman, P.J.A., Allen, A.L., Needelman, B.A., Sharpley, A.N., Vadas, P.A., Saporito, L.S., Folmar, G.J., Bryant, R.B., 2007. Dynamics of phosphorus transfers from heavily manured Coastal Plain soils to drainage ditches. J. Soil Water Conserv. 62, 225-235.

Kleinman, P.J.A., Sharpley, A.N., McDowell, R.W., Flaten, D.N., Buda, A.R., Tao, L., Bergstrom, L., Zhu, Q., 2011b. Managing agricultural phosphorus for water quality protection: principles for progress. Plant Soil 349, 169-182.

Lazzarotto, P., 2005. Modeling phosphorus runoff at the catchment scale. Swiss Federal Institute of Technology (ETH), Zurich.

Lazzarotto, P., Prasuhn, V., Butscher, E., Crespi, C., Fluhler, H., Stamm, C., 2005. Phosphorus export dynamics from two Swiss grassland catchments. J. Hydrol. 304, 139-150.

Leh, M.D., Chaubey, I., 2009. GIS-Based Predictive Models of Hillslope Runoff Generation Processes(1). J. Am. Water Resour. Assoc. 45, 844-856.

Lehmann, H.-J., Valli, C., Fischler, M., Gujer, H.-U., Schrenk, K., Siegenthaler, A., Zbinden, U., Altorfer, M., Dettwiler, J., Liechti, P., Lagger, S., Eberele, T. 1998. Konzept zur Verminderung der Phosphorbelastung von oberirdischen Gewässern aus der landwirtschaftlichen Bewirtschaftung. Bundesamt für Landwirtschaft / Bundesamt für Umwelt, Wald und Landwirtschaft.

Lindenschmidt, K.E., Ollesch, G., Rode, M., 2004. Physically-based hydrological modelling for nonpoint dissolved phosphorus transport in small and medium-sized river basins. Hydrol. Sci. J. 49, 495-510.

McDowell, R.W., Srinivasan, M.S., 2009. Identifying critical source areas for water quality: 2. Validating the approach for phosphorus and sediment losses in grazed headwater catchments. J. Hydrol. 379, 68-80.

Pionke, H.B., Gburek, W.J., Sharpley, A.N., 2000. Critical source area controls on water quality in an agricultural watershed located in the Chesapeake Basin. Ecol. Eng. 14, 325-335.

Pionke, H.B., Gburek, W.J., Sharpley, A.N., Zollweg, J.A., 1997. Hydrological and chemical controls on phosphorus loss from catchments. In: Tunney H., et al. (Eds.), Phosphorus loss from soil to water, CAB International Press, Cambridge, pp. 225-242.

Prasuhn, V., Sieber, U., 2005. Changes in diffuse phosphorus and nitrogen inputs into surface waters in the Rhine watershed in Switzerland. Aquat. Sci. 67, 363-371.

Prasuhn, V., Lazzarotto, P., 2005. Abschwemmung von Phosphor aus Grasland im Einzugsgebiet des Sempachersees. Schriftenreihe der FAL 57.

Radcliffe, D.E., Freer, J., Schoumans, O., 2009. Diffuse phosphorus models in the united states and europe: Their usages, scales, and uncertainties. J. Environ. Qual. 38, 1956-1967.

Reaney, S.M., Lane, S.N., Heathwaite, A.L., Dugdale, L.J., 2011. Risk-based modelling of diffuse land use impacts from rural landscapes upon salmonid fry abundance. Ecol. Model. 222, 1016-1029.

Roberts, W.M., Stutter, M.I., Haygarth, P.M., 2012. Phosphorus Retention and Remobilization in Vegetated Buff er Strips: A Review. J. Environ. Qual. 41, 389-399.

Rodriguez, H.G., Popp, J., Maringanti, C., Chaubey, I., 2011. Selection and placement of best management practices used to reduce water quality degradation in Lincoln Lake watershed. Water Resour. Res. 47.

Sanchez, M., Boll, J., 2005. The effect of flow path and mixing layer on phosphorus release: Physical mechanisms and temperature effects. J. Environ. Qual. 34, 1600-1609.

Schmocker-Fackel, P., Naef, F., Scherrer, S., 2007. Identifying runoff processes on the plot and catchment scale. Hydrol. Earth. Sys. Sc. 11, 891-906.

Schoumans, O.F., Chardon, W.J., Bechmann, M., Gascuel-Odoux, C., Hofman, G., Kronvang, B., Litaor, M.I., Lo Porto, A., Newell-Price, P., Rubaek, G. 2011. Mitigation options for reducing nutrient emissions from agriculture. A study amongst European member states of Cost action 869. Alterra Wageningen UR, Wageningen.

Schoumans, O.F., Silgram, M., Groenendijk, P., Bouraoui, F., Andersen, H.E., Kronvang, B., Behrendt, H., Arheimer, B., Johnsson, H., Panagopoulos, Y., Mimikou, M., Lo Porto, A., Reisser, H., Le Gall, G., Barr, A., Anthony, S.G., 2009. Description of nine nutrient loss models: capabilities and suitability based on their characteristics. J. Environ. Monitor. 11, 506-514.

Sharpley, A.N., 1993. Assessing phophorus bioavailability in agricultural soils and runoff. Fert. Res. 36, 259-272.

Sharpley, A.N., Chapra, S.C., Wedepohl, R., Sims, J.T., Daniel, T.C., Reddy, K.R., 1994. Managing agricultural phophorus for protection of surface waters - issues and options. J. Environ. Qual. 23, 437-451.

Sharpley, A.N., Weld, J.L., Beegle, D.B., Kleinman, P.J.A., Gburek, W.J., Moore, P.A., Mullins, G., 2003. Development of phosphorus indices for nutrient management planning strategies in the United States. J. Soil Water Conserv. 58, 137-152.

Shigaki, F., Sharpley, A., Prochnow, L.I., 2007. Rainfall intensity and phosphorus source effects on phosphorus transport in surface runoff from soil trays. Sci. Total Environ. 373, 334-343.

Smith, K.A., Jackson, D.R., Withers, P.J.A., 2001. Nutrient losses by surface run-off following the application of organic manures to arable land. 2. Phosphorus. Environ. Pollut. 112, 53-60.

Smith, V.H., Joye, S.B., Howarth, R.W., 2006. Eutrophication of freshwater and marine ecosystems. Limnol. Oceanogr. 51, 351-355.

Spiess, E., 2011. Nitrogen, phosphorus and potassium balances and cycles of Swiss agriculture from 1975 to 2008. Nutr. Cycl. Agroecosys. 91, 351-365.

Srinivasan, M.S., Kleinman, P.J.A., Sharpley, A.N., Buob, T., W.J.Gburek, 2007. Hydrology of Small Field Plots Used to Study Phosphorus Runoff under Simulated Rainfall. J. Environ. Qual. 36, 1833-1842.

Stadelmann, P., Lovas, R., Butscher, E., 2002. 20 Jahre Sanierung und Überwachung des Baldeggersees. Mitteilungen der Naturforschenden Gesellschaft Luzern Band 37.

Stamm, C., Flühler, H., Gächter, R., Leuenberger, J., Wunderli, H., 1998. Preferential transport of phosphorus in drained grassland soils. J. Environ. Qual. 27, 515-522.

Stutter, M.I., Chardon, W.J., Kronvang, B., 2012. Riparian Buffer Strips as a Multifunctional Management Tool in Agricultural Landscapes: Introduction. J. Environ. Qual. 41, 297-303.

Vadas, P.A., Kleinman, P.J.A., Sharpley, A.N., Turner, B.L., 2005. Relating soil phosphorus to dissolved phosphorus in runoff: A single extraction coefficient for water quality modeling. J. Environ. Qual. 34, 572-580.

Vadas, P.A., Jokela, W.E., Franklin, D.H., Endale, D.M., 2011. The effect of rain and runoff when assessing timing of manure application and dissolved phosphorus loss in runoff. J. Am. Water Resour. Assoc. 47, 877-886.

Vadas, P.A., Srinivasan, M.S., Kleinman, P.J.A., Schmidt, J.P., Allen, A.L., 2007. Hydrology and groundwater nutrient concentrations in a ditch-drained agroecosystem. J. Soil Water Conserv. 62, 178-188.

Van Vuuren, D.P., Bouwman, A.F., Beusen, A.H.W., 2010. Phosphorus demand for the 1970-2100 period: A scenario analysis of resource depletion. Global Environ. Chang. 20, 428-439.

Wade, A.J., Whitehead, P.G., Butterfield, D., 2002. The Integrated Catchments model of Phosphorus dynamics (INCA-P), a new approach for multiple source assessment in heterogeneous river systems: model structure and equations. Hydrol. Earth. Sys. Sc. 6, 583-606.

Weld, J., Sharpley, A.N., 2007. Phosphorus indices. In: Radcliffe, D. E., Cabrera, M. L. (Eds.), Modeling phosphorus in the environment. CRC Press, Boca Raton, pp. 3-19.

White, M.J., Storm, D.E., Busteed, P.R., Stoodley, S.H., Phillips, S.J., 2009. Evaluating nonpoint source critical source area contributions at the watershed scale. J. Environ. Qual. 38, 1654-1663.

2

Phosphorus losses in runoff from manured grassland of different soil P status at two rainfall intensities

Claudia Hahn, Volker Prasuhn, Christian Stamm, Rainer Schulin

Published in Agriculture, Ecosystems and Environment153 (2012) 65-74

Abstract

In many areas, excessive manure application on agricultural land has led to a substantial build-up of soil phosphorus (P) stocks, increasing the risks for diffuse pollution of surface waters. Recent studies highlight the need to differentiate between runoff types for better prediction of these risks. In a factorial field-plot experiment we investigated the role of soil-P status, band-applied manure and rainfall intensity on P losses from two Swiss grassland sites. Artificial rainfall was applied on each plot first at medium intensity using a sprinkler and then at high intensity using a watering can, simulating two different runoff conditions. Under both conditions, dissolved reactive P (DRP) in runoff increased linearly with water soluble P in the soil (WSP), but the extraction coefficients differed substantially between the two phases of runoff generation. It was 0.017 kg L^{-1} for runoff generated with the watering can (WCR), and 0.085 kg L^{-1} for runoff generated with the sprinkler (SR). Manure application increased DRP losses, but did not override the effect of soil P status. Phosphorus losses with runoff were more sensitive to soil P status for SR than for WCR. Reducing soil-P is therefore crucial to reduce runoff-P.

2.1 Introduction

While phosphorus (P) losses from point-sources were reduced substantially in many countries over the last three decades, diffuse P losses from agricultural land are still resulting in substantial eutrophication of surface water bodies, which is an important problem around the world. In many areas, excessive fertilizer and manure applications have led to an increase in soil P levels (Kleinman et al., 2011; Leinweber et al., 2002; Sharpley et al., 1994). On permanent grassland, P concentrations can be especially high at the soil surface due to the absence of tillage (Schärer et al., 2007). In Switzerland, this problem is particularly well documented for the catchment areas of Lake Sempach and Lake Baldegg on the Swiss Plateau. Here, intensive livestock production and unfavorable hydrological conditions have led to severe eutrophication problems (Gächter, 1987; Herzog, 2005). These areas are characterized by a high percentage of permanent grassland. As the P retention capacity of the top soil becomes exhausted with increasing P input not only freshly applied manure and P fertilizer are at risk of being carried into streams and lakes via surface runoff and macropore flow to tile-drains (Stamm et al., 2002), but also the P that has accumulated close to the soil surface.

Many studies have investigated the relationship between P in soil and P in runoff and analyzed the effect of manure on P losses with surface waters (McDowell et al., 2001; Pote et al., 1999; Pote et al., 1996; Shigaki et al., 2007; Vadas et al., 2005). With regard to soil P it has been generally reported that the dissolved P concentration in runoff depends on the soil P concentration. However, there are contradictory reports on the general relationship between these two variables. Vadas et al. (2005) compared the relationship between water-extractable soil P and reactive P in filtered runoff samples for 20 soils. The slope of the regression lines, the so-called extraction coefficients, varied between 0.006 and 0.018 kg L^{-1}. However, extraction coefficients from 17 of the 20 soils did not differ significantly. This suggests that a single extraction coefficient may be used across a wide range of soils, management practices, runoff conditions and experimental methods to describe the relationship between P concentrations in soil and P concentrations in runoff. This is in contrast to earlier work (e.g. Sharpley et al., 1994), reporting that the relationship between soil and runoff P depended on site-specific factors such as runoff type, soil management and topographic conditions. As mentioned by Kleinman et al. (2006), part of the contradiction may be due to the fact that the studies reviewed by Vadas et al. (2005) only simulated infiltration excess runoff (IER). Kleinman et al. (2006) found the highest P mass losses with saturation excess runoff (SER). In line with these findings various other studies recently highlighted the need to differentiate between runoff types when linking soil P status with P

losses in runoff (Leh and Chaubey, 2009; Lindenschmidt et al., 2004; McDowell and Srinivasan, 2009; Radcliffe et al., 2009; Sanchez and Boll, 2005). Runoff generated by events of different intensity and duration may in particular differ in: (a) soil depth over which rain and soil solution mix during runoff generation, and (b) contact time between infiltrating rain and soil particles. According to Nash et al. (2002), these are the main factors influencing solute mobilization and export in runoff. Kleinman et al. (2006) hypothesized that the mixture of soil solution and rain differs between SER and IER, as IER mainly consists of rainwater, whereas SER is characterized by a higher percentage of soil solution water.

Manure application to soil is a third important factor controlling P losses, apart from soil P status (largely controlled by soil type and grazing history) and runoff types. It can affect P losses in two ways. Firstly, it increases the P pool available for transport. Volf et al. (2007), found that adding manure to soils can increase P extraction coefficients. Shigaki et al. (2007) found that dissolved reactive P (DRP) significantly increased in runoff with increasing water soluble P (WSP) from sources such as fertilizers or manure one day after application. In many studies (Sharpley et al., 1994; Vadas et al., 2004; Withers et al., 2003) the DRP concentration in runoff decreased rapidly with increasing time lag between manure application and the subsequent runoff event. This decrease was often attributed to increasing sorption of the released manure P to soil. Vadas et al. (2011) gave manure decomposition and bioturbation as reasons for the decrease in manure P availability. Secondly, manure application may also affect the generation of runoff. Burkhardt et al. (2005) and Smith et al. (2001) found that manure application increased surface runoff, probably due to soil sealing. In contrast, Srinivasan et al. (2007) found no effect from manure on runoff volume. Instead, they reported a delay in runoff at dry sites caused by manure absorbing rainwater. A possible factor influencing the effect of manure on runoff generation is the way in which manure is applied. In contrast to surface spreading, band spreading and manure injection application result in some exposure of the soil's surface and this may result in reduced soil sealing or water absorption by manure. Swiss authorities introduced incentives to increase the use of band application of manure with the aim to reduce ammonia emissions. While it was beyond the scope of this study to analyse the effect of band application as an additional factor of our experimental design, we used this method of manure application on all of our plots because it is rapidly becoming common practice in Switzerland.

The effects of surface-spread manure and soil-P on P in runoff have been addressed in various studies. However, more research is needed to understand whether and how the rainfall intensity and runoff type influence the relationship between these two factors and runoff-P on grasslands. Thus we performed a factorial field plot experiment with controlled

water application, simulating two types of runoff generating rainfall events (an extremely high-intensity event of very short duration and a medium intensity event of longer duration) on a grassland site in Switzerland in order to (1) assess the influence of these different events on the relationship between soil P - and runoff P, (2) investigate the effect of manure on DRP losses with runoff generated by the two different types of events, and (3) assess how a time delay between manure application and runoff event affects P concentrations in runoff.

2.2 Materials and methods

2.2.1 Study sites

Simulated rainfall experiments were carried out within the catchment area of Lake Baldegg (Fig. 2-1), a lake in central Switzerland with a history of serious eutrophication problems due to agricultural P inputs (Gächter, 1987; Herzog, 2005). The region is characterized by intensive animal production (dairy and pig farms, 2.4 livestock units per ha (Herzog, 2005)) and intensively manured permanent grassland (four to six cuts per year). In the past, P was applied far in excess of crop demand. This caused an increase in the soil P stocks, primarily close to the surface in grassland soils (e.g. Stamm et al., 1998).

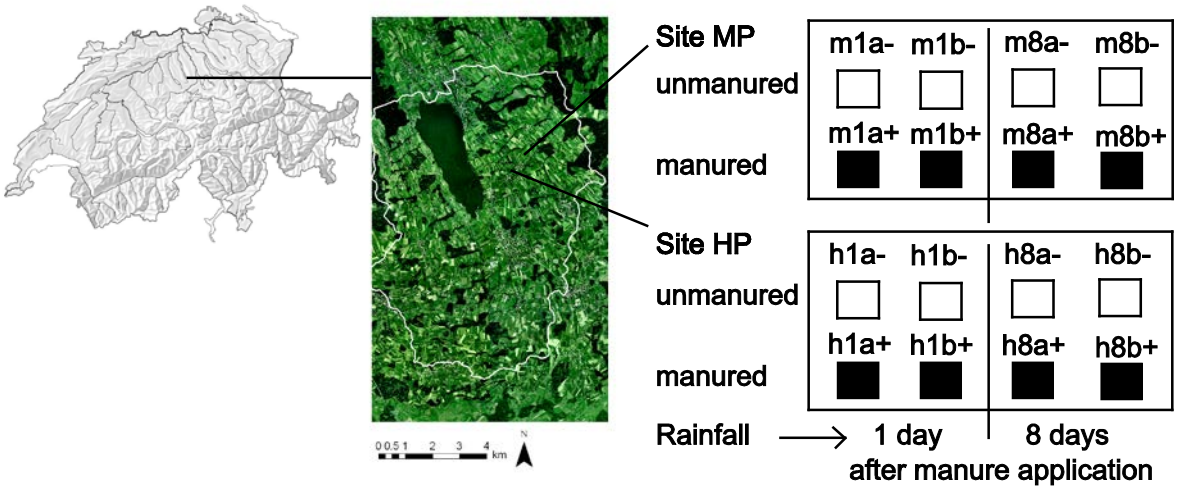

Figure 2-1: Location of study sites in Switzerland (map on the left) and experimental design. Site HP = high-P site; Site MP = medium-P site. Plot names consist of four different parts: m = medium-P site or h = high-P site, 1 = runoff collected 1 day after treatment or 8 = runoff collected 8 days after treatment, a = replicate 1 of 2 or b = replicate 2 of 2, + = manure or - = no manure.

The average annual precipitation is approximately 1140 mm (Herzog, 2005), which is quite uniformly distributed over the year. The soil parent material varies between upper freshwater molasse and moraines of the Würm glaciation (Bodenkarte Hochdorf 1983). For this reason the soils are generally loamy and of low permeability, favoring the generation of surface runoff and preferential flow through cracks and biopores to the many subsurface drainage systems (Stamm et al., 1998).

Plot experiments with artificial rainfall were carried out on two different sites with different P status (Fig. 2-1) covered by permanent grassland. The vegetation was a high-yielding *Trifolio-Lolion* association. Both sites were intensively managed for silage and hay production (5 cuts per year). Manure was usually applied at the beginning of the growing period and after each harvest (Liebisch, 2011).

Site 1 (medium-P; site MP) was characterized by a significantly lower P concentration in the top 5 cm of the soil than Site 2 (high-P; site HP; Table 2-1). Site MP was situated on the upper part of a south-west facing 5.2 to 8.7° slope, approximately 720 m above sea level. The soil was a deep gleyic Cambisol (IUSS Working group WRB, 2006) with a loamy soil texture. Site HP was located approximately 570 m above sea level on a south facing 8.7 to 22.9° midslope. The soil was a calcaric Cambisol (IUSS Working group WRB, 2006), with some gleyic features, a loamy soil texture and an intermediate soil depth. The saturated hydraulic conductivity K_s was estimated using the pedo-transfer function proposed by Cosby et al. (1984):

$$\log(K_s) = 0.804 + 0.0126\ Sand_{\%} - 0.0064\ Clay_{\%}$$

On each site, we collected 30 soil samples (0 to 5 cm) and combined them into one composite sample per site. Within the upper 5 cm both sites showed a similar texture. Despite different Ca concentrations (see Table 2-1), the P buffering capacity (Frossard and Sinaj, 1996) was very similar in both soils (Site MP = 0.58; Site HP = 0.57) (F. Liebisch, personal communication, 2009). However, the quantity of isotopically exchangeable P within 1 min (E1min), as defined by Frossard and Sinaj (1996), was different in the two soils. Site HP was characterized by a higher E1min (E1min = 6.74 + 0.57 mg L-1) than the medium-P site, with E1min = 2.28 + 0.59 mg L-1 (F. Liebisch, personal communication, 2009).

Table 2-1: Soil characteristics for both study sites, determined for composite samples (30 samples, 0-5 cm depth) of each site

	pH	C_{org} [a]	Humus	Clay	Silt	Sand	Ca [b]	WSP [c]	P [b]	P-CO_2 [d]
		%					mg / kg			
Site MP [e]	6.6	3.45	5.9	23.0	31.2	39.9	2992	10.4	45.6	25.7
Site HP [f]	7.5	4.11	7.1	25.1	35.1	32.7	54168	26.1	164.0	78.8

[a] organic carbon
[b] AAE10, extraction with ammonium acetate and EDTA
[c] mean value of water soluble phosphorus from soil samples collected from all plots
[d] P-CO_2 = 0.0356 mg P_2O_5 per 100g soil
[e] medium-P site
[f] high-P site

2.2.2 Runoff plots

On each study site we installed eight 1x1 m runoff plots within an area of 20 by 20 m. The 20 x 20 m area was fenced off for the duration of the experiments and no manure was applied the experimental year prior the experiments. The plots were randomly distributed over the area. The upper and lateral sides of each plot were confined by plastic sheets, which were pushed approximately 5 to 10 cm into the soil and protruded 10 cm out of the soil. The upper frame was 2 m long and the irrigated area covered 1.75 x 1.4 m, in order to ensure uniform irrigation conditions within the enclosed 1x1 m runoff plot (Fig. 2-2). This setup also allowed for soil moisture measurements and soil sampling adjacent to the plot. A gutter was installed at the lower side of the plots to collect surface runoff and subsurface runoff from the upper 5 cm of the soil in a bucket. During the experiments the gutter was covered to avoid direct input of irrigation water. We installed two tensiometers on either side of each plot, one at 10 cm and one at 25 cm depth. Suction was measured with a pressure transducer (DMG 2120, Ballmoos Elektronik AG, Horgen, Switzerland). Additionally, we inserted six 2-rod TDR probes, two probes of 10, 15 and 25 cm depth each, vertically in the soil, to measure the volumetric soil water content ($m^3\ m^{-3}$). The signal was recorded by means of a Tektronix 1502B device and stored by a data logger (CR10 Campbell Scientific, Inc.). The SMDRX50, 50 OHM multiplexer from Campbell Scientific, Inc. was used to manage multiple probes. Water content (θ) was calculated from the temperature-corrected dielectric constant (ε) according to the equation given by Topp et al. (1980):

$$\theta = -5.3\times10^{-2} + 2.92\times10^{-2}\,\varepsilon - 5.5\times10^{-4}\,\varepsilon^2 + 4.3\times10^{-6}\,\varepsilon^3$$

Soil water potential and water content measurements were carried out before and after the sprinkler experiment as well as prior to manure application.

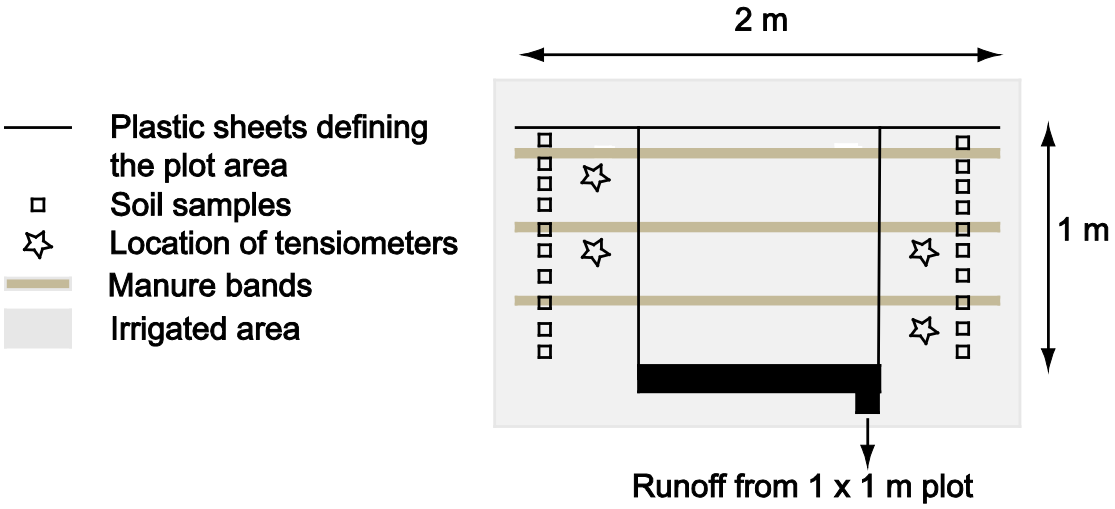

Figure 2-2: Design of the experimental runoff plots. Plastic sheets define the 1m^2 runoff area. Four tensiometers are installed beside the runoff area.

2.2.3 Artificial rainfall experiments

2.2.3.1 Experimental design

Manure was applied on four randomly chosen plots out of the eight plots on each site (Fig. 2-1). The other four plots were treated in the same way except for the manure application. Before the manure was applied, the grass on the manure plot and the corresponding unmanured plot was cut to approximately 7 cm and removed. The manure was obtained from a farm located in the catchment area and used, after thorough mixing, without further treatment. It consisted of an equal mixture of swine and cow manure, and was diluted with water. Three L per m^2 (i.e. 30 m^3 ha^{-1}) of manure was applied in three strips on each plot using a watering can in order to simulate band application. The P concentration of the manure was 0.57 g L^{-1} and thus the rate of P application was 17.1 kg ha^{-1}. The 5 to 10 cm wide application bands ran parallel to the gutter at 30 cm, 60 cm and 90 cm distance upslope. The amount of manure applied corresponded to typical manure application rates in the area. After manure application manured (+) and unmanured (-) plots were covered with a plastic sheet to protect them from natural rainfall. The first sprinkler experiments were performed on the medium-P site in the last two weeks of June 2008, just after a wet period where 79 mm of rain fell in two weeks. The soil was almost saturated when the plots were

prepared (28.5 ± 26 cm WC). To create similar initial conditions on the high-P site, where the plots were prepared two weeks later, each plot and its surrounding area (2 m x 1.5 m) was watered with 90 to 100 L of deionised water.

Two of the four manured plots were irrigated by artificial rainfall one day after manure application using a portable sprinkler and immediately thereafter by means of a watering can. The other two manured plots received the same sprinkler and watering can treatment 8 days after manure application (abbreviations: 1 and 8). In parallel to each manured plot, one unmanured plot was irrigated in the same way. As we could only irrigate two plots per day, we manured and irrigated the second plots of a pair of replicates (denoted as a and b) with a delay of two days. Figure 2-3 illustrates the timing of the experiments. Due to technical problems, the plot pair m1b-/+ on the medium-P site was prepared and irrigated eight, rather than two, days after the plot pair m1a-/+.

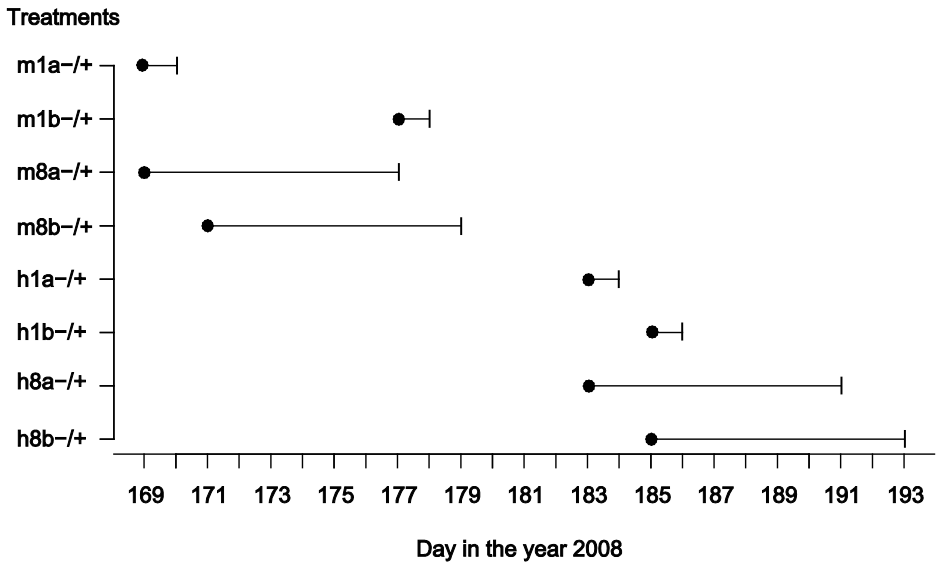

Figure 2-3: Time line for individual experiments. Dots denote the day of manure application, horizontal lines indicate how long plots were covered, and vertical lines mark the day of the sprinkler and watering can experiments. Plot names consist of four different parts: m = medium-P site or h = high-P site, 1 = runoff collected 1 day after treatment or 8 = runoff collected 8 days after treatment, a = replicate 1 of 2 or b = replicate 2 of 2, + = manure or - = no manure. One line comprises two plots: 1 unmanured and 1 manured.

The gutter was installed on the day before the rainfall experiments. Before artificial rainfall was initiated we measured soil water content and matric potential, and took soil

samples from the area laterally adjacent to the runoff plot (Fig. 2-2). Per plot, a total of 20 soil samples were taken from 0 to 5 cm depth, 10 on each side and combined to one composite sample. Six of the 20 samples of each manured plot were taken from the manure bands. Thus, the ratio of soil samples with manure and without manure corresponded to the areal fraction of the manured surface.

2.2.3.2. Sprinkler experiment

The sprinkler used was also used by Schärer et al. (2006) and Schärer et al. (2007) and is described by Flury et al. (1994). The device consisted of a 1.4-m-long spray bar with 6 nozzles. The spray bar was driven by an electric motor back and forth over the plot area, perpendicular to the slope direction. The irrigation intensity was controlled by the speed of the sprinkler bar. During irrigation the nozzles were 48 cm above the soil surface. Artificial rainfall was applied for 90 min at constant intensity of 47 to 48 mm h^{-1}, which corresponds to a 70-year rainfall event (Geiger et al., 1992). Within the last ten years three events with similar rainfall intensity were recorded in the region of the experimental site. Due to the small impact energy of the drops falling from the sprinkler (Flury et al. 1994), a rather high water application rate was needed to generate runoff from the grassland plots. The coefficient of variation of the application rate was measured in separate experiments with 10 cm by 10 cm cups, which were distributed within the 1 m x 1 m plot area. It ranged between 5 and 10 %. In order to guarantee a constant composition of the irrigation water and to best simulate rain water effects on P mobilisation (Schärer et al., 2006), we used deionized water for the sprinkler experiments (electrical conductivity = 8 µS cm^{-1}, pH = 6.7 $\pm$ 0.66, chloride < 0.5 mg L^{-1}, Ca < 0.5 mg L^{-1}, DRP = 8.32 $\pm$ 7.3 µg L^{-1}, TP = 59.5 $\pm$ 81.2 µg L^{-1}). We measured total runoff every 5 min by collecting it in a bucket and using a graduated cylinder to determine the volume. An aliquot of 100 ml was taken for analysis from each sufficiently large runoff sample.

2.2.3.3. Watering can experiment

Immediately after each sprinkler experiment, we recorded soil water potentials and soil water contents. We then applied 11 L of deionized water within one minute with a watering can twice on each plot. Runoff was collected as one integrated sample for each irrigation event until runoff ceased. Analysis was based on the second watering can application. No watering can experiments were carried out on plots m1a- and m1a+ on the medium-P site due to technical difficulties.

The chosen irrigation intensity of 11 mm min^{-1} is very high, but not unrealistic for very short periods (1 min). Within the last 10 years 9 rainfall events were recorded in the region with 1-min intensities exceeding 4 mm min^{-1}. The highest 1-min intensity was recorded in 2007 with 5.33 mm min^{-1}. Dunkerley (2010) reported that rain bursts of similar intensity can occur within longer rainfall events, emphasizing their potential importance for runoff generation and erosion. Although total summer precipitation is predicted to decrease in the future in Switzerland (CH2011, 2011), the frequency of high intensity events is expected to increase (Christensen and Christensen (2003), Beniston et al. (2007)).

2.2.4. Analysis of soil, surface runoff and manure samples

2.2.4.1. Soil and manure samples

All soil samples were stored at 4°C before they were dried for 48 h at 40°C and sieved to 2 mm maximum grain size. The composite soil samples were analyzed for CO_2 saturated water extractable P (P_{CO2}), ammonium acetate and EDTA extractable P (P_{AAE10}) and total P (P_{tot}) according to Swiss reference methods (ART and ACW, 2008 / 2010). For the analysis of P_{CO2} 30 g of soil was mixed with 75 ml CO_2 saturated water (6 mmol CO_2 per 75 ml), shaken for 1 hour and filtered. For the AAE10 extraction 10 g of soil was suspended in 100 ml solution of 3.85 g ammonium acetate and 0.58 g EDTA, shaken for 1 hour and filtered. For the analysis of P_{tot} 5 g of soil was incinerated at 500 °C for 3 hours and digested with 16 ml HCl. Phosphorus concentration in extracts was determined by molybdate colorimetry and a spectrometer measuring at 750 nm.

For the analysis of WSP, subsamples of 3 g of soil were suspended in 30 ml nanopure water and shaken for 16 hours on a reciprocatal (back-and-forth) shaker (GFL 3018). After filtration, the extracts (< 200 nm) were analyzed for P using the malachite green colorimetric method (Ohno and Zibilske, 1991). Manure samples were analyzed for total P using the colorimetric method described by Gericke and Kurmies (1952).

2.2.4.2. Water samples

Runoff water samples were stored overnight at 4°C and analyzed within 24 hours after sampling (Haygarth et al., 1995). After filtration (<450 nm) dissolved reactive phosphorus (DRP) was analyzed using the molybdate colorimetry method (Vogler, 1965). In order to determine total phosphorus (TP), unfiltered samples were digested using potassium persulfate and then analyzed using the molybdate colorimetry method. Electrical conductivity (EC) was measured using a Metrohm Conductometer 712.

2.2.5. Statistical analyses

We used the software package R (R Development Core Team, 2007) for all statistical analyses. In particular, we performed regression analysis, 2-way ANOVA, and covariance analysis, using mixed effects models to account for fixed effects (manure and timing) and random effects (dates). The data were tested for homoscedasticity, normal distribution and equal variances to check whether prerequisites of the tests were met. If conditions for statistical tests were not fulfilled we performed the analysis on log transformed data or adjusted the test. To allow for different variances for each level of factor we performed the covariance analysis using the function "Generalized Least Squares" (gls) within the R package "Linear and Nonlinear Mixed Effects Models" (nlme) (Pinheiro and Bates, 2000). Covariance analysis was performed to test whether different runoff types led to different WSP - DRP relationships and whether manure led to elevated DRP losses and overrides the soil P signal. Wilcoxon and t-tests were used to test for statistical significance of treatment differences.

2.3 Results and discussion

2.3.1 Soil moisture conditions and runoff generation

The plots irrigated one day after manure application were significantly ($p < 0.01$) wetter (10 cm depth: $\theta_{siteMP(plotm1a-,m1a+)} = 0.46 \pm 0.01$ m^3 m^{-3} / $\theta_{siteMP(plotm1b-,m1b+)} = 0.33 \pm 0.05$ m^3 m^{-3}, $\theta_{siteHP} = 0.34 \pm 0.02$ m^3 m^{-3}) than the plots irrigated eight days after manure application ($\theta_{siteMP} = 0.29 \pm 0.02$ m^3 m^{-3}, $\theta_{siteHP} = 0.27 \pm 0.03$ m^3 m^{-3}). Due to the wet period before the start of the experiments, the plots that were irrigated first (m1a- and m1a+) were particularly wet. The differences between the plots disappeared during the sprinkler experiments. After 90 minutes of irrigation, the soil water content exceeded 0.42 m^3 m^{-3} in all medium-P plots and 0.40 m^3 m^{-3} in all high-P plots. Thus, the soil was close to saturation prior to the watering can experiments, with tensiometric water potentials of 6.8 ± 4.2 hPa and 18.2 ± 3.15 hPa, respectively.

The runoff coefficients RC (runoff as percent of irrigation) for the sprinkler experiments were generally low and ranged between 1.9 % and 8.4 % on the medium-P site and between 0.4 and 5.3 % on the high-P site. Exceptionally large runoff (ca. 20 L) was observed on the two m1a plots that were irrigated immediately after the rainfall period before the experiment. Here, the runoff coefficient reached 26.0 (m1a-) and 29.7 % (m1a+), respectively. In contrast, no runoff was observed on one of the manured medium-P plots. This was probably

due to drainage through macropores created by ants, which were observed at that location. Overall, there was a significant small-scale variation in runoff formation (Table 2-2).

Table 2-2: Runoff and phosphorus characteristics for both study sites and both runoff types [a]

			Sprinkler experiment			Watering can experiment		
Site	Plot	WSP	RC	DRP	TP	RC	DRP	TP
		mg kg^{-1}	%	mg L^{-1}	mg L^{-1}	%	mg L^{-1}	mg L^{-1}
Medium-P site (MP)	**unmanured**							
	m1a-	11.11	25.91	0.25	0.32	NA	NA	NA
	m1b-	11.32	3.10	0.52	0.61	43.18	0.28	0.34
	m8a-	9.50	2.93	0.56	0.76	45.45	0.25	0.50
	m8b-	9.85	8.40	1.11	1.52	58.18	0.23	0.26
	manured							
	m1a+	14.13	29.66	2.84	3.72	NA	NA	NA
	m1b+	10.56	0.00	NA	NA	45.00	0.88	1.17
	m8a+	16.52	1.90	0.68	0.95	> 53 [b]	0.63	0.84
	m8b+	16.21	7.04	1.67	2.09	65.91	0.81	0.90
High-P site (HP)	**unmanured**							
	h1a-	28.56	1.68	1.57	1.72	38.18	0.48	0.92
	h1b-	22.03	0.43	0.93	1.10	31.36	0.34	0.68
	h8a-	23.99	3.57	2.30	2.58	34.09	0.46	0.92
	h8b-	30.00	2.10	2.80	3.59	20.91	0.70	1.06
	manured							
	h1a+	31.44	0.39	1.53	1.93	43.64	1.62	2.31
	h1b+	29.40	0.53	0.57	0.75	40.91	1.34	2.17
	h8a+	30.71	2.68	1.80	2.04	17.27	0.91	1.20
	h8b+	37.70	5.27	4.28	5.25	36.36	1.13	1.40

[a] Plot names consist of four different parts: m = medium-P site or h = high-P site, 1 = runoff collected 1 day after treatment or 8 = runoff collected 8 days after treatment, a = replicate 1 of 2 or b = replicate 2 of 2, + = manure or - = no manure. WSP = water soluble P, RC = runoff coefficient, DRP = dissolved reactive P, TP = total P

[b] Estimate of RC based on first watering can experiment

The data suggest that this variability was partly related to antecedent soil water potential (Fig. 2-4). When the soil was very wet prior to the experiment, runoff generation was very pronounced (plots m1a) and at least 30% of the plot area contributed to the collected runoff, including the lowest band of manure application (Fig. 2-2). All other plots were drier before irrigation. They produced less runoff than the other two plots, and the minimum contributing area covered only a small percentage of the plot area. Comparing all respective plot pairs, electrical conductivity measurements (EC) in runoff from manured plots were significantly higher than in runoff from unmanured plots ($p = 0.04$; Table 2-3). Because manure has a very high electrical conductivity this indicates that the area contributing to runoff comprised

of at least one manure band. However, the difference was not significant when all but the wettest plots (m1a- / m1a+) were taken into account. One plot pair (h1b- / h1b+) showed higher electrical conductivity values for the unmanured plot than for the manured plot, suggesting that at very low runoff conditions the manure bands did not necessarily influence runoff quality.

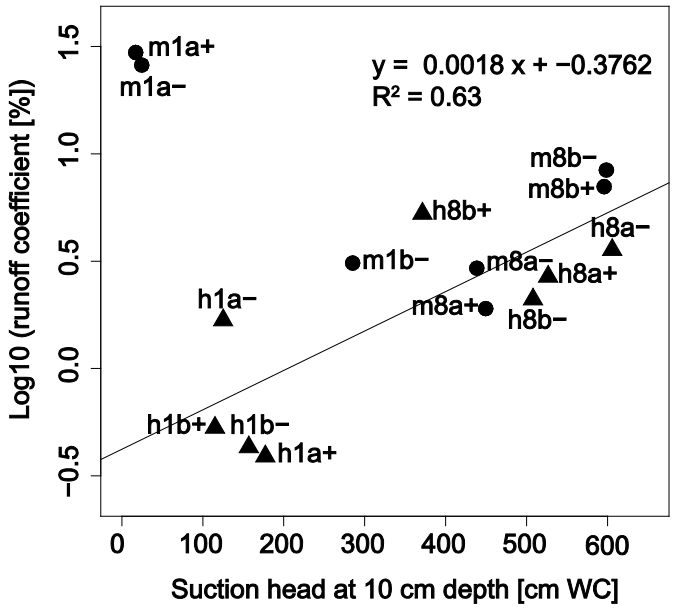

Figure 2-4: Relationship between suction head and the logarithm of the runoff coefficient. Except for the wettest plots, runoff increased with increasing suction head. Plot names consist of four different parts: m = medium-P site or h = high-P site, 1 = runoff collected 1 day after treatment or 8 = runoff collected 8 days after treatment, a = replicate 1 of 2 or b = replicate 2 of 2, + = manure or - = no manure.

Runoff increased with increasing initial soil water suction, except for the two wettest plots (Fig. 2-4). Thus, under dry conditions runoff may have partially resulted from inhibition of infiltration due to hydrophobicity effects. Similar observations were reported by Kleinman et al. (2006). The results are also consistent with findings of Doerr et al. (2006), who investigated water repellency in surface soil samples of different textural types in humid temperate regions. Repellency was found at most of the permanently vegetated sites where the water content of the upper 5 cm of the soil was below 28% by volume. The TDR measurements of soil moisture content taken over a depth of 10 cm in our experiment were comparable to this threshold.

In the sprinkler experiments the soil was gradually wetted, and flow towards the gutter started as subsurface flow. Preferential flow along roots was observed before near-surface runoff was intercepted by the gutter. Despite the high irrigation intensity, which exceeded the estimated K_s values (14.5 mm h^{-1} and 11.4 mm h^{-1}), observations indicate that the sprinkler intensity initially did not exceed infiltration rate, but led to local saturation of the soil. In contrast, runoff almost immediately appeared on the soil surface when the water was applied by means of the watering can, indicating that the application rate exceeded the infiltration rate. The runoff rates were always higher after the second than after the first watering can application due to increased soil water saturation. The runoff coefficients ranged from 17 to 45 % for the first watering can application, and from 43 to 66 % for the second application on the medium-P plots. On the high-P plots, the runoff coefficients ranged from 9 to 31 % for the first application and from 17 to 43 % for the second application. The highest runoff volume (7.25 L) was reported on plot m8b+. The high runoff coefficients strongly suggest that the area contributing to runoff formation was large enough to include at least one manure band. This is supported by the fact that the unmanured plots exhibited significantly ($p = 0.01$) lower EC values than the manured plots (Table 2-3).

The differences in runoff generation between the two irrigation modes are reflected in the EC of the runoff water. Electrical conductivity was 4 to 5.5 times higher in sprinkler-generated runoff than in watering can generated runoff (Table 2-3), indicating a larger contribution of the resident soil solution to the runoff in the first case. Assuming that dissolution of electrolytes from the solid phase was negligible, we calculated the mixing ratios between resident soil solution and irrigation water based on the EC values. The EC of the irrigation water was often below detection limit or very low (8 µS cm^{-1} (at 20°C)). Based on EC values considered typical for non-saline soils (Blume et al., 2010), the EC of the soil solution (EC_{soil}) was set to range between 400 and 700 µS cm^{-1} (at 20°C). Table 2-4 shows that the estimated contribution of resident soil solution to runoff was much higher in the sprinkler experiments than in the watering can experiments. Regarding unmanured plots, runoff generated with the sprinkler consisted of 8 to 13 % soil solution on site MP and of 21 to 37 % soil solution on site HP. Runoff generated with the watering can comprised only 1 to 2 % soil solution (site MP) or 3 to 5 % soil solution (site HP). Obviously, the mode of irrigation strongly influenced the way water interacted with the soil. Given that we neglected any dissolution or desorption of electrolytes from the soil matrix, these estimates represent upper limits for the percentages of soil solution in the sampled runoff. Hence, the watering can runoff hardly contained pre-event soil solution.

Table 2-3: Electrical conductivity measurements (EC) with standard deviation, estimations of the proportion of soil solution in runoff, and measured and calculated DRP concentrations in watering can runoff with standard deviation. Calculation of the proportion of soil solution in runoff is based on two electrical conductivity values for the soil solution EC_{soil} (400 and 700 µS cm^{-1}) to assess the possible range.

	Electrical conductivity [µS cm^{-1}]			Proportion of soil solution in runoff [%]				DRP in watering can Runoff [mg L^{-1}]	
	Sprinkler experiment	Watering can experiment	sprinkler /watering can	EC_{soil} = 400		EC_{soil} = 700		measured	calculated
				Sprinkler	Watering can	Sprinkler	Watering can		
Site MP unmanured	60.8 ± 34	14.7 ± 3.2	4.14	13	2	8	1	0.25 ± 0.03	0.08 ± 0.04
Site MP manured	108.3 ± 29	31.3 ± 7.6	3.46	26	6	15	3	0.77 ± 0.13	0.24 ± 0.13
mean MP	81.1 ± 38.8	23 ± 10.5	3.53	19	4	11	2	0.51 ± 0.3	0.14 ± 0.11
Site HP unmanured	152 ± 36.6	27.5 ± 1.3	5.53	37	5	21	3	0.5 ± 0.15	0.29 ± 0.16
Site HP manured	194 ± 67	49.3 ± 5.1	3.94	47	11	27	6	1.25 ± 0.3	0.44 ± 0.25
mean HP	173 ± 56.4	38.4 ± 12.1	4.51	42	8	24	4	0.87 ± 0.46	0.37 ±0.2

In contrast to Burkhardt et al. (2005), we found no significant manure effect on runoff generation. Runoff volumes are in line with findings of Srinivasan et al. (2007), but at odds with findings of Withers et al. (2003) and Smith et al. (2001), who reported soil surface sealing after slurry application and reduced rain infiltration. The difference in reported manure effects may be attributed to the use of different manure application methods. The studies mentioned above observed an increase in runoff generation for plots treated with surface applied manure. As we simulated band application of manure, we did not cover the whole plot area with manure and thus the effect of manure on runoff generation may have been too small to become statistically significant. The results indicate that P losses with runoff resulting from soil sealing caused by manure (Smith et al., 2001) may be reduced by band application of manure.

Table 2-4: Dissolved reactive phosphorus (DRP) loads [mg m^{-2}] relative to the applied rainfall [L m^{-2}]

Plot	Medium-P Site		High-P Site	
	Sprinkler experiment	Watering can experiment	Sprinkler experiment	Watering can experiment
	mg DRP m^{-2} / L rain m^{-2}			
unmanured				
m1a-	0.064	NA	0.026	0.184
m1b-	0.016	0.120	0.004	0.105
m8a-	0.016	0.113	0.082	0.158
m8b-	0.093	0.131	0.059	0.147
manured				
m1a+	0.844	NA	0.006	0.706
m1b+	No runoff occured	0.394	0.003	0.549
m8a+	0.013	> 0.334	0.048	0.157
m8b+	0.118	0.533	0.225	0.409

2.3.2. Relationship between soil P and runoff P

WSP concentrations on the medium-P site were significantly lower than WSP concentrations on the high-P site (Table 2-2). The data illustrates the variability of WSP within one site, as seen in the WSP values for the unmanured plots. These site-differences translated into differences in DRP concentrations in runoff. This relationship could be described by a linear relationship between the WSP concentration in the topsoil and the DRP concentration in the runoff (Fig. 2-5). The slope of the regression line was significantly steeper for runoff generated with the sprinkler (slope = 0.085 kg L^{-1}) than for runoff generated with the watering can (slope = 0.017 kg L^{-1}). Regression analysis of the DRP -

WSP relationship gave an R^2 of 0.81 (p = 0.006) for the watering can experiments and an R^2 of 0.68 (p = 0.012) for the sprinkler experiments. The higher p-value and lower R^2 can be attributed to the higher variability in DRP found in the sprinkler-generated runoff.

Vadas et al. (2005) reported that the extraction coefficient ranged between 0.006 to 0.018 kg L^{-1} in 10 studies covering a total of 20 different soils. This range covers the value found here for watering can generated runoff but not for the sprinkler-generated runoff. According to Kleinman et al. (2006), Vadas et al. (2005) included only studies on IER in their analysis. Although our experimental conditions did not allow for complete soil saturation across the profile, on-site observations and EC values indicate that the water travelled through and interacted with the soil in different manners during both types of experiments. The rate of water application with the sprinkler did not initially exceed the infiltration rate of the topsoil as was the case with the watering can, but it was high enough to locally saturate the soil.

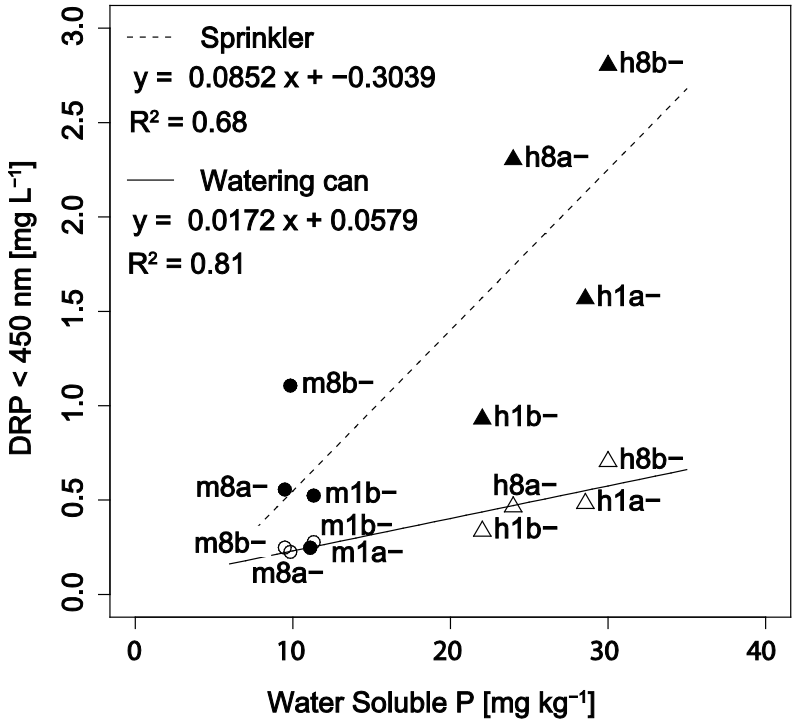

Figure 2-5: Linear relationships between water soluble phosphorus concentrations in soil (WSP) and dissolved reactive phosphorus concentrations in runoff (DRP) from unmanured plots for watering can runoff (WCR) and sprinkler runoff (SR). The slope of the regression line was significantly steeper for SR than for WCR. Plot names consist of four different parts: m = medium-P site or h = high-P site, 1 = runoff collected 1 day after treatment or 8 = runoff collected 8 days after treatment, a = replicate 1 of 2 or b = replicate 2 of 2, + = manure or - = no manure.

On the high-P plots, sprinkler irrigation led to significantly higher DRP concentrations than watering can irrigation ($p = 0.02$). The same tendency was observed in the medium-P soil (Fig. 2-6). However, the difference between the two irrigation methods was not statistically significant. The large scatter of the sprinkler data possibly masked the difference between the two runoff types. More data are needed before reliable conclusions can be drawn.

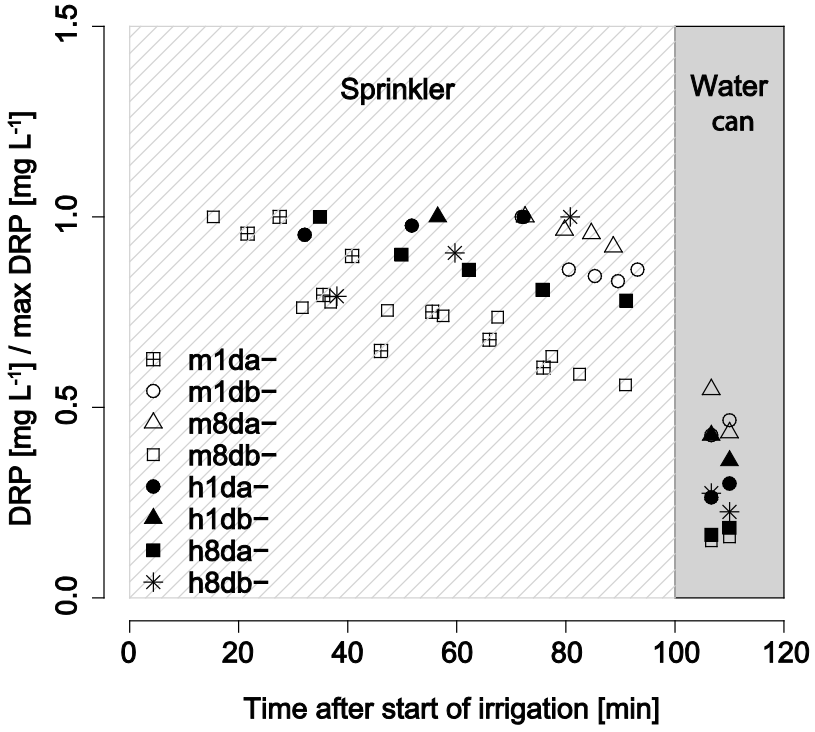

Figure 2-6: Evolution of DRP concentrations relative to the maximum DRP concentration of the respective plot in runoff during the sprinkler and watering can experiments. DRP concentrations are higher in sprinkler runoff than in watering can runoff. This is significant for site HP, but not for site MP. Plot names consist of four different parts: m = medium-P site or h = high-P site, 1 = runoff collected 1 day after treatment or 8 = runoff collected 8 days after treatment, a = replicate 1 of 2 or b = replicate 2 of 2, + = manure or - = no manure.

On all plots, the watering can generated runoff showed lower EC values than the sprinkler-generated runoff. Based on the calculated proportion of soil solution and irrigation water in runoff (see section 2.3.1), and the known DRP concentration in sprinkler-generated runoff, we calculated the DRP concentration for watering can runoff. The DRP concentrations calculated according to the dilution factors were a lot lower than the measured concentrations (Table 2-3). This discrepancy indicates that contact times – even

though they were very short - were long enough to release substantial amounts of P from the soil matrix into the runoff solution. As a result, more DRP was lost with watering can runoff than with sprinkler-generated runoff, given the much higher runoff coefficients of the former (Table 2-4). One possible explanation for that observation could be that the high irrigation rate with the watering can may have mobilized more soil particles than the medium intensity irrigation with the sprinkler due to an increase in runoff energy (Sharpley, 1985). Being poorer in electrolytes, the watering can generated runoff could have mobilized more particle-bound P due to stronger colloidal dispersion. Another reason could be the difference in soil moisture prior to the experiments. Zheng et al. (2004) found that DRP losses can be higher from saturated soils than from freely draining unsaturated soils.

In the absence of manure, higher DRP concentrations were generally found eight days, rather than one day after plot preparation, when soils were more drained. This trend was significant for the sprinkler but not for the watering can experiments. A similar observation, although on a different time scale, was made by Pote et al. (1999) who observed higher DRP concentrations in August than in May and attributed this to: (1) increased DRP generation when microorganisms die and decompose during hot and dry conditions, and (2) DRP released from wilted and dried plant tissue. Due to the covering of our plots with plastic sheets, these processes could partly have played a role in our time frame.

2.3.3. Effect of band applied manure

Three of the four manured medium-P plots yielded sprinkler-generated runoff in which the DRP concentration increased with runoff volume. The concentration of WSP was similar in these plots (Table 2-2), which suggests that the increase was primarily due to increased export of manure-P. Larger runoff volumes were associated with larger contributing areas, routing a larger proportion of runoff from the manure bands to the outlet. The runoff experiments on plot m1a+, which led to high runoff, illustrate the amount of DRP that can be lost from manured medium-P plots if the entire plot area and all manure bands contributed to runoff (~ 3 mg L^{-1}). Sprinkler-generated runoff from this plot resulted in the highest P load observed on any plot and for both runoff types in our study. The highest DRP concentration from the manured high-P plots reached ~ 4 mg L^{-1}.

In contrast to the sprinkler-generated runoff, runoff generated with a watering can always originated from a large fraction of the plot. The application of manure significantly increased the DRP concentrations in runoff, while the effect of soil P was still clearly visible (Fig. 2-7). DRP concentrations in runoff from manured medium-P plots (mean DRP = 0.77 mg L^{-1}) were significantly ($p = 0.02$) lower than DRP concentrations in runoff from manured high-P

plots (mean DRP = 1.25 mg L^{-1}). The intercepts of the regression lines for unmanured and manured plots were significantly different ($p = 3.27 \times 10^{-5}$), whereas the slopes were not (p = 0.28). The same holds true for the total P concentrations in the runoff (p = 0.0048; p = 0.23). These findings suggest that soil P and manure P contributed additively to the DRP found in the runoff. This is in contrast to conclusions drawn by Withers et al. (2003) from a field study conducted in the UK on field plots under arable cropping, the results of Braun et al. (1993), and those of Von Albertini et al. (1993) that found large differences in soil P status were overridden by manure application on grassland. The latter studies were performed in the same region as our study. The difference could be explained by the different way manure was applied (surface versus band spreading). Band application of manure allows for direct contact of rain water with the soil between the manure bands, whereas this is not possible if manure covers the soil completely.

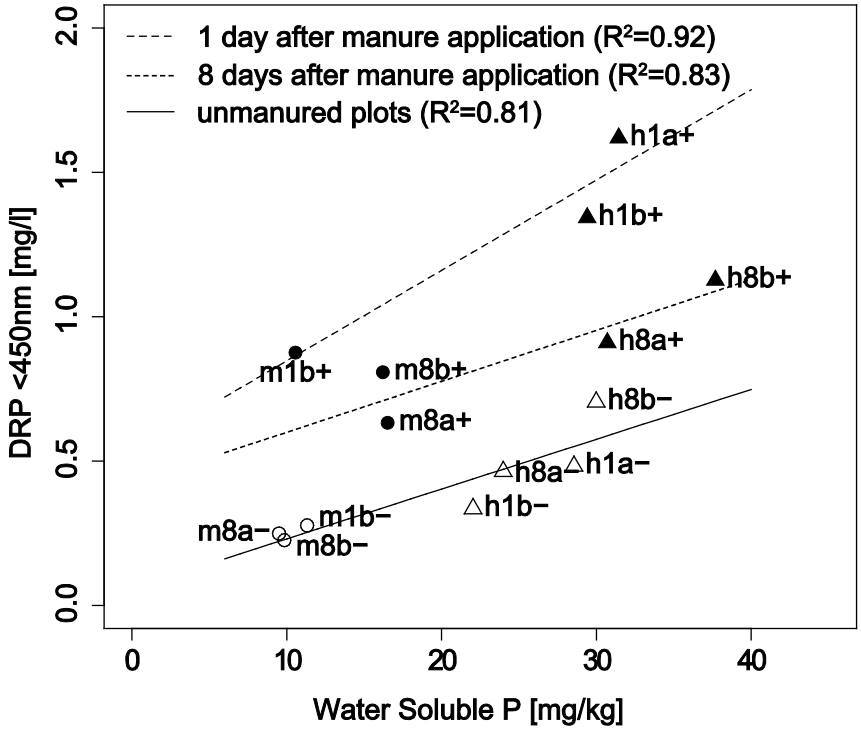

Figure 2-7: Effect of manure on dissolved reactive phosphorus concentration in runoff (DRP) generated with the watering can. Filled symbols define manured plots, empty symbols mark unmanured plots. Manure led to higher P losses, but could not override the effect of the soil P status. The experiments indicate an effect of timing between manure application and runoff event, indicated by dashed lines. Plot names consist of four different parts: m = medium-P site or h = high-P site, 1 = runoff collected 1 day after treatment or 8 = runoff collected 8 days after treatment, a = replicate 1 of 2 or b = replicate 2 of 2, + = manure or - = no manure.

2.3.4. Effect of timing

In the experiments in which irrigation was started one day after manure application, DRP and TP concentrations of watering can generated runoff were higher than in experiments in which irrigation started eight days after manure application (Fig. 2-7). Analysis of covariance showed significant differences in the intercepts for manured plots as compared to the unmanured plots (1 day: $p=1.01 \times 10^{-6}$; 8 days: $p=0.0005$), but no significant differences in slopes (one day: $p=0.098$; eight days: $p=0.955$). Similar effects of the time between manure application and irrigation on DRP in runoff were also observed in several other studies. Shigaki et al. (2007) found that DRP concentrations were lower in runoff generated seven days after manure application (~ 4 times lower) than in runoff generated one day after manure application. Allen and Mallarino (2008) reported that a rainfall event occurring 10 to 16 days after swine manure application resulted in 3.1 times lower runoff DRP concentrations than an event occurring 24 hours after application. They also found that P concentrations of runoff from manured plots became similar to P concentrations in runoff from unmanured control plots five to six months after manure application. Similar results have been reported by Withers et al. (2003) for grassland sites that were similar to those of our study. Figure 2-8 combines our data with data from Braun et al. (1993), which were collected from 30 m x 2 m plots during natural rainfall events. As with Braun et al. (1993), the watering can data indicate a decline of DRP concentration with time (Fig. 2-8). However, more data is needed to achieve statistically reliable results.

Data points from our watering can experiment are in the lower range of observations from Braun et al. (1993). This might be attributed to the difference in manure application or runoff type. However, other factors such as different scales can be important (Dougherty et al., 2004; Dougherty et al., 2008). No such decline with time was observed with the sprinkler because at low runoff conditions the manure bands did not necessarily influence runoff quality. The high DRP concentrations observed on some plots (Fig. 2-8) indicate that band application of manure may not reduce DRP concentrations in surface runoff. Further research is needed to evaluate how different manure application techniques affect P losses with runoff. Johnson et al. (2011) unfortunately did not include band application without aeration.

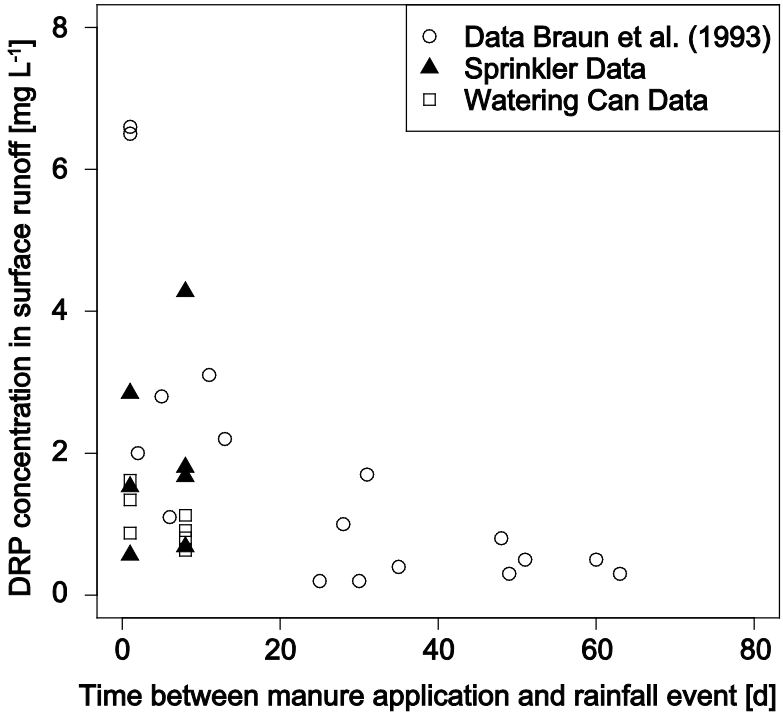

Figure 2-8: Effect of timing between manure application and runoff on dissolved reactive phosphorus (DRP) losses. Comparison with measurements from Braun et al. (1993). Their data was collected from 30 x 2 m plots, during natural rainfall events. The data displayed were collected during events within the vegetation period. DRP concentrations in runoff decrease with increasing time lag.

2.3.5 Multiple regression models

The role of the various factors affecting the DRP concentrations in our experiments can be summarized and quantified by means of multiple regression models (Fig. 2-9). To estimate the DRP concentrations in runoff generated with the sprinkler, the WSP concentration in soil, information on manure application (I_{man}) and on the time lag between manure application (plot covering) and irrigation (T_{man}), and the RCs were needed:

$$DRP = -1.46 - 0.876\ I_{man} + 0.017\ RC + 0.106\ WSP + 0.148\ T_{man} + 0.106\ RC\ I_{man}$$

where I_{man} is an indicator variable that is zero for no manure and one with manure. The model (adjusted $R^2 = 0.83$) shows that DRP was affected by the soil P status, the manure application, the time lag between manure application (plot covering, respectively) and irrigation, and the volume of generated runoff. The latter was not significant for the watering can experiments that could be very well described (adjusted $R^2 = 0.94$) by the model:

$$DRP = -0.085 + 0.924\ I_{man} + 0.014\ T_{man} + 0.021\ WSP - 0.077\ T_{man}\ I_{man}$$

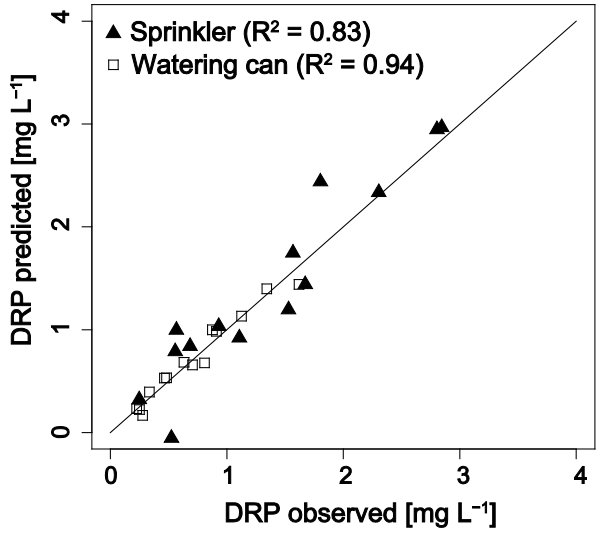

Figure 2-9: Predicted versus observed dissolved reactive phosphorus concentrations (DRP) in runoff. Information on soil P, manure application, the time lag between manure and rainfall and the runoff coefficients were needed for the prediction of DRP losses.

2.3.6 Scale issues

Our experimental setup enabled us to examine the effect of soil-P, manure-P and rainfall intensity on DRP concentrations and loads with runoff at the plot scale. The results cannot simply be upscaled to whole fields or even catchments (Dougherty et al., 2004; Dougherty et al., 2008; Sharpley and Kleinman, 2003; Smith and Pappas, 2010). Our plots had a runoff length of 1 m. Under natural conditions also runoff from further upslope would have flown through the plot. This would probably have led to larger sediment loads and thus higher particulate P (PP) losses. Sharpley and Kleinman (2003) reported that, while PP increased, DRP concentrations in runoff decreased with increasing plot length. They explain this effect with increased sorption of P to mobilised soil particles. In contrast, Dougherty et al. (2004) reviewed several studies where an increase in slope length led to increased DRP concentrations in runoff, which was attributed to longer contact times between the P source and runoff. This could partly explain why DRP concentrations in our watering can experiments were in the lower range (Fig. 2-8) of the values reported by Braun et al. (1993). Another reason may be in the high rainfall intensities commonly used in rainfall simulation experiments (Dunkerley, 2008). Such experiments tend to underestimate DRP concentrations

in runoff and overestimate runoff volumes, compared to frequent natural rain events (Dougherty et al., 2004; Dougherty et al., 2008; Smith and Pappas, 2010). While in field plot studies IER is generated usually (because it is difficult to saturate a plot and the adjacent area within a rainfall simulation experiment), SER can become more relevant at the landscape scale. Buda et al. (2009) showed that different runoff types can occur simultaneously during natural rainfall events at different locations within a catchment. Their study also suggests that due to the variability of P sources within catchments small-scale experiments may be better suited to gain mechanistic understanding of P mobilization processes in soil and losses via runoff than large-scale studies.

2.4 Conclusion

We simulated two different runoff conditions: runoff generated by medium intensity rainfall on initially dry soil and runoff generated by high intensity rainfall on already wet soil. The latter simulates a rain burst occurring within a longer rainfall event. DRP concentrations in runoff depended on the type of simulated rainfall event, the WSP concentration in soil and the manure application. From the linear relationships between soil P and runoff P concentration and the fact that application of manure did not override the effect of soil P status, although P concentrations and losses were increased, we conclude that soil P is an important source for DRP in runoff even in the presence of recently applied manure. Thus, P concentrations in soil need to be reduced in order to reduce DRP losses in runoff. The findings of this study suggest that P losses are more sensitive to soil P status for runoff caused by medium intensity rainfall than for runoff caused by highly intensive storm events. Our results are in line with other studies suggesting that predictions of P losses with runoff might be substantially improved by differentiating between runoff types. In particular, our study shows that this is also valid for grassland soils.

2.5 Acknowledgments:

The project was carried out within the framework of the COST Action 869, and was financially supported by the Swiss State Secretariat for Education and Research SER. We thank all reviewers for their detailed feedback and constructive comments.

2.6 References

Allen, B.L., Mallarino, A.P., 2008. Effect of Liquid Swine Manure Rate, Incorporation, and Timing of Rainfall on Phosphorus Loss with Surface Runoff. J. Environ. Qual. 37, 125-137.

ART, ACW. 2008 / 2010. Forschungsanstalt Agroscope Reckenholz-Tänikon ART, Forschungsanstalt Agroscope Changins-Wädenswil ACW. 1996 (changes 1997-2008, totalP 2010). Schweizerische Referenzmethoden der Forschungsanstalten Agroscope (In German.)

Beniston, M., Stephenson, D.B., Christensen, O.B., Ferro, C.A.T., Frei, C., Goyette, S., Halsnaes, K., Holt, T., Jylha, K., Koffi, B., Palutikof, J., Schoell, R., Semmler, T., Woth, K., 2007. Future extreme events in European climate: an exploration of regional climate model projections. Climatic Change 81, 71-95.

Blume, H.-P., Brümmer, G.W., Horn, R., Kandeler, E., Kögel-Knabner, I., Kretzschmar, R., Stahr, K., Wilke, B.-M., 2010. Lehrbuch der Bodenkunde - Scheffer / Schachtschabel. 16 ed. Spektrum Akademischer Verlag Heidelberg.

Bodenkarte Hochdorf 1983. Landeskarte der Schweiz 1:25000, Blatt 1130 (In German.) Zürich-Reckenholz: Eidg. Forschungsanstalt für landw. Pflanzenbau

Braun, M., Hurni, P., Von Albertini, N., 1993. Abschwemmung von Phosphor auf Grasland an zwei verschiedenen Standorten im Einzugsgebiet des Sempacher Sees. (In German.) Landwirtschaft Schweiz 6, 615-620.

Buda, A.R., Kleinman, P.J.A., Srinivasan, M.S., Bryant, R.B., Feyereisen, G.W., 2009. Effects of hydrology and field management on phosphorus transport in surface runoff. J. Environ. Qual. 38, 2273-2284.

Burkhardt, M., Stamm, C., Waul, C., Singer, H., Muller, S., 2005. Surface runoff and transport of sulfonamide antibiotics and tracers on manured grassland. J. Environ. Qual. 34, 1363-1371.

CH2011, 2011. Swiss Climate Change Scenarios CH2011, published by C2SM, MeteoSwiss, ETH, NCCR Climate and OcCC Zurich, Switzerland, 88 pp.

Christensen, J.H., Christensen, O.B., 2003. Climate modelling: Severe summertime flooding in Europe. Nature 421, 805-806.

Cosby, B.J., Hornberger, G.M., Clapp, R.B., Ginn, T.R., 1984. A Statistical Exploration of the Relationships of Soil Moisture Characteristics to the Physical Properties of Soils. Water Resour. Res. 20, 682-690.

Doerr, S.H., Shakesby, R.A., Dekker, L.W., Ritsema, C.J., 2006. Occurrence, prediction and hydrological effects of water repellency amongst major soil and land-use types in a humid temperate climate. Eur. J. Soil Sci. 57, 741-754.

Dougherty, W.J., Fleming, N.K., Cox, J.W., Chittleborough, D.J., 2004. Phosphorus transfer in surface runoff from intensive pasture systems at various scales: A review. J. Environ. Qual. 33, 1973-1988.

Dougherty, W.J., Nash, D.M., Cox, J.W., Chittleborough, D.J., Fleming, N.K., 2008. Small-scale, high-intensity rainfall simulation under-estimates natural runoff P concentrations from pastures on hill-slopes. Aust. J. Soil Res. 46, 694-702.

Dunkerley, D., 2008. Rain event properties in nature and in rainfall simulation experiments: a comparative review with recommendations for increasingly systematic study and reporting. Hydrol. Process. 22, 4415-4435.

Dunkerley, D.L., 2010. How do the rain rates of sub-event intervals such as the maximum 5- and 15-min rates (I(5) or I(30)) relate to the properties of the enclosing rainfall event? Hydrol. Process. 24, 2425-2439.

Flury, M., Flühler, H., Jury, W.A., Leuenberger, J., 1994. Susceptibility of soils to preferential flow of water: A field study. Water Resour. Res. 30, 9.

Frossard, E., Sinaj, S., 1996. The isotope exchange kinetic technique: A method to describe the availability of inorganic nutrients. Applications to K, P, S and Zn Annual Meeting of Arbeitsgemeinschaft-Stabile-Isotope Berlin, Germany. pp. 61-77.

Gächter, R., 1987. Lake restoration - Why oxygenation and artificial mixing cannot substitute for a decrease in the external phosphorus loading. Schweizerische Zeitschrift Fur Hydrologie-Swiss Journal of Hydrology 49, 170-185.

Geiger, H., Roethlisberger, G., Stehli, A., Zeller, J., 1992. Extreme Point Rainfall of Varying Duration and Return Period 1901 - 1970. In: Institute of Geographie, U. B. (Ed.), Hydrological Atlas of Switzerland. Federal Environmental Office, Bern

Gericke, S., Kurmies, B., 1952. Die kolorimetrische Phosphorsäurebestimmung mit Ammonium-Vandanat-Molybdat und ihre Anwendung in der Pflanzenanalyse. (In German.) Zeitschrift fuer Pflanzenernaehrung, Duengung, Bodenkunde 59, 235-247.

Haygarth, P.M., Ashby, C.D., Jarvis, S.C., 1995. Short term changes in the molybdate reactive phosphorus of stored soil waters. J. Environ. Qual. 24, 1133.

Herzog, P. 2005. Sanierung des Baldegger Sees, Auswertung der Zufluss-Untersuchungen 2000 bis 2004. (In German.) Luzern.

IUSS Working group WRB. 2006. World reference base for soil resources 2006. FAO, Rome.

Johnson, K.N., Kleinman, P.J.A., Beegle, D.B., Elliott, H.A., Saporito, L.S., 2011. Effect of dairy manure slurry application in a no-till system on phosphorus runoff. Nutr. Cycl. Agroecosys. 90, 201-212.

Kleinman, P.J.A., Srinivasan, M.S., Dell, C.J., Schmidt, J.P., Sharpley, A.N., Bryant, R.B., 2006. Role of Rainfall Intensity and Hydrology in Nutrient Transport via Surface Runoff. J. Environ. Qual. 35, 1248-1259.

Kleinman, P.J.A., Sharpley, A.N., McDowell, R.W., Flaten, D.N., Buda, A.R., Tao, L., Bergstrom, L., Zhu, Q., 2011. Managing agricultural phosphorus for water quality protection: principles for progress. Plant Soil 349, 169-182.

Leh, M.D., Chaubey, I., 2009. GIS-Based Predictive Models of Hillslope Runoff Generation Processes(1). J. Am. Water Resour. Assoc. 45, 844-856.

Leinweber, P., Turner, B.L., Meissner, R., 2002. Phosphorus. In: Haygarth, P. M., Jarvis, S. C. (Eds.), Agriculture, Hydrology and Water Quality. CAB International, Wallingford, Oxon, UK, pp. 29-55.

Liebisch, F., 2011. Plant and soil indicators to assess the phosphorus nutrition status of agricultural grasslands. ETH.

Lindenschmidt, K.E., Ollesch, G., Rode, M., 2004. Physically-based hydrological modelling for nonpoint dissolved phosphorus transport in small and medium-sized river basins. Hydrol. Sci. J. 49, 495-510.

McDowell, R., Sharpley, A., Brookes, P., Poulton, P., 2001. Relationship between soil test phosphorus and phosphosrus release to solution. Soil Sci. 166, 137 - 149.

McDowell, R.W., Srinivasan, M.S., 2009. Identifying critical source areas for water quality: 2. Validating the approach for phosphorus and sediment losses in grazed headwater catchments. J. Hydrol. 379, 68-80.

Nash, D., Halliwell, D., Cox, J., 2002. Hydrological Mobilization of Pollutants at the Field / Slope Scale. In: Haygarth, P. M., Jarvis, S. C. (Eds.), Agriculture, Hydrology and Water Quality. CAB International, Wallingford, Oxon, UK, pp. 225 - 242.

Ohno, T., Zibilske, L.M., 1991. Determination of low concentrations of phosphorus in soil extracts using malachite green. Soil Sci. Soc. Am. J. 55, 892-895.

Pinheiro, J.C., Bates, D.M., 2000. Mixed-Effects models in S and S-PLUS. Springer-Verlag, New York.

Pote, D.H., Daniel, T.C., Sharpley, A.N., Moore, P.A., Edwards, D.R., Nichols, D.J., 1996. Relating extractable soil phosphorus to phosphorus losses in runoff. Soil Sci. Soc. Am. J. 60, 855-859.

Pote, D.H., Daniel, T.C., Nichols, D.J., Sharpley, A.N., Moore, P.A., Miller, D.M., Edwards, D.R., 1999. Relationship between phosphorus levels in three ultisols and phosphorus concentrations in runoff. J. Environ. Qual. 28, 170-175.

R Foundation for Statistical Computing. 2007. R: A language and environment for statistical computing. Release 2.6.1. R Foundation for Statistical Computing, Vienna, Austria.

Radcliffe, D.E., Freer, J., Schoumans, O., 2009. Diffuse phosphorus models in the united states and europe: Their usages, scales, and uncertainties. J. Environ. Qual. 38, 1956-1967.

Sanchez, M., Boll, J., 2005. The effect of flow path and mixing layer on phosphorus release: Physical mechanisms and temperature effects. J. Environ. Qual. 34, 1600-1609.

Schärer, M., Vollmer, T., Frossard, E., Stamm, C., Fluhler, H., Sinaj, S., 2006. Effect of water composition on phosphorus concentration in runoff and water-soluble phosphate in two grassland soils. Eur. J. Soil Sci. 57, 228-234.

Schärer, M., Stamm, C., Vollmer, T., Frossard, E., Oberson, A., Flühler, H., Sinaj, S., 2007. Reducing phosphorus losses from over-fertilized grassland soils proves difficult in the short term. Soil Use Manage. 23, 154-164.

Sharpley, A., Kleinman, P., 2003. Effect of rainfall simulator and plot scale on overland flow and phosphorus transport. J. Environ. Qual. 32, 2172-2179.

Sharpley, A.N., 1985. Depth of Surface Soil-Runoff Interaction as Affected by Rainfall, Soil Slope, and Management. Soil Sci. Soc. Am. J. 49, 1010-1015.

Sharpley, A.N., Chapra, S.C., Wedepohl, R., Sims, J.T., Daniel, T.C., Reddy, K.R., 1994. Managing agricultural phophorus for protection of surface waters - issues and options. J. Environ. Qual. 23, 437-451.

Shigaki, F., Sharpley, A., Prochnow, L.I., 2007. Rainfall intensity and phosphorus source effects on phosphorus transport in surface runoff from soil trays. Sci. Total Environ. 373, 334-343.

Smith, D.R., Pappas, E., 2010. Do plot studies generate "directionally" correct assessments of field-level phosphorus losses? J. Soil Water Conserv. 65, 289-297.

Smith, K.A., Jackson, D.R., Withers, P.J.A., 2001. Nutrient losses by surface run-off following the application of organic manures to arable land. 2. Phosphorus. Environ. Pollut. 112, 53-60.

Srinivasan, M.S., Kleinman, P.J.A., Sharpley, A.N., Buob, T., W.J.Gburek, 2007. Hydrology of Small Field Plots Used to Study Phosphorus Runoff under Simulated Rainfall. J. Environ. Qual. 36, 1833-1842.

Stamm, C., Flühler, H., Gächter, R., Leuenberger, J., Wunderli, H., 1998. Preferential transport of phosphorus in drained grassland soils. J. Environ. Qual. 27, 515-522.

Stamm, C., Sermet, R., Leuenberger, J., Wunderli, H., Wydler, H., Flühler, H., Gehre, M., 2002. Multiple tracing of fast solute transport in a drained grassland soil. Geoderma 109, 245-268.

Topp, G.C., Davis, J.L., Annan, A.P., 1980. Electromagnetic determination of soil water content: measurements in coaxial transmission lines. Water Resour. Res. 16, 574-582.

Vadas, P.A., Kleinman, P.J.A., Sharpley, A.N., 2004. A Simple Method to Predict Dissolved Phosphorus in Runoff from Surface-Applied Manures. J. Environ. Qual. 33, 749-756.

Vadas, P.A., Kleinman, P.J.A., Sharpley, A.N., Turner, B.L., 2005. Relating soil phosphorus to dissolved phosphorus in runoff: A single extraction coefficient for water quality modeling. J. Environ. Qual. 34, 572-580.

Vadas, P.A., Jokela, W.E., Franklin, D.H., Endale, D.M., 2011. The effect of rain and runoff when assessing timing of manure application and dissolved phosphorus loss in runoff. J. Am. Water Resour. Assoc. 47, 877-886.

Vogler, P., 1965. Beiträge zur Phosphatanalytik in der Limnologie. II. Die Bestimmung des gelösten Ortophosphates. (In German.) Fortschritte der Wasserchemie und ihrer Grenzgebiete 2.

Volf, C.A., Ontkean, G.R., Bennett, D.R., Chanasyk, D.S., Miller, J.J., 2007. Phosphorus losses in simulated rainfall runoff from manured soils of Alberta. J. Environ. Qual. 36, 730-741.

Von Albertini, N., Braun, M., Hurni, P., 1993. Oberflächenabfluss und Phosphorabschwemmung von Grasland. (In German.) Landwirtschaft Schweiz Band 6 10, 575 - 582.

Withers, P.J.A., Ulén, B., Stamm, C., Bechmann, M., 2003. Incidental phosphorus losses - can they be predicted? J. Plant Nutr. Soil Sc. 166, 459-468.

Zheng, F.L., Huang, C.H., Norton, L.D., 2004. Surface water quality - Effects of near-surface hydraulic gradients on nitrate and phosphorus losses in surface runoff. J. Environ. Qual. 33, 2174-2182.

3

Prediction of dissolved reactive phosphorus losses from small agricultural catchments: calibration and validation of a parsimonious model

Claudia Hahn, Volker Prasuhn, Christian Stamm, Patrick Lazzarotto, Michael W.H. Evangelou, Rainer Schulin

Submitted to Hydrology and Earth System Sciences

Abstract

Eutrophication of surface waters due to diffuse phosphorus (P) losses continues to be a severe water quality problem world-wide, causing the loss of ecosystem functions of the respective water bodies. Phosphorus in runoff often originates from a small fraction of a catchment only. Targeting mitigation measures to these critical source areas (CSA) is expected to be most efficient and cost-effective, but requires suitable tools.

Here we investigated the capability of the parsimonious Rainfall-Runoff-Phosphorus (RRP) model to identify CSA in grassland-dominated catchments based on readily available soil and topographic data. After simultaneous calibration on runoff data from four small hilly catchments on the Swiss Plateau, the model was validated on a different catchment in the same region without further calibration. The RRP model adequately simulated the discharge and dissolved reactive P (DRP) export from the validation catchment. Sensitivity analysis showed that the model predictions were robust with respect to the classification of soils into 'poorly drained' and 'well drained', based on the available soil map. Comparing spatial hydrological model predictions with field data from the validation catchment provided further evidence that the assumptions underlying the model are valid and that the model adequately accounts for the dominant P export processes in the target region. Thus, the parsimonious RRP model is a valuable tool that can be used to determine CSA. Despite the considerable predictive uncertainty regarding the spatial extent of CSAs the RRP can provide guidance for the implementation of mitigation measures. The model helps to identify those parts of a catchment where high DRP losses are expected or can be excluded with high confidence. Legacy P was predicted to be the dominant source for DRP losses and thus, in combination with hydrologic active areas, a high risk for water quality.

3.1 Introduction

Eutrophication of surface waters due to diffuse phosphorus (P) inputs continues to be a severe water quality problem world-wide (Carpenter et al., 1998; Kleinman et al., 2011b), causing e.g. algal blooms, oxygen shortage, fish death and loss of water bodies for recreation and drinking. It has been observed that the majority of P found in the runoff at the outlet of a catchment may originate from a small fraction of the catchment only (Gburek and Sharpley, 1998; Pionke et al., 2000; Pionke et al., 1997). Thus, targeting mitigation options to these critical source areas (CSA) is seen to be particularly efficient and cost-effective (Heathwaite et al., 2003; Schulte et al., 2009; Strauss et al., 2007; White et al., 2009). Critical source areas are characterized by a direct transport connection of available P sources to a receiving water body (Gburek and Sharpley, 1998). Originally, erosion and surface runoff were assumed to be the only relevant transport mechanisms, but now it is recognized that also subsurface flow can significantly contribute to P export (Doody et al., 2012; Kleinman et al., 2007; Kleinman et al., 2011b; Stamm et al., 2002; Watson and Matthews, 2008). Important sources of such P exports are (1) freshly applied fertilizers or manure (Shigaki et al., 2007; Smith et al., 2001; Vadas et al., 2011), and (2) soils that are enriched with P due to excessive fertilizer application in the past (Kleinman et al., 2011a; Vadas et al., 2005). To a much smaller extent also plants can contribute that are freshly grazed, trampled or in decay (Kleinman et al., 2011b). Runoff from locations with freshly applied manure or high soil P concentrations bear particularly high risks for P export. Buda et al. (2009) demonstrated that even sites with relatively low soil P concentrations can deliver very high P loads when runoff is large. However, due to the complexity of the processes controlling diffuse P losses, the identification of CSAs is still difficult (Doody et al., 2012; Kleinman et al., 2011a; Kleinman et al., 2011b).

Various tools exist to describe water and P transport from non-point sources and to identify CSAs (Radcliffe et al., 2009; Schoumans et al., 2009; Sharpley et al., 2003), ranging from site assessment tools such as the P-Index (Weld and Sharpley, 2007) to process-based dynamic models such as SWAT (Arnold et al., 1998), INCA-P (Wade et al., 2002), and ANSWERS-2000 (Beasley et al., 1980). While static models are not able to account for the temporal and spatial variability of runoff and P losses, spatially distributed dynamic models are often over-parameterized (Radcliffe et al., 2009) and require many input data that are often not available. Therefore, as pointed out by Radcliffe et al. (2009), there is a need for parsimonious models that can be used to assess the spatial distribution of P export risks in a catchment. Irrespective of which type of model is used, a model requires validation for the purpose for which it is used. A major problem in validating spatially localized predictions of

P export from a catchment is that P export risks depend on processes that are subject to high local spatial variability and fluctuation in time.

A parsimonious model developed to predict runoff and P losses at the outlets of small agricultural catchments is the Rainfall-Runoff-Phosphorus (RRP) model (Lazzarotto, 2005; Lazzarotto et al., 2006). The RRP model is based on the concept of spatially distributed CSAs that vary in size with hydrological conditions. It describes the export of dissolved reactive phosphorus (DRP). This form is immediately available for algal uptake (Sharpley, 1993; Sharpley et al., 1994) and thus has a direct impact on eutrophication (Kleinman et al., 2011b). The RRP model gave a good description of discharge and DRP losses at the outlet of experimental catchments (Lazzarotto, 2005; Lazzarotto et al., 2006).

In the model it is assumed that two sites with the same topographic position belonging to the same soil type behave the same. In order to keep the number of model parameters low, the model only distinguishes between two soil types, i.e. well and poorly drained soils. This allowed for parameterizing the soil types by simultaneously calibrating the model to four catchments of different soil composition (Lazzarotto, 2005; Lazzarotto et al., 2006). Accordingly, the model should be transferable to other sites without calibration if the topographic and soil information is available. Because the moisture regime is a continuum, assigning the soils to these two classes may be somewhat arbitrary in some cases.

In this study we investigated the validity of RRP model predictions and in particular their sensitivity on the binary classification of soils by water regime classes. First, we calibrated the model simultaneously on runoff data of four small catchments in an agricultural area of Switzerland and then used it to predict runoff and P export from a neighboring catchment. Aside from testing the validity of these model predictions, we investigated the sensitivity of the model predictions on the soil grouping and assessed the spatial performance of various model versions using field data on soil moisture, ground water table, runoff volumes and P concentrations in runoff.

3.2 Materials and methods

3.2.1 The Rainfall-Runoff-Phosphorus (RRP) model

The Rainfall-Runoff-Phosphorus (RRP) model is a parsimonious model for continuous simulations of DRP transport from intensively managed grassland soils into streams in small agricultural catchments. It consists of two sub-models: the semi-distributed rainfall-runoff model and the phosphorus (P) model.

3.2.1.1 Rainfall-Runoff sub-model

The Rainfall-Runoff sub-model is a soil-type based semi-distributed model (Lazzarotto et al., 2006). It is based on the assumptions that (1) areas with the same topographic index λ and class of soil have the same hydrological behavior, and that (2) soils can be divided into two classes, i.e. well and poorly drained soils, having the same hydrologic characteristics within each class. The topographic index λ (Beven and Kirkby, 1979; Kirkby, 1975) is defined as

$$\lambda = \ln(A_{upstream}/\tan\beta) \quad (1)$$

where A is the upslope area draining through the respective location (multiple flow direction algorithm of Quinn et al. (1991)) and β is the local slope at that location. It is an indicator for the wetness of the soil at a given location within the catchment. Catchments are divided into four types of hydrological response units (HRU) differing in runoff dynamics: well drained soils (HRU_1), poorly drained soils (HRU_2), urban areas (HRU_3), and forests (HRU_4). Soil moisture is assumed to be uniform within each HRU. Changes in water storage S_i in HRU_i are calculated in hourly time steps (Δt) from the mass balance equation:

$$S_i(t+\Delta t) = S_i(t) + [rain(t) - et(t) - runoff_i(t)]\Delta t \quad (2)$$

where $rain(t)$, $et(t)$ and $runoff_i(t)$ are the respective rates of rainfall, evapotranspiration and simulated runoff from HRU_i during the time interval Δt. For HRU_1 and HRU_2 the model considers two types of runoff: fast flow $q_{i,fast}$ and slow flow $q_{i,slow}$. The slow flow component, which is given by

$$q_{i,slow}(t) = \Theta_i(t)c_i \quad (3)$$

depends (i) on the parameter c_i determining how much water from HRU_i contributes to baseflow and (ii) on the degree of soil saturation Θ_i, which is defined as the ratio between soil water storage $S_i(t)$ and the maximum soil water storage capacity $S_{i,max}$:

$$\Theta_i = S_i(t)/S_{i,max} \quad (4)$$

The fast flow component includes all types of quickly responding flow, such as preferential flow, saturation excess and Hortonian overland flow. It is the sum of an auto-regressive part describing the recession of fast flow and of a part representing the fraction of rain directly converted into fast flow:

$$q_{i,fast}(t+\Delta t) = a_i q_{i,fast}(t) + b_i rain(t+dt_i)\frac{A_{i,fast}}{A_i} \quad (5)$$

The parameter a_i is the fast flow decline rate, b_i is the proportion of rain that is directly converted into fast flow, dt_i is the time delay between rainfall and runoff in HRU_i, and $A_{i,fast}/A_i$ is the areal fraction of HRU_i that contributes to fast flow. The latter depends on the soil moisture status at time t. For every time step a threshold value $\lambda_{0,i}(t)$ is determined for the topographic index λ of HRU_i:

$$\lambda_{0,i}(t) \propto (1 - \Theta_i(t))^{n_i} \tag{6}$$

Locations with a topographic index higher than this threshold value are attributed to $A_{i,fast}$. The parameter n_i is determined by calibration. In contrast to HRU_1 and HRU_2, all runoff is assumed to occur as fast flow in urban areas (HRU_3):

$$q_{i,fast}(t + \Delta t) = a_3 q_{3,fast}(t) + b_3 rain(t - dt_3) \tag{7}$$

The total catchment response results from the sum of all flow components weighted with their respective areal fractions A_i/A_{total}, with $A_{total} = \sum A_i$. Neglecting runoff from forest areas due to their limited size in the study catchments, this sum was

$$Q(t) = \left(q_{1,slow}(t) + q_{1,fast}(t)\right)\frac{A_1}{A_{total}} + \left(q_{2,slow}(t) + q_{2,fast}(t)\right)\frac{A_2}{A_{total}} + q_{3,fast}(t)\frac{A_3}{A_{total}} \tag{8}$$

in our case.

3.2.1.2 Calibration of the Rainfall-Runoff sub-model

Using Uniform Monte Carlo simulations, the soil parameters (Table 3-1) were determined by simultaneous calibration of the model on four catchments (see Section 3.2.2) that differed in their soil composition and their hydrological response (Lazzarotto et al., 2006). The calibration period extended from July 7 – 17, 2000. This short calibration period proved to be sufficient (Lazzarotto et al., 2006), as conditions varied between very wet and dry. Different parameter combinations were generated using random sampling within the domain of each parameter. The following Nash-Sutcliffe-Criterion (NSC) (Nash and Sutcliffe, 1970), calculated for the four catchments together, was used to assess model performance of each parameter combination:

$$NSC = 1 - \frac{\sum_{k=1}^{4}\sum_{t=t_0}^{te}(Q_{obs}^k(t) - Q_{sim}^k(t))^2}{\sum_{k=1}^{4}\sum_{t=t_0}^{te}(Q_{obs}^k(t) - \bar{Q}_{obs}^k)^2} \tag{9}$$

where $Q_{obs}(t)$ is the observed runoff at time t, $Q_{sim}(t)$ is the simulated runoff at time t, and $\bar{Q}_{obs}$ is the mean observed runoff for the whole time period in catchment k. The evaluated

parameter sets were classified as either 'behavioral' (or 'accepted') for NSC > $NSC_{threshold}$ or 'non-behavioral' for NSC < $NSC_{threshold}$ (Hornberger and Spear, 1981). Behavioral parameter sets were used for model application. Thus, the number of accepted parameter sets (mc) defines the number of simulation results. The 10% quantiles and 90% quantiles of these simulations were used to characterize the uncertainty of the model predictions.

Table 3-1: Parameters of the hydrological response units (HRU_i = 1, 2, 3) that need to be determined during calibration (adopted from Table 2 in Lazzarotto et al., 2006). HRU_1 = well drained, HRU_2 = poorly drained, HRU_3 = urban

Global parameter	Minimum value	Maximum value	property	Used HRU
$S_{i,max}$ [mm]	0	800	Maximum soil water storage capacity	i = 1,2
a_i [-]	0	1	Fast flow decline rate	i = 1,2,3
b_i [-]	0	1	Proportion of rainfall converted into fast flow on the contributing areas	i = 1,2,3
c_i [mm]	0	1	Flow rate between the scaled soil water storage and the slow flow components	i = 1,2
n_i [-]	1	10	Expansion control of areas contributing to fast flow	i = 1,2

For more information on the hydrological model the reader is referred to Lazzarotto et al. (2006). Here, we converted the model from FORTRAN77 to FORTRAN95 in order to make a few modifications (such as corrections of some coding errors and removal of parameter constraints). We will refer to this version of this model in which all soil parameters were calibrated simultaneously as Version 1. In a second model version (Version 2) the urban parameters a_3 and b_3 were separately calibrated using discharge data from six small runoff events in July 2010 recorded in the Stägbach catchment, which is located in the vicinity of the calibration catchments (see Section 3.2.2). As soil moisture was low prior to these six events, runoff from agricultural land could be neglected. The resulting parameter values were a_3 = 0.0968 and b_3 = 0.0894. The third model version (Version 3) was identical to Version 2, but used a different soil classification (see Section 3.2.3.1).

For each of the three model versions more than 500 accepted parameter sets were determined. For each of these sets, a prediction of runoff was calculated for a given

catchment and time period and fed into the P sub-model to calculate a prediction of P export using the P sub-model (see Section 3.2.1.3).

3.2.1.3 The phosphorus model

The Phosphorus (P) sub-model was developed to predict DRP losses at catchment outlets and CSAs within catchments in combination with the Rainfall-Runoff sub-model (Lazzarotto, 2005). The model was developed for the Lippenrütibach catchment, a catchment on the Swiss Plateau, which was also used for calibration of the hydrological sub-model. Previous studies in the study region had shown that DRP concentrations in runoff were strongly correlated with runoff volume (Lazzarotto et al., 2005; Pacini and Gächter, 1999; Stamm et al., 1998), indicating that high rates of P losses were associated with fast runoff. To account for the elevated P concentrations of fast runoff as compared to slow runoff, fast flow is assumed to be composed of 'old' and 'new' water, while slow flow is assumed to consist of 'old' water only. While $q_{i,slow}(t)$ and $q_{i,fast}(t)$ are average values that apply to all cells within an HRU_i, the P sub-model distinguishes between grid cells within the respective HRU_i that actually contribute to fast flow in a given event and cells that do not, assuming that total fast flow is equally distributed among the cells that contribute. Thus, for cells that contribute fast flow $q_{i,fast}(t,x,y)$ is calculated by dividing $q_{i,fast}(t)$ by the areal fraction ($A_{i,fast}(t)/A_i$) of HRU_i that contributes to fast flow, while fast flow $q_{i,fast}(t,x,y)$ from cells that are not contributing is zero. The new water component, $q_{i,new}(t,x,y)$, is assumed to be a constant fraction η of the total fast flow from the contributing area:

$$q_{i,new}(t,x,y) = \eta q_{i,fast}(t)\frac{A_i}{A_{i,fast}}F(t,x,y) \quad (10)$$

where F(t,x,y) is 0 for cells not contributing to fast flow, and 1 for cells contributing to fast flow at time t, and x and y are the central coordinates of the respective cell. The fraction η was estimated from nitrate dilution data collected during runoff events and baseflow conditions as 0.25 ± 0.05 (Lazzarotto, 2005). The flow of old water is the sum of the remaining fast flow and the slow flow of the respective cell, i.e.:

$$q_{i,old}(t,x,y) = (1-\eta)q_{i,fast}(t)\frac{A_i}{A_{i,fast(t)}}F(t,x,y) + q_{i,slow}(t) \quad (11)$$

The DRP loss with old water flow is calculated for every grid cell as

$$L_{i,old}(t,x,y) = DRP_{baseflow}q_{i,old}(t,x,y)gridsize \quad (12)$$

assuming that the concentration of DRP in old water is the same as the DRP concentration of the baseflow, $DRP_{baseflow}$ (0.05 mg L^{-1}). DRP losses associated with new water flow include

incidental P losses from freshly applied manure (DRP_{IPL}) and P losses from soil (DRP_{soil}) enriched in P due to excessive manure applications in the past. DRP_{soil} concentrations were calculated for every pixel from water-soluble soil P (WSP) concentrations. The WSP – DRP relationship was taken from artificial rainfall experiments carried out in the catchment area of Lake Baldegg (Hahn et al., 2012). The WSP concentrations (and thus also the DRP_{soil} concentrations) were assumed to remain constant over the simulation period in the present study.

In contrast, $DRP_{IPL}(t,x,y)$ concentrations in runoff were considered to vary in time. Based on the studies of Braun et al. (1993) and von Albertini et al. (1993) $DRP_{IPL}(t,x,y)$ is assumed to decrease exponentially with increasing time lag $\Delta t_m = t_r - t_a$ between manure application t_a and onset of runoff t_r:

$$DRP_{IPL}(t,x,y) = DRP^0_{IPL}(t,x,y)\exp(-\Delta t_m h) \quad (13)$$

The time t of runoff onset is the time when the respective soil pixel starts to contribute to fast flow (Lazzarotto, 2005). The parameter h was assumed to be the same for well and poorly drained soils: 0.007 +/- 0.004. With each application of manure Δt_m is set to zero, and the $DRP_{IPL}(t,x,y)$ concentration is increased immediately to the new value of $DRP_{IPL}{}^0(t,x,y)$ resulting from the addition of the new DRP to the DRP_{IPL} remaining from the prior applications.

The total DRP load associated with new water is the sum of DRP_{soil} and DRP_{IPL} loss at each pixel:

$$L_{i,new}(t,x,y) = (DRP_{soil}(x,y) + DRP_{IPL}(t,x,y))q_{i,new(t,x,y)}gridsize \quad (14)$$

while the total DRP loss from a pixel at time t is the sum of $L_{i,old}(t,x,y) + L_{i,new}(t,x,y)$, and the total loss of DRP from the catchment is the sum of DRP loss from all soil pixels.

We used Gaussian Error Propagation to account for uncertainty in the model parameters η and h and in the WSP-DRP relationship. Thus, for each mc model run and time step we obtained an error estimate. These were combined with the 10% and 90% quantiles of the hydrological predictions to give the uncertainty of the DRP export predictions.

3.2.2 Study area

The study area was situated on the Swiss Plateau in the vicinity of Lucerne. It is characterized by undulating terrain, ranging between 500 and 800 m altitude above sea level and covered by glacial tills (Lazzarotto et al., 2006). The soils are generally loamy and of

low permeability (Bodenkarte Hochdorf, 1983). Average amounts of annual precipitation in the region range between 1000 and 1200 mm, depending primarily on altitude.

The four catchments used for model calibration (Lippenrütibach (LIP), Greuelbach (GRB), Rotbach (RTB), Meienbach (MEI)) drain into Lake Sempach (Lazzarotto, 2005), whereas the catchment (Stägbach catchment (Stäg)) used for model validation drains into Lake Baldegg (Fig. 3-1). Both lakes have serious eutrophication problems and are artificially aerated. The region is characterized by intensive animal husbandry (dairy and pig farms, 2.4 livestock units per ha (Herzog, 2005), which in the past has resulted in highly increased soil P stocks (Stamm et al., 1998).

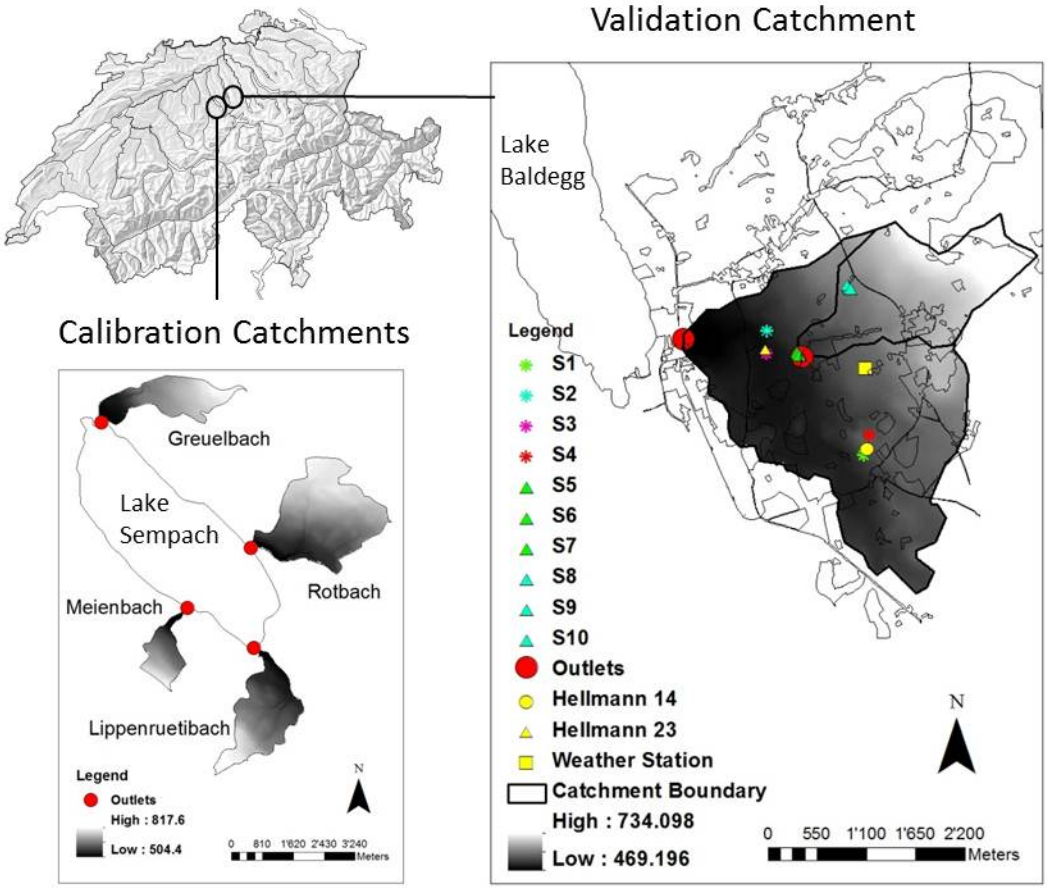

Figure 3-1: Locations of calibration and validation catchments and the installed measurement devices

In addition to the Stägbach catchment as a whole we also used a sub-catchment of the Stägbach catchment, denoted as Stäg2, for validation (Fig. 3-1). Table 3-2 shows that the percentages of urban area, forest, and agricultural area in the validation catchments were in the range of the calibration catchments. Agriculture is the dominating land use in all

catchments, whereas the area classified as urban covered less than 10%. The latter consisted of a few villages and some isolated farms. While the Stäg2 sub-catchment was comparable in size to the calibration catchments, the Stägbach catchment as a whole (8.24 km^2) was larger than all four calibration catchments. More information on the calibration catchments is given by (Lazzarotto et al., 2006). Small differences between the HRU percentiles given here and those by Lazzarotto et al. (2006) are due to the fact that the data had to be processed anew.

Table 3-2: Areal fraction of each hydrological response unit (HRU) on the total catchment area in [%] – No background color = model version, grey background = model Version 3

	Calibration Catchments								Validation Catchments			
	LIP	LIP	RTB	RTB	MEI	MEI	GRB	GRB	Staeg	Staeg	Staeg2	Staeg2
Urban[%]	8.1	8.1	9	8.7	2.5	2.5	8	7.6	9	9	6	6
Forest	16.7	16.7	16	16.4	7.7	7.7	16	16.3	8	8	9.5	9.5
Well	38.6	13.1	56	31.5	74	40.6	61	34.6	66	42	67.2	41.2
Poor	36.6	62.1	19	43.4	15.8	49.2	15	41.5	17	41	17.3	43.3
Area [km^2]	3.3		6.0		1.2		2.6		8.24		2.265	

3.2.3 Model validation

3.2.3.1 Model input data

Precipitation and evapotranspiration

From April till October in 2010 a weather station was installed in the center of the Stägbach catchment to obtain representative precipitation data for the Stägbach catchment. The station was equipped with a R102/R102H tipping bucket rain gauge. Data was recorded every 15 minutes. For two short time periods (28.05. – 08.06.2010 and 21.07. – 01.08.2010) no data was recorded at this weather station, due to technical problems. For these periods we used precipitation data from the nearest weather station (Hochdorf, data from uwe Canton Lucerne), which is located less than 2 km away from the Stägbach catchment. All other data gaps were filled with mean precipitation data from the three closest weather stations (Buchs, Lucerne, Cham, source: Swiss Federal Office of Meteorology and Climatology) surrounding the catchment. Two Hellmann rain gauges were installed in the catchment to check for spatial variability in rainfall.

For the global radiation data we used evapotranspiration data from the three weather stations Buchs, Lucerne and Cham (source: Swiss Federal Office of Meteorology and Climatology). These data are based on the Primault formula. They were available at daily

resolution, but using mean global radiation data from the same three MeteoSwiss stations, we derived estimates of hourly evapotranspiration.

Topographic index and HRU determination

The Topographic Index λ (Quinn, 1991) was determined on a 25-m resolution digital elevation model (DEM), which is available for whole Switzerland (source: Swiss Federal Office of Topography), using the open source GIS software Saga 2.0. The convergence coefficient was set to 1. Urban areas and forests were identified using aerial photographs (source: Swiss Federal Office of Topography). The data was processed and prepared for model input using ArcGIS (ArcGIS Desktop 10 Service Pack 2, ESRI) and the software package R (R Development Core Team, 2007).

Soil classification into drainage classes

The assignment of soils to the two classes of well and poorly drained soils was based on the local soil map (Bodenkarte Hochdorf, 1983). In model Version 1 and 2 we followed Lazzarotto et al. (2006), who classified Eutric and Dystric Cambisols and Eutric Regosols as well drained soils and Gleyic Cambisols and Eutric Gleysols as poorly drained soils. To investigate the sensitivity of the model to this classification, we compared Version 2 with Version3. In the latter we also assigned soils considered well drained by Lazzarotto et al. (2006) although showing signs of temporary water stagnation or water-logging according to the soil map to the poorly drained soils. Accordingly the areal fraction occupied by the poorly drained HRU was larger in Version 3 than in Version 1 and 2 (Table 3-2).

Soil P status and manure application

A map of the spatial distribution of soil P concentrations was constructed from data of soil P analyses farmers have to provide to local authorities every 5 years. With the help of the farmers the available data on soil P status were assigned to individual fields. Some farmers did not cooperate. In these cases we used P data obtained from the environmental protection agency of the Canton Lucerne and attributed area weighted mean P values to the respective management units.

Some farmers also provided detailed data on the amounts, locations and times of manure application on their farms. For the other farms, that covered more than 80% of the area, the manure P pool was neglected. In contrast, manure application data was complete for the Lippenrütibach catchment, one of the calibration catchments, in the year 1999.

3.2.3.2 Model validation

Discharge measurements

At the outlet of the Stägbach catchment a 6712 Full-size Portable Sampler (ISCO, USA) was used to determine discharge and collect water samples. In addition, the water level was recorded every minute by means of a Bubbler Flow Module. Further flow and water level measurements (dilution method) were taken by a consulting company ('Büro für Wasser und Umwelt' BWU) working for the cantonal environmental protection agency. They provided us also with the level-discharge data necessary to calculate the discharge from the level data.

The discharge at the outlet of Stäg2 was estimated from the discharge at the outlet of the entire catchment using a relationship that was determined on the basis of eight manual measurements of flow velocity profiles and water levels at the outlet of Stäg2 between the beginning of June and the end of July 2010, using a current meter (MiniAir2) and a measuring rod. From these measurements we calculated the discharge across the entire flow profile for each of these eight occasions and related it to the discharge from the entire catchment. The discharge estimates for Stäg2 based on this relationship were validated by measurements with a 6712 Full-size Portable Sampler equipped with a 750 Area Velocity Module (ISCO, USA) installed at the outlet of sub-catchment Stäg2. Unfortunately, no continuous automatic measurements were available because the instruments were dislocated during the extreme rain event in June 2010 and partly damaged. Discharge estimations based on the Stäg catchment were very similar to discharge values deduced from the relationship between the manual discharge measurements and the automatic flow velocity data. Only during the high runoff event end of July and afterwards, the two graphs differed. This period was therefore not taken into account for model assessment.

Water samples

Using the before-mentioned 6712 Full-size Portable Sampler, flow-proportional water samples were collected automatically at the outlet of the Stägbach catchment and the Stäg2 sub-catchment. A pre-defined water level (Stäg) or flow velocity (Stäg2 sub-catchment) threshold was set, and when it was reached, samples were taken automatically every 15 minutes. Four subsequent samples were collected in the same bottle, resulting in one composite sample every hour, as long as the water level (or the velocity, respectively) was above the threshold. After a runoff event, samples were collected and stored at 4 °C till analysis. In addition, we took grab samples each time we went into the field, at least once a week. Dissolved reactive phosphorus (DRP) was analyzed by means of the molybdate colorimetry method (Vogler, 1965) after filtration (<450 nm) of sample solution. In order to

determine total phosphorus (TP), unfiltered samples were digested in potassium persulfate before they were analyzed for P using the molybdate colorimetry method. Electrical conductivity (EC) was measured using a Metrohm Conductometer 712.

Soil moisture measurements

On four grassland sites (Table 3-3) soil water content was monitored at 10 and 30 cm depth using six horizontally inserted 2-rod TDR probes at each depth. The signal was recorded by means of a TDR100 and stored by a data logger (CR10X Campbell Scientific, Inc.). The volumetric soil water content (m^3 m^{-3}) was calculated using the equation given by Topp et al. (1980). Volumetric soil samples were taken at each of the four soil water monitoring locations using steel cylinders to determine soil bulk density and porosity.

Table 3-3: Site characteristics of the four permanent measurement stations in the Stägbach catchment

	S1		S2		S3		S4	
HRU	well drained		well drained		poorly drained		well drained	
topographic index	7.16		10.65		11.13		7.27	
soil map	vertically permeable soil		vertically permeable soil		ground-/slope water dominated soil		vertically permeable soil, partly ground- or slope water influenced	
soil	calcaric Cambisol		eutric Cambisol		eutric Cambisol		eutric Cambisol	
texture (FAO)	loam		sandy clay loam		loam		loam	
soil depth	10 cm	30 cm	10 cm	30 cm	10 cm	30 cm	10 cm	30 cm
Clay [%]	20.94 +/- 0.66	22.14 +/- 1.03	25.63 +/- 1.26	26.52 +/- 2.11	25.25 +/- 0.13	19.62 +/-0.35	17.80 +/- 1.39	18.99 +/- 2.27
Silt [%]	32.99 +/- 1.24	38.98 +/- 0.91	36.27 +/-3.41	39.78 +/- 0.09	46.39 +/- 0.82	44.03 +/- 0.56	32.40 +/ 0.47	35.03 +/- 0.2
Sand [%]	46.07 +/- 0.58	38.88 +/-0.12	38.10 +/ 3.75	33.71 +/- 2.02	28.36 +/- 0.95	36.34 +/- 0.21	49.80 +/- 0.92	45.97 +/- 2.07
pH	7.02	7.16	6.05	6.26	5.32	5.45	5.89	6.59
pore volume [%]	52	47	54	49	41	41	53	44

Piezometer and overland flow detectors

Furthermore, we installed a piezometer equipped with a light plummet and an overland-flow-detector (OFD; see (Doppler et al., 2012)) at each soil water monitoring station and 6 other locations. Readings of these instruments were taken approximately once a week normally and more often after rainfall events.

3.3 Results

3.3.1 Model performance at the catchment outlet

3.3.1.1 The Rainfall-Runoff model

Model calibration with data from the year 2000

Without separate calibration of the urban parameters (Version 1) the model performed poorly. Out of seven million Monte-Carlo (MC) simulations, no parameter set achieved a NSC value > 0.5; 661 parameter sets yielded a NSC > 0.4. Separate calibration of the urban parameters (Version 2) improved the model results substantially and resulted in 724 accepted parameter sets from 5 million MC runs when the threshold value was set to 0.6, with 25%, 50%, and 75% quantiles of 0.61, 0.61 and 0.63, respectively. Changing the classification of the soils (Version 3) decreased the performance for the calibration period, so that the NSC threshold had to be reduced to 0.5 to obtain 606 accepted parameter sets, with 25%, 50% and 75% NSC quantiles of 0.51, 0.52 and 0.53 respectively.

Comparison of predictions for the Lippenrütibach catchment

Before we applied the calibrated model to the Stägbach catchment, we compared hydrological predictions for the Lippenrütibach catchment (LIP), one of the calibration catchments, for the year 1999. The same data had been used for validation by Lazzarotto et al. (2006). Figure 3-2A shows a fair agreement between simulations (Version 2) and measurements. Predictions were again better for the model version with separate calibration of the urban HRU parameters a_3 and b_3 (Version 2) than for the corrected original version of the model (Version 1) (Table 3-4). This improvement was in particular due to better prediction of small peaks, which were overestimated by the original model (Lazzarotto et al., 2006). However, two other problems, which had already been identified by Lazzarotto et al. (2006), remained unsolved: (1) Some high runoff peaks were still underestimated, and (2) baseflow declined too fast after long periods with no rainfall (Fig. 3-2B).

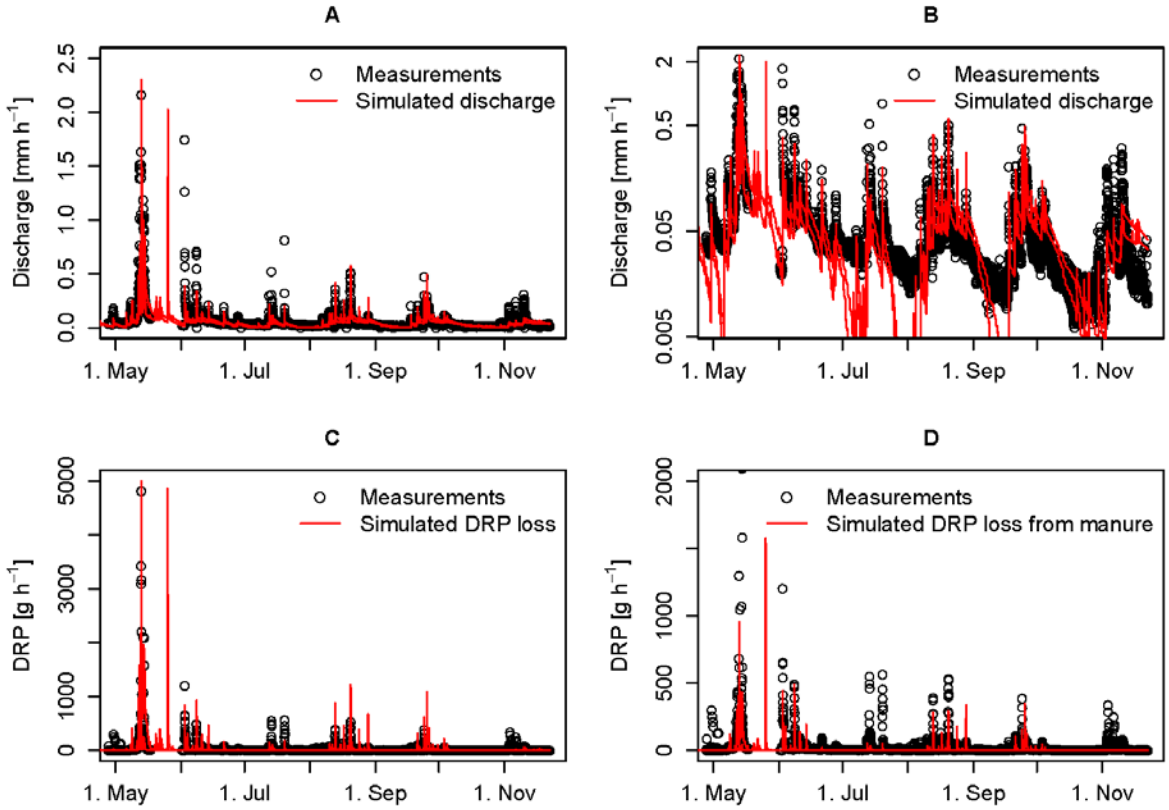

Figure 3-2: Simulations (lines) using RRP Version 2 versus measured (points) discharge and DRP loss from the Lippenrütibach catchment in 1999. The y-axis in figures on the right are in logarithmic scale (B) or focus on a certain part of the value range (D).

Table 3-4: Performance of different model versions in three catchments (Lippenrütibach catchment LIP, Stägbach catchment Stäg, Stägbach sub-catchment Stäg2), measured with the Nash-Sutcliffe-Criteria (NSC) (Nash and Sutcliffe, 1970)

Model version	Lip			Stäg			Stäg2			Calibration
	NSC quantiles									
	25%	50%	75%	25%	50%	75%	25%	50%	75%	$NSC_{threshold}$
Version 1	0.42	0.44	0.46	0.50	0.61	0.70	0.65	0.71	0.78	0.4
Version 2	0.48	0.50	0.52	0.53	0.62	0.71	0.66	0.72	0.80	0.6
Version 3	0.44	0.46	0.48	0.62	0.68	0.75	0.68	0.74	0.80	0.5

Version 1 – corrected original model
Version 2 – separate urban parameter calibration
Version 3 – separate urban parameter calibration + different soil classification

Model validation - Stägbach 2010

To test how well the model performs when applied outside the watersheds used for calibration, we applied the calibrated Version 2 model to the Stägbach catchment for a forward prediction of discharge during the year 2010 and compared predictions with measurements. Figures 3-3 and 3-4 show that the model performed well for the entire catchment as well as for the Stäg2 sub-catchment. The median NSC values were 0.62 and 0.72, respectively (Table 3-4).

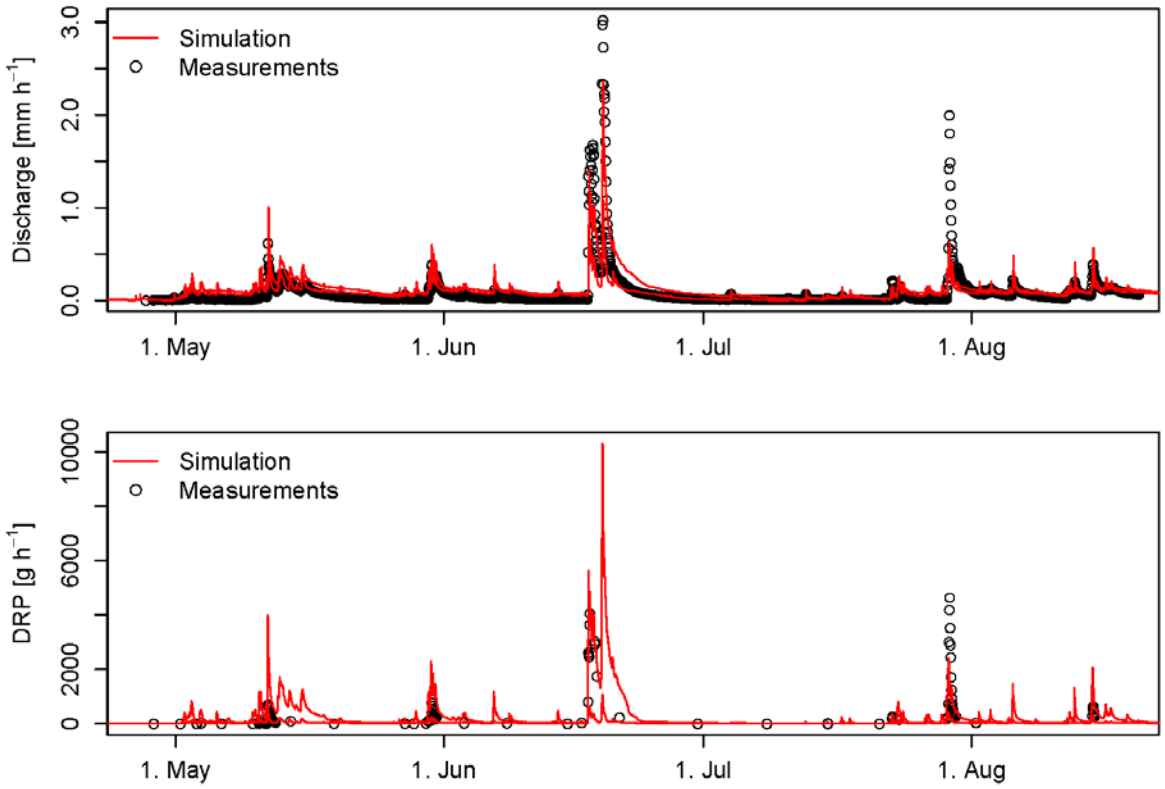

Figure 3-3: Simulations (lines) using RRP Version 2 versus measured (points) discharge and DRP loss from the Stägbach catchment in 2010.

With the global parameter c_{well} ranging mainly between 0.7 and 0.92 (25% and 75% quantiles), and c_{poor} ranging between 0.33 and 0.61, more baseflow was predicted to come from the well-drained than from the poorly drained HRU. Thus, the relatively high amount of well drained soils within the validation catchments as compared with the calibration catchments (Table 3-2), led to a baseflow overestimation in both validation catchments. Due to the general overestimation of baseflow, accelerated baseflow decline as observed for the Lippenrütibach catchment in 1999, was only observed during the very dry period in summer.

The underestimation of discharge during the large event end of July (h=5000) was probably due to the fact that no rain data was available from the Stägbach weather station for this event, while spatial variability of rainfall was very high in the study area, as indicated by the Hellmann rain gauges. One Hellmann rain gauge collected 126 mm rain while the other one only collected 88 mm within the same time frame.

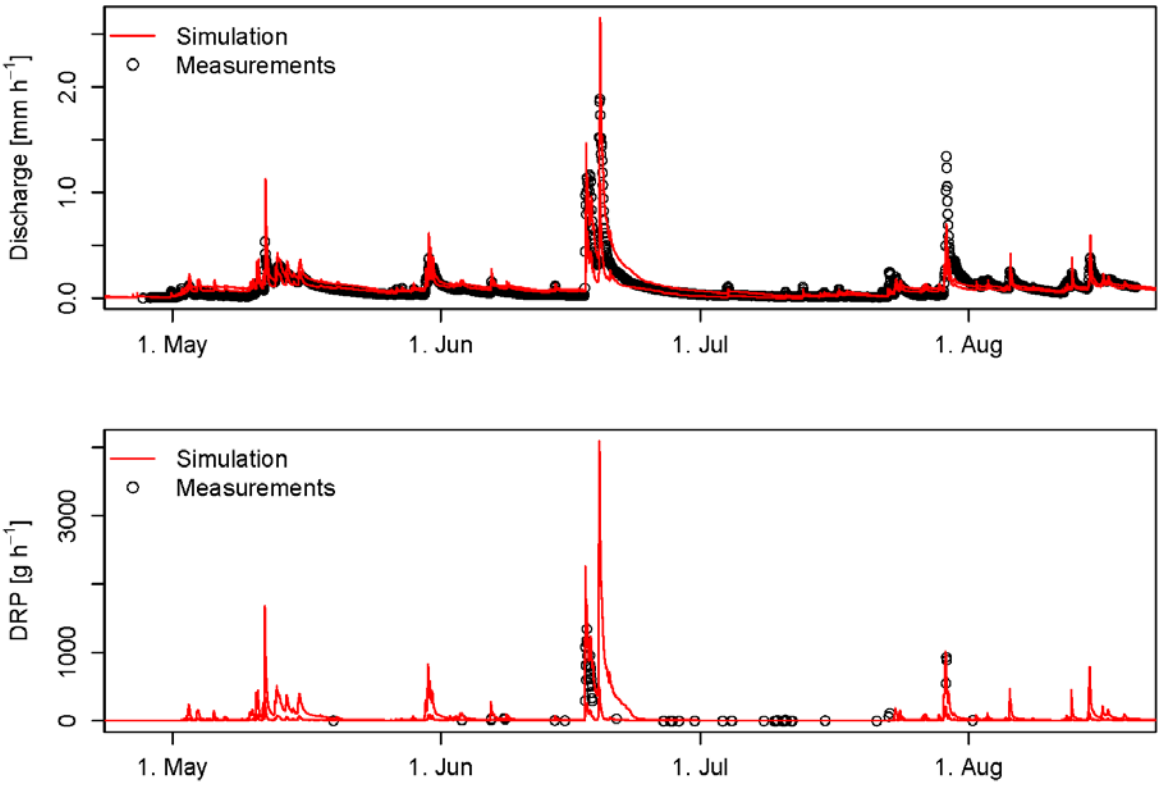

Figure 3-4: Simulations (lines) using RRP Version 2 versus measured (points) discharge and DRP loss from the Stägbach sub-catchment Stäg2 in 2010.

Influence of soil classification – model Version 3

As in the calibration, Version 3 did not perform as well as Version 2 also in the validation for the Lippenrütibach catchment (Table 3-4), as runoff peaks were slightly lower in simulations with Version 3 than with Version 2. The higher value of c_{poor} and the higher areal percentage of HRU_{poor} (62.1%) resulted in higher slow flow from poorly drained soils, which led to lower soil moisture and thus to lower peak flows. In contrast, the change in soil classification from Version 2 to Version 3 improved model predictions for the entire Stägbach catchment and the Stäg2 sub-catchment (Table 3-4). The improvement was due to better simulations of baseflow and of the large runoff event in June. This can be attributed to

the lower value of c_{well} (25% and 75% quantiles: 0.31, 0.75) and the lower areal fraction of well drained soils in Version 3 (Table 3-2), resulting in higher soil moisture and consequently also in higher peak flows. The larger area of poorly drained soils also led to steeper decline of the hydrographs (Fig. 3-5), due to a larger contribution of the poorly drained HRU to fast flow.

Apart from these rather small differences, both versions of the model simulated the discharge dynamics of the study catchments quite well.

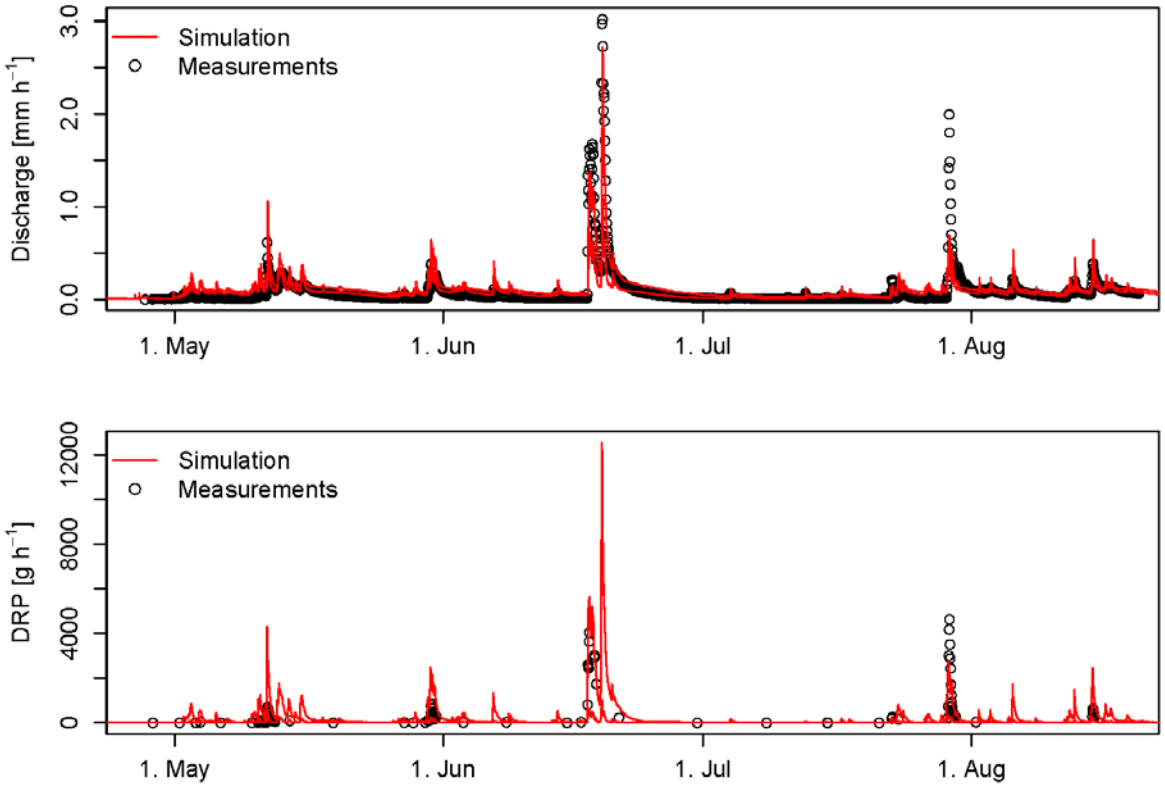

Figure 3-5: Simulations (lines) using RRP Version 3 versus measured (points) discharge and DRP loss from the Stägbach catchment in 2010.

3.3.1.2 The phosphorus model

The simulated DRP losses for the Lippenrütibach catchment in the year 1999 and the Stägbach catchments in the year 2010 are in fair agreement with the measurements (Fig. 3-2C, 3-3, 3-4). There was little difference between Version 2 and 3 of the model. The predictions of DRP loads mainly depended on runoff prediction. For example, DRP losses from the Lippenrütibach catchment were underpredicted for the events at the beginning of June, in July and November 1999, for which runoff was underestimated as well. On the other

hand discharge and DRP load were well predicted for the large events in May 1999 (Lippenrütibach) and in June 2010 (Stägbach). Unfortunately, in the Stägbach catchments no samples were collected during the second peak of the extreme event because the sampling device was either clogged (Stäg) or dislocated (Stäg2).

The simulated loss of DRP from the Lippenrütibach catchment that was attributable to recently applied manure (Fig. 3-2D) was about 1/5 of the total DRP loss (Fig. 3-2C) during the large event in May, and less than half of the total simulated DRP load in most of the other events. Thus, most DRP lost with runoff came from the soils according to the model. In the Stägbach catchments, a good fit between simulations and measurements was obtained despite the limited availability of manure application data, suggesting again that soil P was the main source for the DRP losses with runoff.

3.3.2 Spatial model performance

3.3.2.1 Hydrological risk areas

For each time step, we constructed maps showing for each pixel the fraction of accepted parameter sets (out of a total of 724 accepted sets for Version 2 and 606 accepted sets for Version 3) that resulted in fast flow in that pixel at the respective time. These maps give a picture of the uncertainty in the prediction of fast flow at the specific time across the catchment for the respective model version. For simplicity, we refer to the fraction of accepted parameter sets predicting fast flow as ‘risks’ of fast flow. This measure reflects how sensitive the fast flow prediction is towards changes of the parameter sets. We introduce four classes and denote values ranging between 0 and 0.2 a low risk, values between 0.2 and 0.5 a medium risk, values between 0.5 – 0.8 a high risk, and values between 0.8 and 1 a very high risk of fast flow.

The spatial extent of risk areas changes with time. For the small runoff event of May 14, 2010, 7% of the agricultural area in the Stägbach catchment was classified as very high risk area, whereas for the large event in June (19.06.2010) 16% (Version 2) or even 21% (Version 3) of the agricultural area were very high risk area. Also the percentage of high and medium risk areas within the catchment increased during this event (Table 3-5). On the other hand, large fractions of the catchment were considered at low risk during the small event by both model versions (76 and 48%, respectively). However, during the June event, model version 3 predicted a low risk for only 13% of the catchment, while this percentage was higher (44%) for model version 2. Hence, based on the model results one cannot exclude the risk for DRP losses from a considerable fraction of the area.

Table 3-5: Spatial extent of risk classes in the Stägbach catchment for different model versions and two runoff events in 2010 – relative to the total agricultural area in %

Risk classes	Low	Medium	High	Very high
Risk values	0-0.2	0.2-0.5	0.5-0.8	0.8-1
Version 2				
small event in May	76	12	5	7
large event in June	44	23	17	16
Version 3				
small event in May	48	41	4	7
large event in June	13	50	16	21

The spatial patterns of predicted fast flow risk areas were very similar for model versions 2 and 3 (Table 3-5, Fig. 3-6).

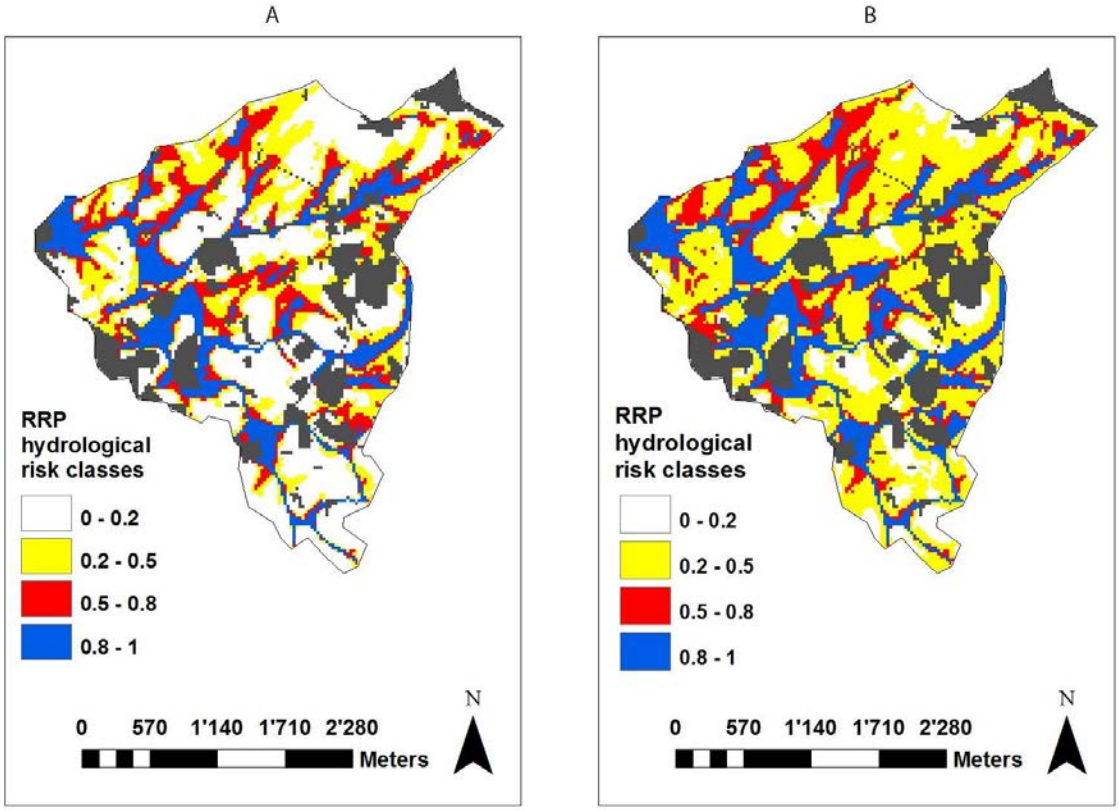

Figure 3-6: Risk maps for the extreme event of June 2010 in the Stägbach catchment, obtained with model versions 2 (left) and 3 (right). Grey shading denotes forested and urban areas

The major difference was that the medium risk was more prevalent and the low risk class less frequent in Version 3 than in Version 2. This can be attributed to the lower overall runoff in Version 3 simulations, which led to higher soil moisture predictions and thus lower topographical threshold values.

3.3.2.2. Spatial predictions of DRP losses from soil

In the RRP model, the risk of P loss depends on the combination of runoff risk and the presence of DRP at a given location. While manure is a DRP source that decreases rapidly after application and can be managed, soil DRP has much slower dynamics and is always present as a source (Kleinman et al., 2011a). Areas with high simulated DRP loads were mainly distributed along the stream network, or in flat areas with high soil P concentrations a bit further away from the stream (Fig. 3-7). There was little difference between the two model versions regarding the area that is expected to contribute the most. The extent of the hatched area in Figure 3-7 however was larger for Version 3 than for Version 2. The hatched area illustrates where less than 80% of the simulations resulted in the same distribution of fast flow generation and thus indicates where model predictions were fairly uncertain. Accounting for all model predictions we calculated the average DRP load for each pixel. For 90% of the agricultural area in the Stägbach catchment, the average DRP load calculated over the whole simulation period was below 14.9 mg h^{-1} $pixel^{-1}$ for Version 2 and below 13.7 mg h^{-1} $pixel^{-1}$ for Version 3. The remaining 10% of the agricultural area delivered more than half of the total load exported from agricultural land (Version 2: 52%, Version 3: 54%). Neglecting winter months, the estimated yearly DRP loads from these 10% of the agricultural area averaged 3.4 kg ha^{-1} (Version 2) and 3.1 kg ha^{-1} (Version 3).

During the large runoff event in June 2010, much higher loads per hour were simulated. Again, 10 % of the agricultural area delivered more than 50% of the DRP load from the total agricultural area. The estimated load per hectare for these 10% of the area averaged 24 g ha^{-1} h^{-1} (Version 2) and 29 g ha^{-1} h^{-1} (Version 3) during this event.

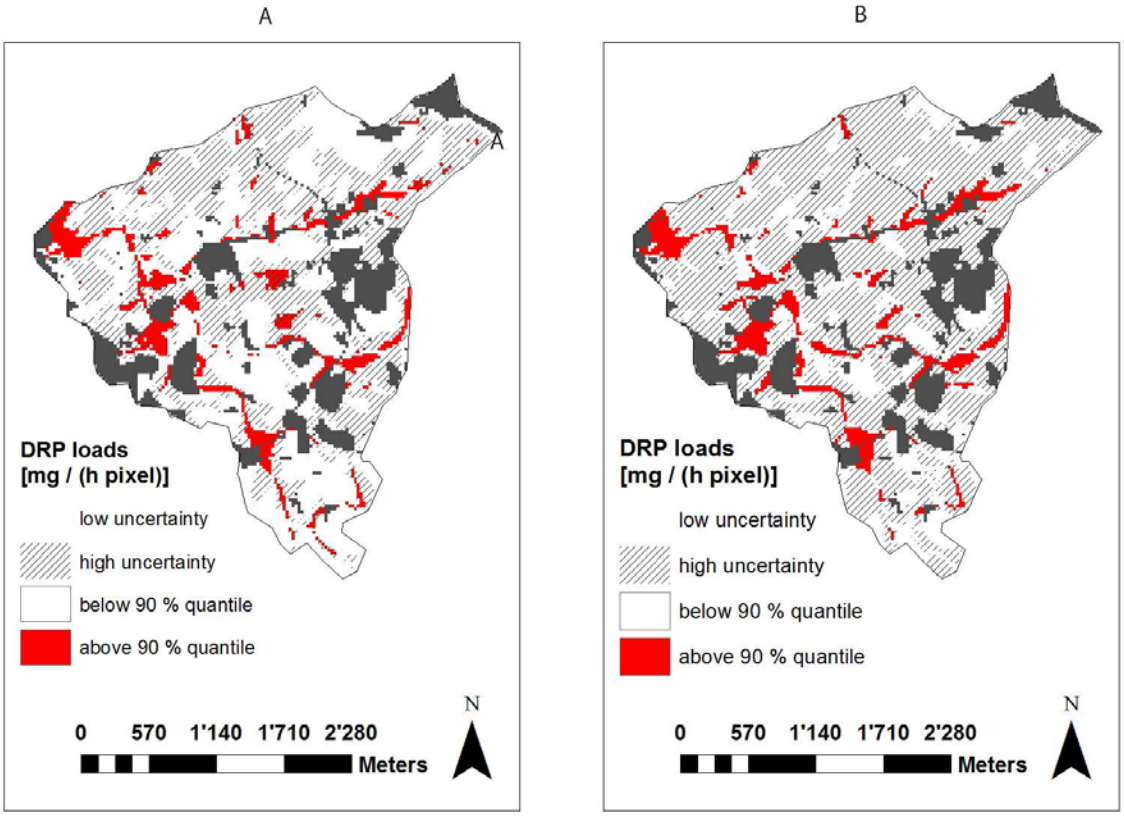

Figure 3-7: Simulated distribution of DRP loads in the Stägbach catchment during the large event in June 2010 obtained by averaging over all Monte-Carlo simulations. Red colour shows the area (10% of the total agricultural area) where according to the simulations more than 50% of the total DRP loss occurred. Areas for which less than 80% of the simulations resulted in the same distribution of fast flow generation are hatched. Grey shading denotes forested and urban areas.

3.3.3 Spatial model performance and field measurements

3.3.3.1 Test of model assumptions

The data from the 4 permanent measurement stations shown in Figure 3-8 supported the assumptions underlying the model that (1) soil water saturation increases with topographic index λ, and that (2) well-drained soils are drier than poorly drained soils. The location of Station S3, which was situated in the poorly drained HRU of the Stägbach catchment, had the highest λ (11.13) and showed the highest water saturation over the whole measurement period. In contrast, the location of Station S1, which was situated in the well-drained HRU, had the lowest λ value (7.16) and always showed the lowest soil water saturation. Station S2, which was also situated in the well-drained HRU but at a location with a higher λ value (10.65) than S1, showed a soil water saturation between that of S1 and S3 and similar to that

of Station 4. The latter also had a similar topographic index (λ = 7.27) as Station 2, while it had an intermediate position with respect to the classification by drainage classes. Station 4 was situated in the poorly drained HRU according to the soil classification used in Version 3 of the model but in the well-drained HRU according to the classification used in Version 2. Thus, the results suggest that soil moisture was more closely related to topographic index than to soil drainage category.

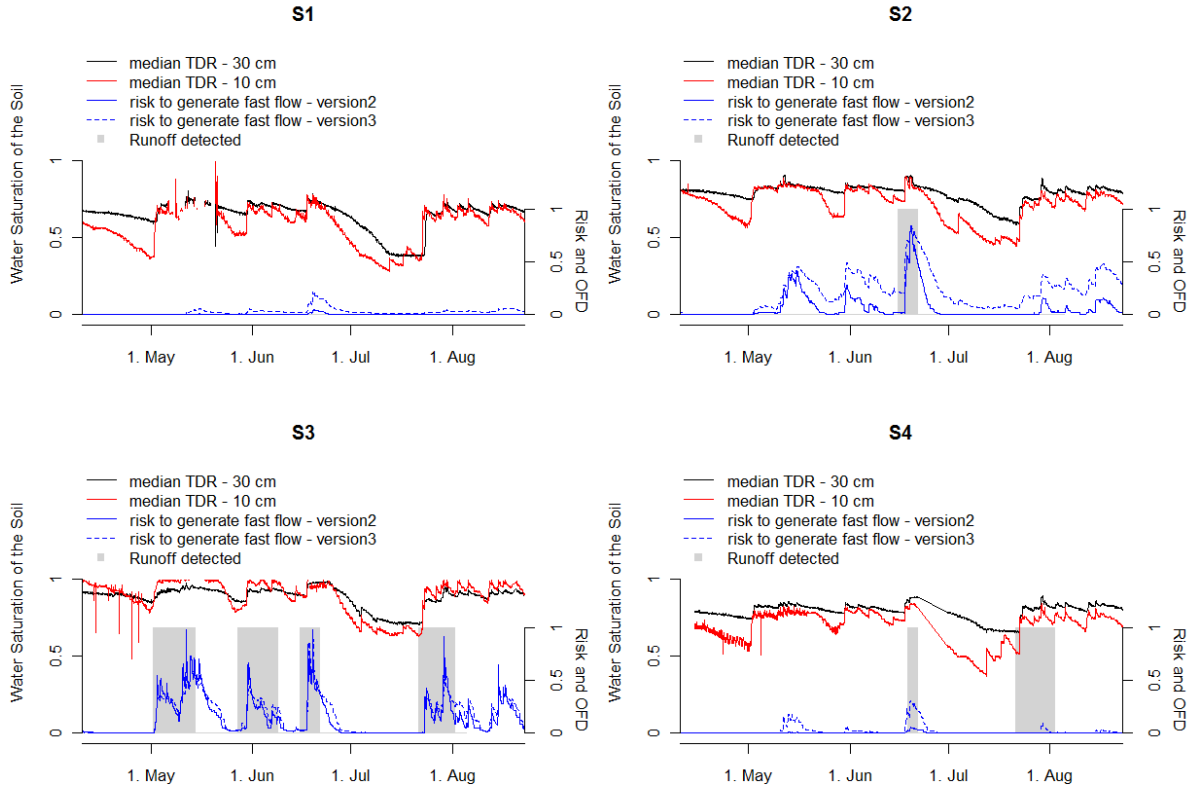

Figure 3-8: Comparison of soil moisture measurements, runoff measurements (with Overland-Flow-Detectors OFD) and model predictions of fast flow risks at the four permanent soil moisture measurement stations in the Stägbach catchment for the year 2010.

3.3.3.2 Model predictions and soil moisture measurements

Figure 3-8 furthermore shows that the predicted risk of fast flow was closely related to measured soil water saturation, confirming the validity of the hydrological simulations presented before. At the two stations with high λ values (S2, S3) the predicted risk of fast flow strongly increased when soil moisture approached full saturation, while there was generally a very low risk of fast flow with comparatively little response to variations in soil

moisture at the two stations with low λ values (S1, S4). Version 3 consistently predicted higher risks of fast flow than Version 2, in line with the results presented in Section 3.3.2.1.

3.3.3.3 Model predictions and OFD measurements

The model predictions of fast flow risks were also in reasonable agreement with runoff data recorded by the OFD (Fig. 3-8). Surface runoff occurred at sites S2 and S3 when both model versions predicted a risk of fast flow above 0.75. No runoff was collected when the predicted risk was below 0.5. On the other hand, runoff was never observed at station S1, for which the predicted risk values were always below 0.05 for model Version 2 and 0.225 for model Version 3. Some over-prediction of runoff risks may be due to the fact that OFDs only collect surface runoff, whereas predicted fast flow also includes preferential flow in the RFP model. This may in particular have been the case at station S7, which was one of the 6 other measurement stations that were not permanently operated. For this location both model versions often predicted high fast flow risks, sometimes even in all simulations, but runoff was collected only once with the installed OFD. This station was located close to a brook where a large amount of the simulated runoff may actually have been due to subsurface flow.

In contrast to stations S1, S2, S3 and S7, the risk of runoff from station S4 was underestimated. Surface runoff was collected at S4 during the extreme event in June, while model Version 2 predicted fast flow only in 6% of the simulations. Similarly, no elevated risk was predicted for the event at the end of July, when 10 ml of runoff were collected (Fig. 3-8). Using model Version 3 substantially higher risks of fast flow were predicted for S4 than by Version 2, but even for the extreme event in June the predicted risk still did not exceed a value of 0.3. Similar under-predictions of runoff risks were also obtained for one event at sites S5, S8 and S10, where runoff was collected by the OFD, while the predicted risks remained below 0.1 for model Version 2 and below 0.3 for model Version 3. At two of the three locations infiltration excess runoff or runoff from a street further up-slope may have had some influence.

3.3.3.4 Model predictions and groundwater measurements

While OFD-recorded runoff data only showed a rather loose relationship to the prediction of fast flow events, there were close relationships between groundwater levels recorded by the piezometers and the fraction of accepted parameter sets that resulted in the prediction of fast flow (Fig. 3-9). Even changes in groundwater table at relatively low levels were associated with changes in risk predictions, in particular with model Version 3.

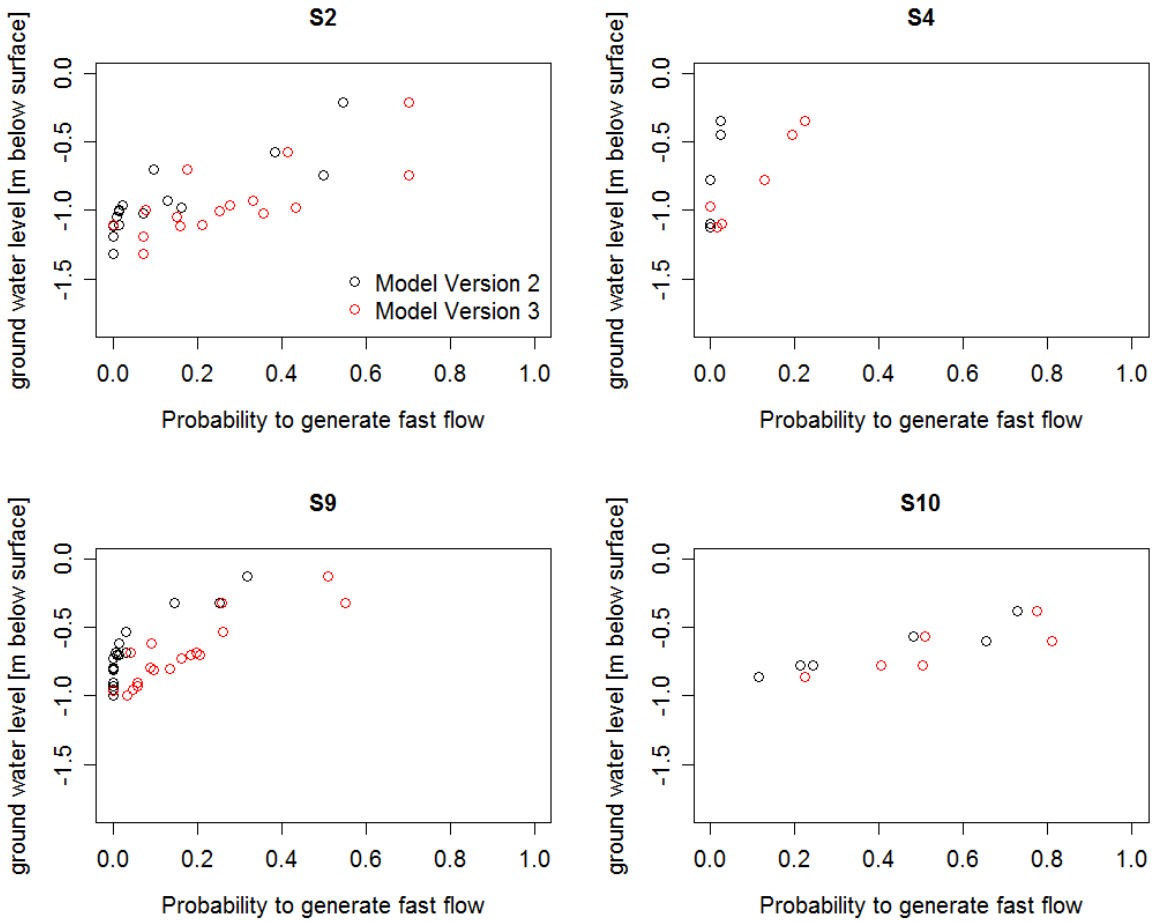

Figure 3-9: Comparison of model predictions with ground water level measurements at 10 locations within the Stägbach catchment for the year 2010

3.4 Discussion

Despite the low amount of input data required, the predictions of the RRP model were in good agreement with the measurements, especially after separate calibration of the HRU parameters. The latter improved the prediction of small runoff peaks, which were overestimated by the original model (Lazzarotto et al., 2006). The fact that the model adequately predicted discharge and DRP export at the outlet of a catchment and sub-catchment that had not been used for calibration is evidence for the validity of the underlying concept and assumptions. The comparison of hydrological model predictions with measurements of soil moisture, surface runoff and groundwater levels at various locations within the Stägbach catchment provides further support to this conclusion. Of course, model

application is always limited to situations that fulfill the assumptions on which a model is based (Radcliffe et al., 2009; Schoumans et al., 2009).

One of the inherent assumptions of the RRP model is that soil can be represented as a single compartment (Lazzarotto et al., 2006). This simplification leads to an accelerated baseflow decline during dry conditions. This may limit the usefulness of the model for areas dominated by highly permeable soils and for long dry periods. Limited performance during dry periods may furthermore be explained with the role of the topographic index λ in the model. Western et al. (1999) found that the spatial organization of soil moisture could be well described by topography during wet periods, when surface and subsurface lateral redistribution of water occurs. During dry periods they observed little spatial organization of soil moisture. Thus, triggering fast flow by a threshold based on the topographic index is assumed to perform better for wet than for dry soil conditions. Furthermore, the λ does not account for differences in soil moisture caused by aspect (Kopecky and Cizkova, 2010). This might partially explains the limited differentiation between S1 and S4. Another drawback of the RRP model is that it disregards connectivity. Although the measurements showed that the model did not identify all locations of high fast flow risk, we do not consider the soil representation and disregard of connectivity a major problem for the target region because in the hilly areas of the Swiss Plateau, soils are generally of low permeability and often directly connected to streams or lakes through artificial subsurface drains. Since baseflow simulations are less important for DRP losses than high flow conditions, the use of λ is justifiable. It however restricts fast flow generation, including infiltration excess runoff (IER), to potentially wet areas and therefore may underestimates the extent of IER generating areas.

Due to the crucial role of hydrology for P losses, which was also pointed out by (Kleinman et al., 2011a), the accuracy of predictions of DRP loads at the catchment outlets mainly depended on the quality of the hydrological simulations, an observation also made by Hively et al. (2006). The good agreement between predictions and measurements obtained when discharge was described well indicates that the model adequately captured all relevant processes in our catchments. Thus, there was no need to incorporate further processes, such as those proposed by Vadas et al. (2011). They suggested relating DRP concentrations to the runoff-to-rain ratio. According to them, a higher runoff to rain ratio leads to higher DRP concentrations in runoff from manured soils. Based on data from 9 studies, Vadas et al. (2011) showed that a high runoff-to-rain ratio often means that runoff starts in an earlier phase of an event than in events with a low ratio. This was considered important because concentrations of P released from manure decrease with time during an event (Sharpley and

Moyer, 2000). While the RRP model worked well in our study without such a refinement, it would be easy to incorporate this relationship if deemed appropriate for other applications.

According to our simulations, most DRP lost with runoff originated from P-enriched soils. Using a fully distributed model Hively et al. (2006) came to a similar conclusion for a rural watershed in the New York State. These findings support the conclusions of Kleinman et al., (2011a) who announced that legacy P remains to represent a high and permanent risk of P export into waters that needs to be reduced. Also manure application can lead to substantial P loads in runoff (Shigaki et al., 2007; Withers et al., 2003).

Unfortunately, the capability of models to determine the sources of P in catchment discharge has still not been tested by direct measurements. This lack of validation also includes the capability of models to allocate the spatial origin of P losses from a catchment (White et al., 2009). Till now validation is mainly based on the comparison of P concentrations in different stream segments (Gburek and Sharpley, (1998). Further development of isotopic methods such as that of Tamburini et al. (2010) is needed to determine the sources of P (manure, legacy P) found in runoff. While tracers have been used to determine source areas of eroded sediments (Stevens and Quinton, 2008) and pesticides (Doppler et al., 2012; Leu et al., 2004), the identification of source areas for P losses remains challenging.

Our model predictions were quite robust with respect to the two schemes of binary soil classification by drainage capacity compared in our study. This did not only apply to discharge predictions but also to the delineation of CSAs within the catchment, which makes the model valuable for the identification of CSAs within catchments. Our findings suggest that soil drainage capacity was less important for soil moisture status and thus also for the risk of fast flow generation in our study area than topography.

In accordance with the ‘variable source area’ concept (Ward, 1984) and observations of Gburek and Sharpley (1998), the RRP model predicted an increase in runoff generating areas with increasing soil moisture. If enriched with P sources that can be easily mobilized, these hydrologically active areas can be a severe threat for water quality (Gburek and Sharpley, 1998). In the Stägbach catchment, areas with high simulated DRP loads, averaged over the monitoring period, were mainly situated along the stream network. According to our simulations, the 10% of the area contributing the most delivered more than 50% of the total DRP export from the Stägbach catchment. Pionke et al. (2000) and White et al. (2009) obtained similar results. Pionke et al., (2000) calculated that the majority of the DRP exported from the Brown catchment into the Chesapeake Bay derived from 11% of the catchment area, while simulations of P export from 6 catchments in Oklahoma by White et

al. (2009) predicted that on average 5% of the area yielded 34% of the exported P loads. However, the model results and their uncertainty demonstrate also that one cannot exclude the possibility that large fractions (40 - 50%) of the catchment may contribute (see Fig. 3-7).

Our findings provide further support to suggestions of previous authors that management strategies to reduce P transfer from agricultural areas into surface water bodies should focus on the prevention and reduction of P accumulation in soils close to streams and in particular restrict fertilizer and manure applications in these areas.

3.5 Conclusion

Our results demonstrate that the RRP model is able to make useful predictions of discharge and DRP losses from grassland dominated catchments. The validity of the underlying concept is further supported by the agreement between spatial predictions of runoff generation risks with ground measurements of soil moisture, surface runoff and groundwater levels. The predictions were sufficiently robust with respect to the binary classification of soil drainage capacity to allow the use of conventional soil maps to assign the soils of the simulated catchment to these classes. The hydrological predictions were in line with the CSA concept and highlight the dominant role of topography. While the model suggests that the 10% of the catchment area contributing the most delivered more than 50% of the total DRP load the result also reveal a considerable risk that larger fractions of the catchments contribute as well. For practical applications this means that targeting the 10% of high risk areas will most probably reduce DRP losses, however more areal options may be needed to reduce them to a sufficient degree. According to the model, the actual measures should focus on legacy P as it was the dominant source for DRP losses. These findings confirm conclusions of previous authors that P enrichment in soils of hydrological active areas presents a high risk for water quality and needs to be reduced. The parsimonious RRP model is a suitable tool to delineate risk areas and guide the implementation of mitigation measures.

3.6 Acknowledgements

Without the help of many people the field work would not have been possible. We are thankful to people from the Soil Protection Group (ETH) and from the Water Protection and Nutrient and Pollutant Flows Group (ART), Tobias Doppler, Hans Wunderli and Marlies

Sommer. We also thank the local farmers for their cooperation. This study was carried out within the framework of the COST Action 869. The Swiss State Secretariat for Education and Research SER financially supported the project.

3.7 References

Arnold, J.G., Srinivasan, R., Muttiah, R.S., Williams, J.R., 1998. Large area hydrologic modeling and assessment - Part 1: Model development. J. Am. Water Resour. Assoc. 34, 73-89.

Beasley, D.B., Huggins, L.F., Monke, E.J., 1980. ANSWERS - a model for watershed planning. T. Asae 23, 938-944.

Beven, K.J., Kirkby, M.J., 1979. A physically based, variable contributing area model of basin hydrology. Hydrol. Sci. Bull. 24.

Bodenkarte Hochdorf 1983. Landeskarte der Schweiz 1:25000, Blatt 1130 (In German.) Zürich-Reckenholz: Eidg. Forschungsanstalt für landw. Pflanzenbau

Braun, M., Hurni, P., Von Albertini, N., 1993. Abschwemmung von Phosphor auf Grasland an zwei verschiedenen Standorten im Einzugsgebiet des Sempacher Sees. (In German.) Landwirtschaft Schweiz 6, 615-620.

Buda, A.R., Kleinman, P.J.A., Srinivasan, M.S., Bryant, R.B., Feyereisen, G.W., 2009. Effects of hydrology and field management on phosphorus transport in surface runoff. J. Environ. Qual. 38, 2273-2284.

Carpenter, S.R., Caraco, N.F., Correll, D.L., Howarth, R.W., Sharpley, A.N., Smith, V.H., 1998. Nonpoint pollution of surface waters with phosphorus and nitrogen. Ecol. Appl. 8, 559-568.

Doody, D.G., Archbold, M., Foy, R.N., Flynn, R., 2012. Approaches to the implementation of the Water Framework Directive: Targeting mitigation measures at critical source areas of diffuse phosphorus in Irish catchments. J. Environ. Manage. 93, 225-234.

Doppler, T., Camenzuli, L., Hirzel, G., Krauss, M., Lück, A., Stamm, C., 2012. Spatial variability of herbicide mobilisation and transport at catchment scale: insights from a field experiment. Hydrol. Earth. Sys. Sc. 16, 1947-1967.

Gburek, W.J., Sharpley, A.N., 1998. Hydrologic controls on phosphorus loss from upland agricultural watersheds. J. Environ. Qual. 27, 267-277.

Hahn, C., Prasuhn, V., Stamm, C., Schulin, R., 2012. Phosphorus losses in runoff from manured grassland of different soil P status at two rainfall intensities. Agr. Ecosyst. Environ. 153, 65-74.

Heathwaite, L., Sharpley, A., Bechmann, M., 2003. The conceptual basis for a decision support framework to assess the risk of phosphorus loss at the field scale across Europe. J. Plant Nutr. Soil Sc. 166, 447-458.

Herzog, P. 2005. Sanierung des Baldegger Sees, Auswertung der Zufluss-Untersuchungen 2000 bis 2004. (In German.) Luzern.

Hively, W.D., Gerard-Marchant, P., Steenhuis, T.S., 2006. Distributed hydrological modeling of total dissolved phosphorus transport in an agricultural landscape, part II: dissolved phosphorus transport. Hydrol. Earth. Sys. Sc. 10, 263-276.

Hornberger, G.M., Spear, R.C., 1981. An approach to the preliminary-analysis of environmental systems. J. Environ. Manage. 12, 7-18.

Kirkby, M., 1975. Hydrograph modelling strategies. In: Peel, R., et al. (Eds.), Processes in Physical and Human Geography. Heinemann, Lodon, pp. 69-90.

Kleinman, P.J.A., Sharpley, A.N., Buda, A.R., McDowell, R.W., Allen, A.L., 2011a. Soil controls of phosphorus in runoff: Management barriers and opportunities. Can. J. Soil Sci. 91, 329-338.

Kleinman, P.J.A., Allen, A.L., Needelman, B.A., Sharpley, A.N., Vadas, P.A., Saporito, L.S., Folmar, G.J., Bryant, R.B., 2007. Dynamics of phosphorus transfers from heavily manured Coastal Plain soils to drainage ditches. J. Soil Water Conserv. 62, 225-235.

Kleinman, P.J.A., Sharpley, A.N., McDowell, R.W., Flaten, D.N., Buda, A.R., Tao, L., Bergstrom, L., Zhu, Q., 2011b. Managing agricultural phosphorus for water quality protection: principles for progress. Plant Soil 349, 169-182.

Kopecky, M., Cizkova, S., 2010. Using topographic wetness index in vegetation ecology: does the algorithm matter? Applied Vegetation Science 13, 450-459.

Lazzarotto, P., 2005. Modeling phosphorus runoff at the catchment scale. Swiss Federal Institute of Technology (ETH), Zurich.

Lazzarotto, P., Stamm, C., Prasuhn, V., Fluhler, H., 2006. A parsimonious soil-type based rainfall-runoff model simultaneously tested in four small agricultural catchments. J. Hydrol. 321, 21-38.

Lazzarotto, P., Prasuhn, V., Butscher, E., Crespi, C., Fluhler, H., Stamm, C., 2005. Phosphorus export dynamics from two Swiss grassland catchments. J. Hydrol. 304, 139-150.

Leu, C., Singer, H., Stamm, C., Muller, S.R., Schwarzenbach, R.P., 2004. Variability of herbicide losses from 13 fields to surface water within a small catchment after a controlled herbicide application. Environ. Sci. Technol 38, 3835-3841.

Nash, J.E., Sutcliffe, J.V., 1970. River flow forecasting through conceptual models part I — A discussion of principles. J. Hydrol. 10, 282-290.

Pacini, N., Gächter, R., 1999. Speciation of riverine particulate phosphorus during rain events. Biogeochemistry 47, 87-109.

Pionke, H.B., Gburek, W.J., Sharpley, A.N., 2000. Critical source area controls on water quality in an agricultural watershed located in the Chesapeake Basin. Ecol. Eng. 14, 325-335.

Pionke, H.B., Gburek, W.J., Sharpley, A.N., Zollweg, J.A., 1997. Hydrological and chemical controls on phosphorus loss from catchments. In: Tunney H., et al. (Eds.),

Phosphorus loss from soil to water, CAB International Press, Cambridge, pp. 225-242.

Quinn, P., Beven, K., Chevallier, P., Planchon, O., 1991. The prediction of hillslope flow paths for distributed hydrological modeling using digital terrain models. Hydrol. Process. 5, 59-79.

R Foundation for Statistical Computing. 2007. R: A language and environment for statistical computing. Release 2.6.1. R Foundation for Statistical Computing, Vienna, Austria.

Radcliffe, D.E., Freer, J., Schoumans, O., 2009. Diffuse phosphorus models in the united states and europe: Their usages, scales, and uncertainties. J. Environ. Qual. 38, 1956-1967.

Schoumans, O.F., Silgram, M., Groenendijk, P., Bouraoui, F., Andersen, H.E., Kronvang, B., Behrendt, H., Arheimer, B., Johnsson, H., Panagopoulos, Y., Mimikou, M., Lo Porto, A., Reisser, H., Le Gall, G., Barr, A., Anthony, S.G., 2009. Description of nine nutrient loss models: capabilities and suitability based on their characteristics. J. Environ. Monitor. 11, 506-514.

Schulte, R.P.O., Doody, D.G., Byrne, P., Cockerill, C., Carton, O.T., 2009. Lough Melvin: Developing cost-effective measures to prevent phosphorus enrichment of a unique aquatic habitat. Tearmann 7, 211-228.

Sharpley, A., Moyer, B., 2000. Phosphorus forms in manure and compost and their release during simulated rainfall. J. Environ. Qual. 29, 2053-2053.

Sharpley, A.N., 1993. Assessing phophorus bioavailability in agricultural soils and runoff. Fert. Res. 36, 259-272.

Sharpley, A.N., Chapra, S.C., Wedepohl, R., Sims, J.T., Daniel, T.C., Reddy, K.R., 1994. Managing agricultural phophorus for protection of surface waters - issues and options. J. Environ. Qual. 23, 437-451.

Sharpley, A.N., Weld, J.L., Beegle, D.B., Kleinman, P.J.A., Gburek, W.J., Moore, P.A., Mullins, G., 2003. Development of phosphorus indices for nutrient management planning strategies in the United States. J. Soil Water Conserv. 58, 137-152.

Shigaki, F., Sharpley, A., Prochnow, L.I., 2007. Rainfall intensity and phosphorus source effects on phosphorus transport in surface runoff from soil trays. Sci. Total Environ. 373, 334-343.

Smith, K.A., Jackson, D.R., Withers, P.J.A., 2001. Nutrient losses by surface run-off following the application of organic manures to arable land. 2. Phosphorus. Environ. Pollut. 112, 53-60.

Stamm, C., Flühler, H., Gächter, R., Leuenberger, J., Wunderli, H., 1998. Preferential transport of phosphorus in drained grassland soils. J. Environ. Qual. 27, 515-522.

Stamm, C., Sermet, R., Leuenberger, J., Wunderli, H., Wydler, H., Flühler, H., Gehre, M., 2002. Multiple tracing of fast solute transport in a drained grassland soil. Geoderma 109, 245-268.

Stevens, C.J., Quinton, J.N., 2008. Investigating source areas of eroded sediments transported in concentrated overland flow using rare earth element tracers. Catena 74, 31-36.

Strauss, P., Leone, A., Ripa, M.N., Turpin, N., Lescot, J.M., Laplana, R., 2007. Using critical source areas for targeting cost-effective best management practices to mitigate phosphorus and sediment transfer at the watershed scale. Soil Use Manage. 23, 144-153.

Tamburini, F., Bernasconi, S.M., Angert, A., Weiner, T., Frossard, E., 2010. A method for the analysis of the delta O-18 of inorganic phosphate extracted from soils with HCl. Eur. J. Soil Sci. 61, 1025-1032.

Topp, G.C., Davis, J.L., Annan, A.P., 1980. Electromagnetic determination of soil water content: measurements in coaxial transmission lines. Water Resour. Res. 16, 574-582.

Vadas, P.A., Kleinman, P.J.A., Sharpley, A.N., Turner, B.L., 2005. Relating soil phosphorus to dissolved phosphorus in runoff: A single extraction coefficient for water quality modeling. J. Environ. Qual. 34, 572-580.

Vadas, P.A., Jokela, W.E., Franklin, D.H., Endale, D.M., 2011. The effect of rain and runoff when assessing timing of manure application and dissolved phosphorus loss in runoff. J. Am. Water Resour. Assoc. 47, 877-886.

Vogler, P., 1965. Beiträge zur Phosphatanalytik in der Limnologie. II. Die Bestimmung des gelösten Ortophosphates. (In German.) Fortschritte der Wasserchemie und ihrer Grenzgebiete 2.

Von Albertini, N., Braun, M., Hurni, P., 1993. Oberflächenabfluss und Phosphorabschwemmung von Grasland. (In German.) Landwirtschaft Schweiz Band 6 10, 575 - 582.

Wade, A.J., Whitehead, P.G., Butterfield, D., 2002. The Integrated Catchments model of Phosphorus dynamics (INCA-P), a new approach for multiple source assessment in heterogeneous river systems: model structure and equations. Hydrol. Earth. Sys. Sc. 6, 583-606.

Ward, R.C., 1984. On the response to precipitation of headwater streams in humid areas J. Hydrol. 74, 171-189.

Watson, C.J., Matthews, D.I., 2008. A 10-year study of phosphorus balances and the impact of grazed grassland on total P redistribution within the soil profile. Eur. J. Soil Sci. 59, 1171-1176.

Weld, J., Sharpley, A.N., 2007. Phosphorus indices. In: Radcliffe, D. E., Cabrera, M. L. (Eds.), Modeling phosphorus in the environment. CRC Press, Boca Raton, pp. 3-19.

Western, A.W., Grayson, R.B., Bloschl, G., Willgoose, G.R., McMahon, T.A., 1999. Observed spatial organization of soil moisture and its relation to terrain indices. Water Resour. Res. 35, 797-810.

White, M.J., Storm, D.E., Busteed, P.R., Stoodley, S.H., Phillips, S.J., 2009. Evaluating nonpoint source critical source area contributions at the watershed scale. J. Environ. Qual. 38, 1654-1663.

Withers, P.J.A., Ulén, B., Stamm, C., Bechmann, M., 2003. Incidental phosphorus losses - can they be predicted? J. Plant Nutr. Soil Sc. 166, 459-468.

4

A comparison of three simple approaches to identify critical areas for runoff and dissolved reactive phosphorus losses

Claudia Hahn, Volker Prasuhn, Christian Stamm, Dave G. Milledge, Rainer Schulin

Submitted to the Journal of Environmental Management

Abstract

Diffuse phosphorus (P) losses are the main cause for eutrophication of surface waters in many regions. Implementing mitigation measures on critical source areas (CSA) is seen to be the most effective way to reduce P-losses. Thus, tools are needed that delineate CSA on the basis of available data. We compared three models based on different approaches and sets of input data: the Rainfall Runoff Phosphorus (RRP) model, the Dominant Runoff Processes (DoRP) model, and the Sensitive Catchment Integrated Modeling Analysis Platform (SCIMAP). The RRP model is a parsimonious dynamic model using the topographic index and a binary soil classification to simulate discharge and P-losses. The DoRP model distinguishes 8 soil classes based on soil and geological maps. It does not account for topography when calculating runoff. SCIMAP assesses runoff risks solely on the basis of topography using the network index. Compared to surface runoff and soil moisture data available from a catchment in Switzerland, the RRP model and SCIMAP made better predictions than the DoRP model, suggesting that in our study area topography was more important for CSA delineation than soil data. The study demonstrates that simple models using readily available data provide very useful information for CSA delineation.

4.1 Introduction

Diffuse phosphorus (P) losses from agricultural land continue to be a severe problem for water quality, causing eutrophication of many surface waters (Buda et al., 2012; Kleinman et al., 2011b; Schoumans et al., 2009). The European Union (EU) Water Framework Directive (WFD) calls for restoration of all water bodies to good quality by 2015 if possible, and 2027 at the latest (Hering et al., 2010). Since P losses from point sources, which can be identified and targeted rather easily, were substantially reduced over the last two decades (Dubrovsky et al., 2010), diffuse P losses from agricultural areas are now the main cause of eutrophication of water bodies in many countries (Carpenter et al., 1998; Sharpley et al., 1994). Thus, in order to meet the WFD goal, the focus now needs to be directed to measures by which these diffuse inputs can effectively be reduced.

A wide range of different mitigation options were proposed and discussed within COST Action 869 (Schoumans et al., 2011). Some measures aim to prevent or intercept P transfer by runoff from fields to surface waters, (e.g. buffer strips (Roberts et al., 2012; Stutter et al., 2012)); others focus on the immobilization of P sources in soil and manure by adding P sorbing agents (Buda et al., 2012).

Several studies reported that most P found in runoff at the catchment outlet originated from rather small areas within the catchment (Gburek and Sharpley, 1998; Pionke et al., 2000; Pionke et al., 1997). Targeting these critical source areas (CSAs) seems to be the most efficient and cost-effective approach to mitigate the water pollution problem (Doody et al., 2012; Heathwaite et al., 2003; Rodriguez et al., 2011; Schulte et al., 2009).

Kleinman et al. (2011b) reviewed source and transport factors that need to be considered when addressing diffuse P losses and CSA delineation. Distinguishing chronic or legacy sources and acute or temporary sources, the main P sources are pools of legacy P in soils due to excessive fertilizer application in the past and temporary increases in available P resulting from current applications of manure or fertilizer. Decaying crop residues can also play a role as a temporary P source (Kleinman et al., 2011b; Pote et al., 1999). While proper crop nutrition and soil management according to codes of best practices can reduce acute sources very effectively, sources of legacy P are more difficult to deal with as they can persist for a long time (Kleinman et al., 2011a). In earlier studies erosion and surface runoff were considered the main or only transport mechanisms carrying P to streams. More recently, other processes have been recognized to transport substantial amounts of P to surface waters (Doody et al., 2012; Kleinman et al., 2011b) such as subsurface flow (Kleinman et al., 2009), and tile drain flow (Kleinman et al., 2007; Stamm et al., 1998; Vadas et al., 2007).

Given the diversity of sources and transport processes involved in diffuse P losses, the identification of CSAs in a catchment is a challenging task. Various tools have been developed to model diffuse P losses and to delineate CSAs (Krueger et al., 2012; Radcliffe et al., 2009; Schoumans et al., 2009), ranging from rather simple site-assessment tools to complex physically based catchment models. The former are usually easy to apply but are often too simplistic, whereas the latter are generally too complex for practical applications and usually require input data that are not easily available. As pointed out by various authors (Heathwaite et al., 2007; Radcliffe et al., 2009; Srinivasan and McDowell, 2007), there is a need for parsimonious process-based and easy-to-use, but nonetheless sound and reliable models that are easy to parameterize and can assist water protection policy and agricultural P management in targeting effective and cost-efficient water protection and mitigation measures to the most critical areas.

Here we compare three tools that can be used to predict critical source areas in catchments based on different approaches and input data: the Rainfall Runoff Phosphorus (RRP) model, the Dominant Runoff Processes (DoRP) model, and the Sensitive Catchment Integrated Modeling Analysis Platform (SCIMAP). The Rainfall Runoff Phosphorus (RRP) model is a dynamic, parsimonious model that simulates runoff and dissolved reactive P (DRP) losses from a catchment, using the topographic index λ proposed by Beven and Kirkby (1979) and a binary soil classification by drainage capacity to simulate a site's hydrological responses to rainfall events (Hahn et al., in review; Lazzarotto, 2005). The DoRP model, which was proposed by Schmocker-Fackel et al. (2007), distinguishes 8 soil classes by drainage and soil water storage capacities, based on soil and geological maps, but does not account for topography when calculating runoff. In contrast, SCIMAP, which was proposed by Lane et al. (2006), assesses runoff risks solely on the basis of topography, using the network index NI introduced by Lane et al. (2004). This network index is derived from the topographic index λ by correcting it for reduced topographic connectivity of locations that are not directly connected to a stream. RRP and SCIMAP provide a framework to combine these hydrological predictions with pollutant source data to identify CSAs.

We tested the three approaches by applying them to two catchments located in a grassland-dominated hilly region of the Swiss Plateau. First, we investigated the importance of topography relative to soil properties in defining runoff risks by comparing the ability of the RRP and DoRP models to reproduce observed runoff patterns. We then compared the RRP model to SCIMAP to test the impact of applying a simpler, time integrated model. The RRP model was used as reference because it had been compared to experimental data on soil moisture, runoff generation and groundwater levels in an earlier publication (Hahn et al., in review; Lazzarotto, 2005). By comparing the three approaches (RRP, DoRP, SCIMAP), we

investigate the importance of connectivity and detailed soil data for the delineation of CSA and identify the benefits of a parsimonious dynamic model using soil and topographical information.

4.2 Materials and methods

4.2.1 Model concepts

4.2.1.1 The Rainfall-Runoff-Phosphorus (RRP) model

The RRP model is a parsimonious dynamic model developed by Lazzarotto (2005) to predict dissolved reactive P (DRP) losses from small agricultural catchments. The model consists of a hydrological and a P sub-model. For this study we used Version 2 of the model, which has been developed and described in detail by (Hahn et al., in review).

The hydrological sub-model (Lazzarotto et al., 2006), referred to here as Rainfall-Runoff model, is a semi-distributed hydrological model with an hourly time resolution that uses soil and topographic information to describe the dynamics of the system. It is based on the concept that areas with the same topographic index λ and the same soil drainage capacity have the same hydrological behavior. The topographic index λ (Beven and Kirkby, 1979; Kirkby, 1975) is an indicator of the wetness of the soil at a given location within a catchment and is determined by the upslope contributing area and the local slope of a location. Soils are divided into 2 drainage classes, well drained and poorly drained soils, the ensembles of which form a poorly-drained and a well-drained hydrological response unit (HRU), respectively. The discharge from both of these two HRUs is composed of a fast and a slow flow component. The former comprises all kinds of quickly responding flow, including preferential flow, saturation excess runoff and Hortonian overland flow. The slow flow component is an approximation of the baseflow. The model was simultaneously calibrated (Uniform Monte Carlo method) on discharge data from four catchments draining into Lake Sempach (Hahn et al., in review; Lazzarotto et al., 2006). Using the modified Nash-Sutcliffe criterion NSC (Nash and Sutcliffe, 1970) as defined by Lazzarotto et al. (Lazzarotto et al., 2006) and a NSC threshold value of 0.6, 724 parameter sets, out of 5 million, were judged behavioral and used for model application (Hahn et al., in review).

The P-model assigns a constant P concentration, observed during baseflow (Lazzarotto, 2005), to baseflow runoff. For areas where fast flow occurs, P loads comprise incidental P losses from manure, P losses from topsoil, which might be enriched with P due to P

application in excess of crop demands in the past (also called legacy P), and losses associated with baseflow.

4.2.1.2 The Dominant Runoff Processes (DoRP) assessment scheme

In contrast to the simplification in the RRP model regarding the soil data, the GIS-based DoRP model presented by Schmocker-Fackel et al. (2007) classifies the soil hydrology in a more differentiated way based on several soil attributes contained in a standard soil map and information about the parent material obtained from geological maps. The approach is based on the study of Scherrer and Naef (2003), who developed decision schemes to determine the dominant runoff process (DoRP) of a soil profile. Schmocker-Fackel et al. (2007) simplified these schemes to reduce data requirements and to enable automatic GIS-based mapping of DoRPs at catchment scale. The DoRP maps were used for flood discharge simulations, but they can also be used to determine risk areas for pesticide or P losses and erosion.

The DoRP model distinguishes between the following runoff processes: Hortonian Overland Flow (HOF), Saturated Overland Flow (SOF), fast Subsurface Flow (SSF) and Deep Percolation (DP). For SOF and SSF to occur an impermeable layer in the soil profile is required. According to the drainable porosity of a profile, three classes of soil water storage capacity are distinguished: STO1 = very low (0 – 40 mm), STO2 = medium (40 – 100 mm), STO3 = large (100 – 200 mm), where the numbers in parentheses give the total volume of drainable porosity per unit area above the impermeable layer (in mm). Schmocker-Fackel et al. (2007) used a soil map, a geological map, a forest map and a land-use map to determine the occurrence of DP and HOF and to determine the storage classes STO1, STO2, STO3. Apart from roads and other artificially sealed areas, HOF is assumed to occur on soils with very low infiltration capacity, e.g. due to soil surface sealing, water-repellency or compaction, at very high rainfall intensity (> 50 mm h^{-1}). At lower intensities, these areas are assigned to another runoff process. Information on slope is needed to differentiate between SOF and SSF. SOF was observed to occur below a slope of 15%, and SSF on slopes above 15% (Schmocker-Fackel et al., 2007). If drainage data is available, SSF can be further differentiated into drainage flow and natural SSF. Following the terminology of Schmocker-Fackel et al. (2007) SOF and SSF runoff from soil with storage capacity STO_i (i=1,2,3) is denoted as SSF_i and SOF_i, respectively.

Areas dominated by DP are assumed to generate no runoff; instead, rain falling on these areas infiltrates and is delivered to groundwater. As STO1 areas are saturated much faster than STO2 areas and these faster than STO3 areas under the same initial conditions, the risk of runoff is highest on areas with HOF, followed by STO1, STO2 and STO3 areas in a given

event. Furthermore, SSF areas are assumed to drain faster than SOF areas. Following Schmocker-Fackel et al. (2007) we used storage capacities of 5 mm for HOF and 20 mm, 70 mm and 150 mm for STO1, STO2 and STO3 areas, respectively. While the DoRP classification of soils gives a qualitative assessment of the hydrological behavior of a given location, the DoRP model also includes a simple bucket model to make quantitative discharge predictions (Schmocker-Fackel et al., 2007). Neglecting lateral flow, runoff is generated, as soon as rainfall exceeds the soil's storage capacity at a given location. To account for antecedent soil moisture conditions, all rain water is stored for 5 days in the soil, if storage capacity is available, and is then removed.

4.2.1.3 SCIMAP

The Sensitive Catchment Integrated Modeling Analysis Platform (SCIMAP) estimates the risk of pollutant loss from a location x to a stream or other receiving water body. This locational risk p_x^{gc} (Reaney et al., (2011) indicates whether a pollutant is both available at a location and can be delivered to the water body. It is calculated by multiplying two relative site indicators, the availability risk at point x (p_x^g) and the connection risk (p_x^c), the risk that it can be delivered to a water body:

$$p_x^{gc} = p_x^g p_x^c$$

In this study, which focuses on DRP losses the availability risk is defined by the P availability (source factor). The connection risk is the likelihood that runoff is generated and delivered to a stream (transport factor). The availability risk for dissolved P losses can be related to the concentration of legacy P in the soil, which is a permanent P source. Given that the relationship between water extractable P concentrations (WSP) in the soil and DRP in runoff was found to be linear in many studies (Hahn et al., 2012; Vadas et al., 2005), we normalized the WSP data by the maximum WSP value. In line with the original SCIMAP concept, this normalization was carried out for each catchment separately. To allow for comparisons across catchments, we also modified this normalization procedure to account for the value range in both catchments.

Following (Reaney et al., 2011), the connection risk was derived from the Network Index (NI), which is a connectivity index equivalent to the topographic index λ but corrected for locations of reduced connectivity (Lane et al., 2004). Although cells with a higher λ are more likely to be saturated than cells with a lower λ, water from these cells might not reach the stream network, if drier cells along the flow path enable infiltration. Assuming that the contribution of an upslope location to stream runoff is limited by the lowest λ value further

downslope along the flow path, the NI assigns the lowest λ value found further downslope along that flow path to all cells further upslope that otherwise would have a higher λ value. The NI then needs to be related to p_x^c. Based on a comparison with a distributed hydrological model (Lane et al., 2009), Reaney et al. (2011) suggested a p_x^c of 0 for NI values below their 5% quantile and 1 for values above the 95% quantile, with a linear p_x^c to NI relationship in between (i.e. from $p_x^c = 0$ at the 5% quantile to $p_x^c = 1$ at the 95% quantile). Again, this normalization does not allow comparisons across catchments. We modified this procedure by deriving quantiles for the pooled data sets of both catchments.

4.2.2 Study sites

We applied the three approaches to the Lippenrütibach catchment (3.3 km^2) and the Stägbach catchment (8.24 km^2), which are both situated in the hilly area of the Swiss Plateau northwest of Lucerne (Fig. 4-1). The former drains into Lake Sempach, whereas the latter drains into Lake Baldegg. Both lakes have a legacy of eutrophication and are artificially aerated to avoid oxygen depletion in the lower part of the water column. The region is characterized by intensive livestock production (diary and pig farms, 2.4 livestock units per ha (Herzog, 2005)) and intensively manured permanent grassland (4 to 6 cuts and manure applications per year). Soil P levels are elevated due to a legacy of P inputs in excess of crop demands. The average annual precipitation ranges from 1000 to 1200 mm. The catchments are characterized by hilly terrain that undulates between altitudes from 500 to 800 m above sea level. The landscape shows strong molding by the Würm glaciation. The parent material varies between upper freshwater molasse and moraines (Bodenkarte Hochdorf, 1983). The soils are predominantly eutric and gleyic Cambisols, with loamy texture (Bodenkarte Hochdorf, 1983; AGBA, 1993). Less than 10% of the two catchment areas are covered by settlements, roads and other constructed features. Forests account for 17% of the Lippenrütibach catchment and 8 % of the Stägbach catchment. The remaining area is used for agriculture.

The Lippenrütibach catchment (LIP) is one of the four catchments that were used for the calibration of the RRP model, using discharge data and DRP analyses of runoff collected from the 7th until the 17th of July 2000. In the present study we applied the model to the period from March until November 1999, for which precipitation, ET, discharge, and manure application data were available that had not been used for model calibration. For the Stägbach catchment (Stäg) we used data collected in 2010 to run the RRP model and to validate model results. In addition to discharge and DRP measurements at the catchment outlet, permanent soil moisture measurements at four locations (S1 to S4) as well as

groundwater level and Overland Flow Detector (OFD) measurements at 10 stations (S1 to S10) were available for validation. For more details the reader is referred to Hahn et al. (in review).

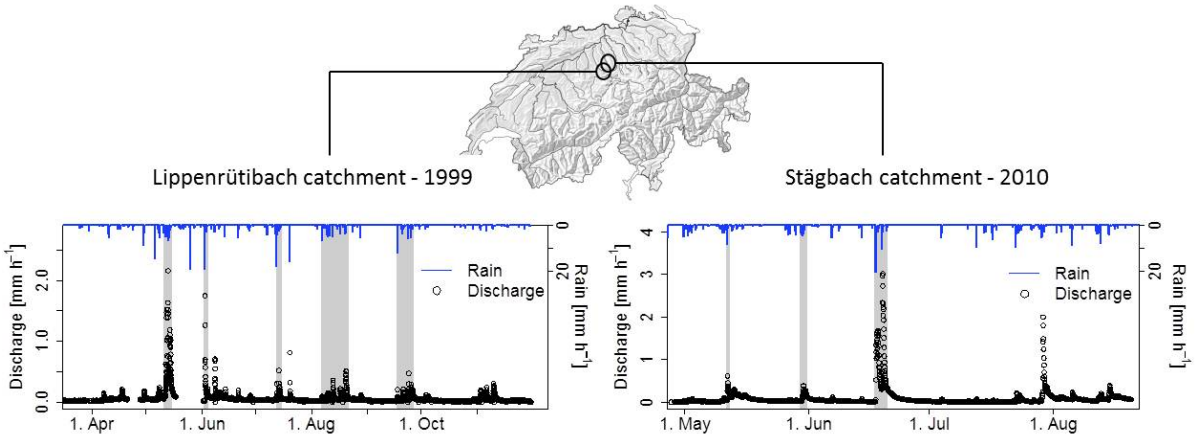

Figure 4-1: Location of study areas and the rainfall & discharge characteristics for the respective monitored year. Grey shading indicates the events for which discharge was calculated using the Dominant Runoff Processes approach

4.3 Results

4.3.1 Hydrology

4.3.1.1 RRP

The RRP model predicted the discharge dynamics at the outlet of the Lippenrütibach and the Stägbach catchment fairly well, with median NSC values of 0.5 and 0.62, respectively (Hahn et al., in review). To characterize the uncertainty of fast flow predictions, we constructed maps showing the fraction of the accepted parameter sets that predicted fast flow for each pixel at a given time (Fig. 4-2A). Values between 0 and 0.2 are considered to indicate a low risk, values between 0.2 and 0.5 a medium risk, values between 0.5 – 0.8 a high risk, and values between 0.8 and 1 a very high risk of fast flow. For both catchments the percentage of high-risk areas increased with soil moisture (Table 4-1). The percentage of the respective agricultural areas with very high predicted runoff risk varied between 9% for small events and 27% for large events in the Lippenrütibach catchment, and between 7 and 16% in the Stägbach catchment. Runoff measurements from OFDs installed at different locations within the Stägbach catchment were in good agreement with these predictions. For example, runoff was collected at 5 out of 7 locations during the large event in June 2010, but

at only 2 locations during the small event in May. The RRP model was able to capture the temporal soil moisture and runoff patterns in three out of the four locations where soil moisture was monitored continuously in 10 and 30 cm depth and runoff was collected using OFDs. Only for one site (S4) the RRP model underestimated runoff risks (Hahn et al., in review).

RRP model – 2A
Hydrological risk areas during the largest event of the monitored year
0-0.2 low risk, 0.2-0.5 medium risk, 0.5-0.8 high risk, 0.8-1 very high risk

DoRP – 2B
DP – deep percolation
SOF – saturation overland flow
SSF – subsurface flow
1-3 – storage classes,
1 = lowest storage capacity

SCIMAP – 2C
connection risk
= Network Index scaled between the 5 % and 95% quantiles

Lippenrütibach

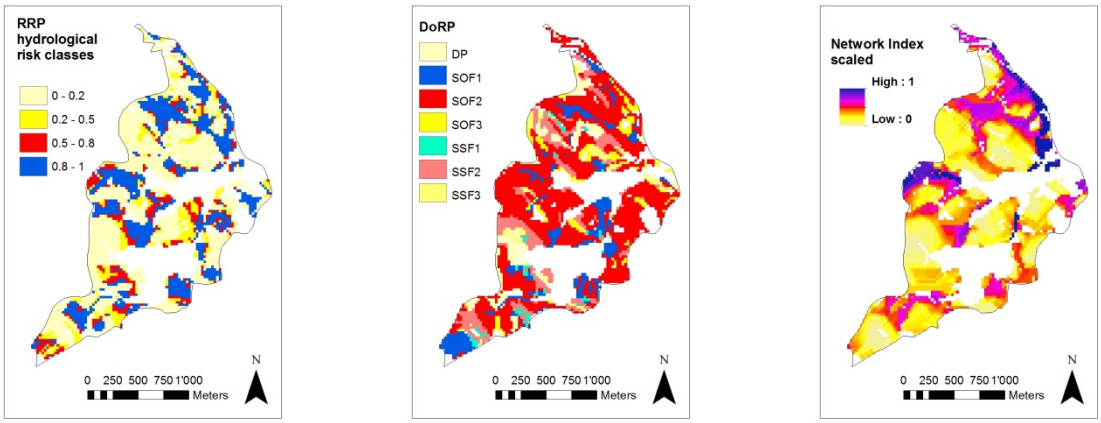

Stägbach

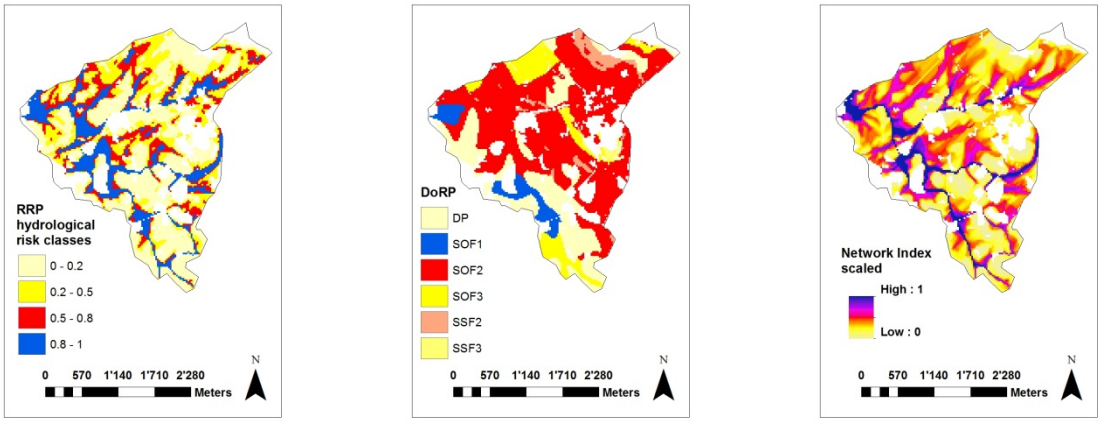

Figure 4-2: Spatial distribution of hydrological risk areas as determined with the three models for the Lippenrütibach catchment and the Stägbach catchment

Table 4-1: Spatial extent of hydrological risk classes for a large and a small runoff event in the Lippenrütibach and the Stägbach catchment – relative to the total agricultural area in %

	low	medium	high	very high
	---------- % ----------			
Lippenrütibach 1999				
Small event in August	71	13	7	9
Large event in May	49	12	12	27
Stägbach 2010				
Small event in May	76	12	5	7
Large event in June	44	23	17	16

4.3.1.2 DoRP

Discharge predictions of the DoRP model are based on an extremely simple model concept of a limited storage volume characteristic for each soil type (see above). Despite its simplicity and the lack of any calibration, the predicted discharge volumes for different events correlated reasonably well with the measured values. However, the slope deviates from the 1 to 1 line in both catchments with an underestimation for the Stägbach catchment and an overestimation for the Lippenrütibach (Fig. 4-3). However, no reliable statement for the Stägbach catchment is possible due to the limited number of observations. The model thus proved to be useful to predict the discharge of an event relative to discharge of other events from the same catchment, but cannot be used to predict discharge from another catchment without re-calibration. This is in contrast to the RRP model that yielded satisfactory results without site-specific calibration.

Given the large percentages of STO2 areas in the two catchments (Table 4-2), the runoff contributing area predicted by the DoRP model increased sharply as soon as rainfall plus antecedent moisture exceeded the storage capacity of this class of soils.

Table 4-2: Areal percentage of each dominant runoff process (DoRP) in the Lippenrütibach catchment and the Stägbach catchment [%] – relative to the total agricultural area. STO1 – low storage capacity, STO2 – intermediate storage capacity, STO3 – high storage capacity, DP – deep drainage

	STO1	STO2	STO3	DP
	---------- % ----------			
LIP	14	69	9	8
Stäg	5.5	60.5	11.2	22.8

The difference between simulated and measured discharge increased with increasing event size (Fig. 4-3) suggesting that either storage capacities need to be calibrated or more differentiation between locations in STO2 is needed.

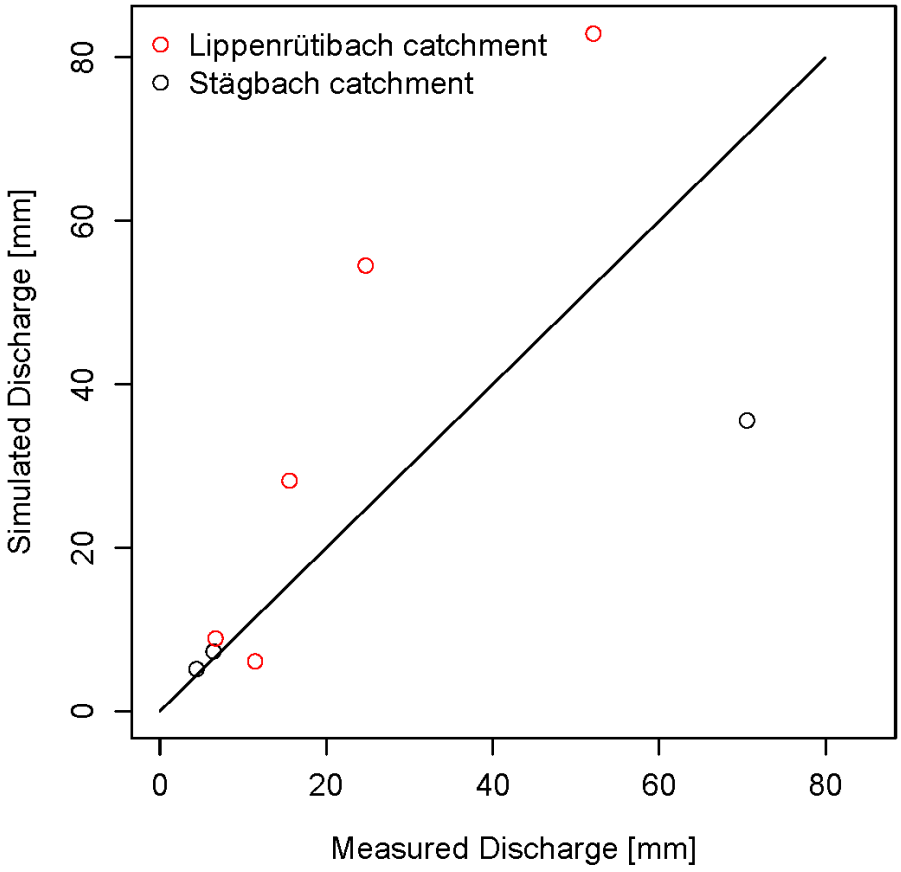

Figure 4-3: Comparison of discharge estimations for runoff events in the year 1999 (Lippenrütibach catchment) and 2010 (Stägbach catchment) derived with the DoRP approach and the measured discharge. The respective runoff events are indicated in Figure 4-1 by grey shading.

Surface overland flow from soils of storage class 2 (SOF2) was the most prevalent runoff category in both catchments (Fig. 4-2B). Three of the four permanent measurement stations (S2, S3 and S4) in the Stägbach catchment were situated on soils of this category, while S1 was classified as DP. Indeed, S1 was the only station where surface runoff was never detected during the whole monitoring period and where the ground water table never rose above a level of 0.5 m below the soil surface. Thus, in contrast to the RRP model, the DoRP model differentiated correctly between S1 and S4, but not between S2, S3 and S4, although S2, S3 and S4 also showed substantial differences in their soil moisture and runoff regimes (Hahn et al., in review). The fact that S2, S3 and S4 were in line with RRP predictions

suggests that topography was in general a better predictor for the runoff responsiveness of a location to rainfall events than hydraulic soil properties.

4.3.1.3 Comparison of RRP and DoRP

The highest observed P losses occurred during the largest event in each of the two catchments during the study period. Thus, we used these two events (Fig. 4-1) to compare the DoRP assessment of the soils of the two catchments with risk classes determined by the RRP model. In general, the extreme risk classes (very high or very low) agree well between the two approaches. On the one hand, very high fast flow risks according to the RRP model were strongly associated with soils of low (STO1) to medium (STO2) storage capacity (Table 4-3). On the other hand, the DoRP storage classes DP and STO3 primarily fell into the categories of low fast flow risks according to RRP (Table 4-4). The intermediate categories in each approach were distributed across the classes of the other approach in much more heterogeneous manner. This holds true especially for the DoRP storage class STO2, which contains for example 45.6% of RRP low risk class areas but also 29.7% of very high risk during the largest runoff event in the Lippenrütibach catchment (Table 4-4). The STO2 class dominates in both study areas, which explains why DoRP allows for little spatial differentiation.

Table 4-3: Amount of RRP risk class pixel within the DoRP storage classes in percent of the total amount of pixel within one risk class [%].The areal extent of the RRP risk classes during the large runoff events (Lippenrütibach: May 1999, Stägbach: June 2010, see Fig. 4-1) was taken for comparison. STO1 – low storage capacity, STO2 – intermediate storage capacity, STO3 – high storage capacity, DP – deep drainage

	DoRP storage classes				
	STO1	STO2	STO3	DP	sum
RRP risk classes	Lippenrütibach catchment				
low	3.1	65.1	16.2	15.6	100
medium	24.8	68.1	2.7	4.3	100
high	25.8	71.5	2.3	0.4	100
very high	23.4	75.6	0.9	0.1	100
	Stägbach catchment				
low	0.6	48.1	12.3	38.9	100
medium	2.5	65.3	14.7	17.6	100
high	6.5	75.6	9.7	8.2	100
very high	21.4	70.9	5.2	2.5	100

Table 4-4: Amount of RRP risk class pixel within the DoRP storage classes in percent of the total area of the storage classes [%].The areal extent of the RRP risk classes during the large runoff events (Lippenrütibach: May 1999, Stägbach: June 2010) was taken for comparison. STO1 – low storage capacity, STO2 – intermediate storage capacity, STO3 – high storage capacity, DP – deep drainage

	DoRP storage classes			
	STO1	STO2	STO3	DP
RRP risk classes	Lippenrütibach catchment			
low	10.6	45.6	90.1	92.6
medium	21.6	12.0	3.8	6.5
high	22.5	12.6	3.2	0.6
very high	45.3	29.7	2.9	0.3
sum	100	100	100	100
	Stägbach catchment			
low	5.2	34.7	47.8	74.5
medium	10.4	24.6	29.8	17.6
high	20.4	21.4	14.7	6.1
very high	64.1	19.2	7.6	1.8
sum	100	100	100	100

One reason for the relatively good match between the two models regarding the extreme risk classes is that all STO1 soils were classified as poorly drained soils in the RRP model and that locations with low soil water storage capacity tended to have large λ values (Fig. 4-4). These relationships can be understood as an expression of the dependence of soil formation processes on topography and position within the landscape.

4.3.1.4 Comparison of RRP and SCIMAP

In contrast to the RRP and the DoRP model, SCIMAP cannot be used to predict discharge since it is a time integrated rather than dynamic model and so does not make discharge predictions. However, it is the only one of the three approaches that accounts for connectivity when identifying runoff risks within a catchment. This aspect however, does not seem to play a major role in our study areas. A comparison between the topographic index λ and network index NI reveals only minor differences (see Fig. 4-SI_1). Accordingly, it is not surprising that the spatial NI patterns are similar to the RRP risk classes as can be seen in Fig. 4-2 for the largest event during the respective monitoring periods for the two study areas.

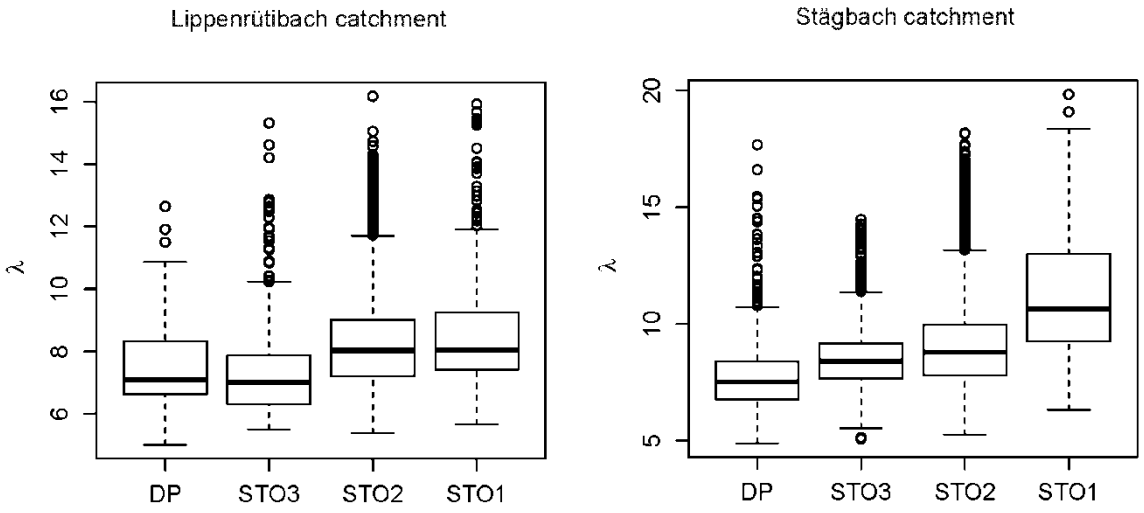

Figure 4-4: Boxplots – the distribution of the Topographic Index λ within the DoRP storage classes. DP – Deep Percolation, STO1 – low storage capacity, STO2 – intermediate storage capacity, STO3 – high storage capacity

Figure 4-5A shows that there were close relationships between the NI and the risk of fast flow predicted by the RRP model. The scatter is due to pixels where the topographic index λ differs from the network index NI. For such locations the risk might be overestimated by the RRP model, unless there is a direct connection to a stream that does not directly depend on topography, e.g. a connection via tile drains. In Figure 4-5B these pixels were not displayed to avoid the influence of connectivity when comparing the RRP hydrological risk with the SCIMAP connection risk.

As should be expected, well-drained locations were predicted by the RRP model to have lower fast flow risk than poorly drained locations with the same NI (Fig. 4-5). For the Lippenrütibach catchment this observation was even more pronounced.

Because SCIMAP yields a static risk assessment while RRP predicts risk for fast flow as a function of time it is useful to compare the SCIMAP prediction with RRP predictions for discharge events of different magnitude (Fig. 4-5B). For small events, the SCIMAP risk predictions are systematically larger than for those resulting from RRP (all RRP results lay below the 1:1 line in Fig. 4-5B). For large events, the situation is more complex. According to the RRP model, a considerable areal fraction has a higher risk than according to SCIMAP. On well drained soils this relationship turns to the opposite for RRP low risk areas. For poorly drained soils, RRP yields systematically higher risk values than SCIMAP. The average RRP risk over the monitoring period does not show a risk of 1 because it is an average of storm flow events and low flow. Even after rescaling the RRP risk to range

between 0 and 1 to enable a fair comparison the average RRP risk predictions are always lower than the SCIMAP risk predictions. The average risk integrates periods of large and small storm flows as well as very low runoff events and therefore continues to increase until quite high NI values are reached (Fig. 4-5A). At a SCIMAP connection risk of 1 the average RRP risk ranges between 0.2 and 0.6 (Fig. 4-5B). This is because the scaling between the 5% and 95% quantiles does not enable a fine enough differentiation between high NI values. Therefore, SCIMAP differentiates in space less than the dynamic RRP model. Hence, SCIMAP agrees better with RRP predictions for larger events.

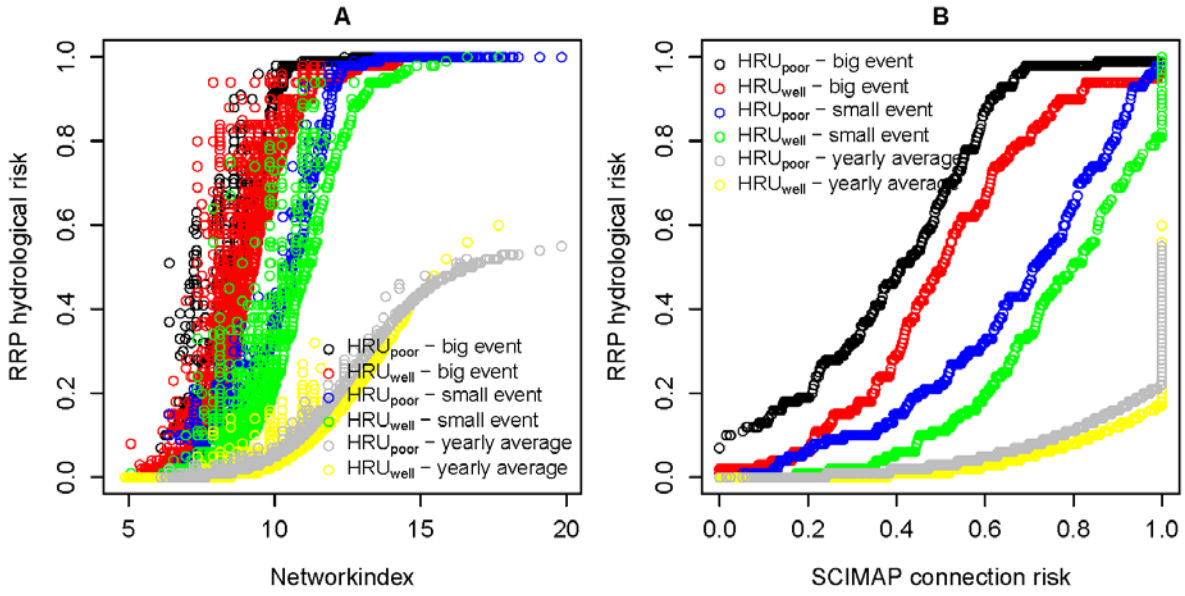

Figure 4-5: RRP hydrological risk predictions for both hydrological response units (HRU_{well} and HRU_{poor}) during two different rainfall events and for the whole monitoring period versus the Network Index (4-5A) and versus the original SCIMAP connection risk (4-5B).

4.3.1.5 Comparison of all three model predictions

Despite the differences between RRP and SCIMAP described above, their spatial predictions of areas prone to fast flow processes and hence to DRP losses are much more similar to each other than to the DoRP risk predictions (Fig. 4-2). Many topographic features where RRP and SCIMAP predict a high risk for runoff generation are not reflected at all in the DoRP model. Despite a more refined soil classification such features may get lost in the DoRP classification. Interestingly, this is not always the case. The two SOF1 areas (DoRP) in the Stägbach catchment for example, appear very clearly in both RRP and SCIMAP. In

general however, DoRP seems rather coarse in its classification compared to differentiation indicated by the other two models.

Interestingly, the incorporation of soil information, which is part of the RRP model concept, caused very little change in spatial patterns relative to SCIMAP, which is solely based on topographic information. Accounting for soil drainage classes in the RRP approach resulted only in two small differences between Figure 4-2A and C, observed in the south western part of LIP and the north eastern part on Stäg. Accounting for connectivity (SCIMAP) had little influence on the spatial pattern of predicted hydrological risk areas relative to those predicted based on the original topographic index (Fig. 4-2A+C).

4.3.2 Critical areas for phosphorus losses

4.3.2.1 Comparison of RRP and SCIMAP

As shown by Hahn et al. (in review), the RRP model produced good predictions of P loads at the outlet of the Stägbach catchment and one of its sub-catchments. Spatial RRP predictions of runoff risks were also in good (qualitative) agreement with local measurements of soil moisture, groundwater levels and surface runoff. This gives confidence that the RRP model reflects the main processes and is a valid tool to delineate CSA for P exports into the streams of the study catchments. Given the good performance of the RRP model, it is interesting that SCIMAP predicted similar areas with high risk of DRP loss and that this agreement appears to be better for high-runoff events than for the average DRP load during the simulation period (Fig. 4-6, 4-7). Thus SCIMAP appears to have good potential to be used at least as a first screening tool for the identification of critical source areas.

4.3.2.2 Relationship between NI and the connection risk used in SCIMAP

The original SCIMAP model prescribes a static linear relationship between NI and the connection risk p_x^c from 0 at the 5% NI quantile to 1 at the 95% quantile. This approach has some limitations. First, one cannot assume that this mapping of NI to the connection risk is invariant in time. The comparison with the RRP model shown above indicates that the SCIMAP assessment reflects mainly larger events in our study areas. Second, the 5 and 95% thresholds make the method insensitive to certain parts in the catchment. Assigning a connection risk of 0 to areas with very low NI values is reasonable for single runoff events as well as for an entire monitoring period. Assigning the value 1 to cells with a NI higher than the 95% quantile is appropriate for large events, but not necessarily for aggregated risks

over a period of time or small events (Fig. 4-5B). This can be seen in Figure 4-7A and 4-7C, which show a considerable scatter for any SCIMAP locational risk.

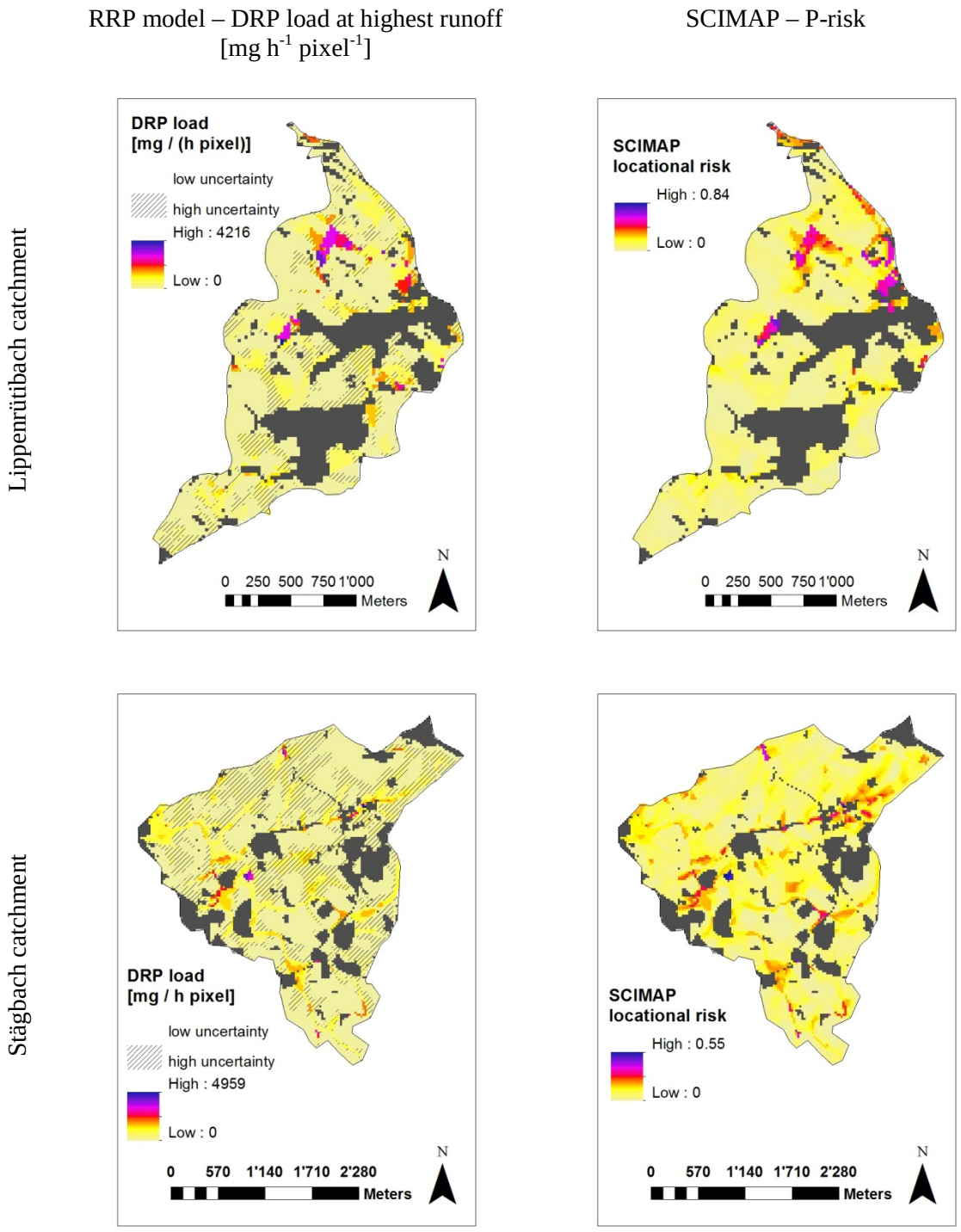

Figure 4-6: Spatial model results for P losses as predicted with the RRP model and the SCIMAP model, grey areas are forested or urban areas. Areas for which less than 80% of the RRP simulations resulted in the same distribution of fast flow generation are hatched.

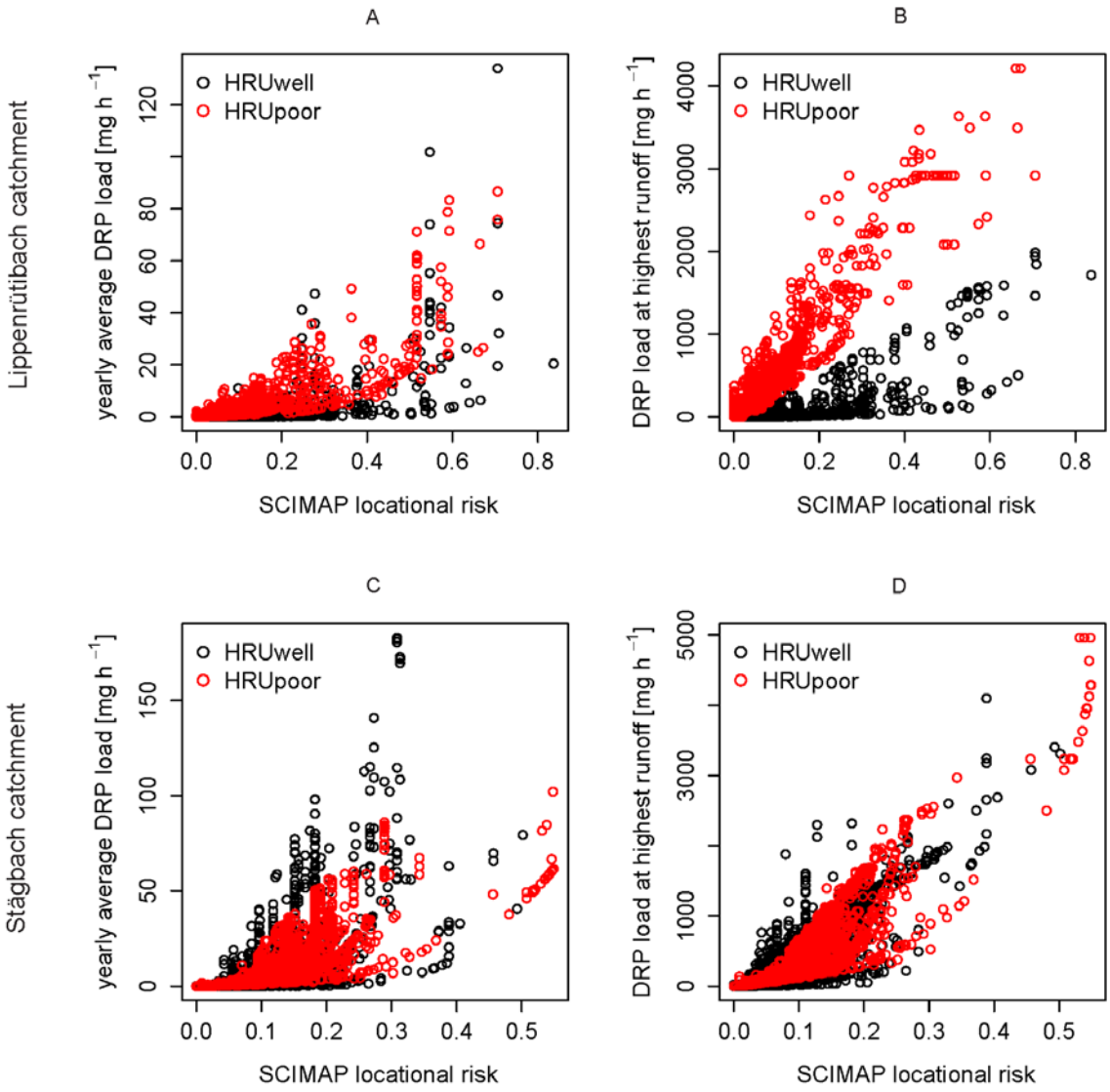

Figure 4-7: Comparison of the P load calculated with the RRP model, that differentiates between well and poorly drained hydrological response units (HRU_{well}, HRU_{poor}), for the entire monitoring period and the highest runoff event with the locational risk for P losses predicted using the SCIMAP approach

The scatter is reduced upon using the maximum NI value for scaling of the risk/NI relationship (Fig. 4-8). This can be explained by a more appropriate estimation of risks in areas upstream compared to downstream areas close to the catchment outlet. The latter are characterized by very high λ and NI values and, according to the RRP model contributed to runoff most often, even during very small events. With the 5 to 95% scaling cells further upstream were assigned the same high risk as downstream, while using the maximum NI for

scaling enabled a differentiation between high NI values and thus between upstream and downstream areas.

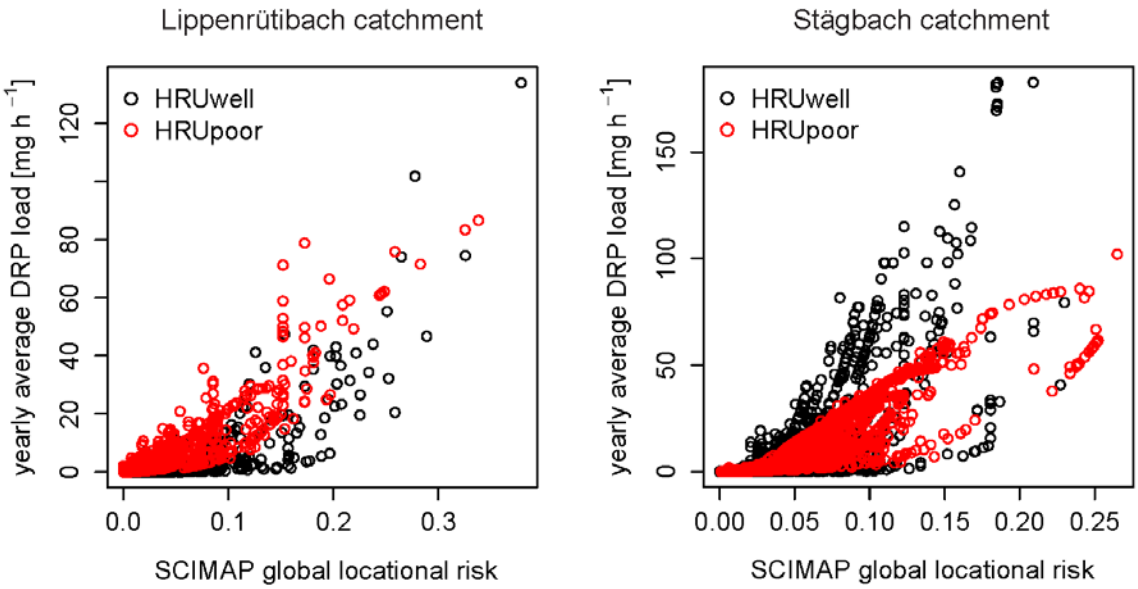

Figure 4-8: Comparison between the average DRP loads for the whole monitoring periods predicted by the RRP model for both hydrological response units (HRU_{well}, HRU_{poor}) and the global SCIMAP locational risk estimations. For the global locational risk we set the delivery risk to 0 at Network Index NI≤6, the 5 % quantile, and to 1 at NI≥20, the maximum NI of both catchments and scaled linearly for NI in between. The source factor (generation risk) was normalized by dividing with the maximum WSP of all catchments. In our catchments the difference to the original locational risk resulted mainly from the changed delivery risk delineation.

A third limitation of the original SCIMAP approach is that the normalization procedure removes differences between different catchments. To enable a comparison between catchments, the generation risk (source factor) and the delivery risk (transport factor) have been scaled differently. The source factor was divided by the maximum value of all catchments of interest, instead of dividing it by the maximum value of the respective catchment. Adjusting the transport factor is less straightforward. The highest NI value of the two catchments studied here was 20, the lowest 4.7. The 5% quantile of all NI values was 6 and based on our RRP model predictions the runoff risk of cells with NI values lower than 6 can be neglected. Thus, we set the transport factor to 0 at NI $\leq$ 5% quantile and to 1 at NI $\geq$ NI-maximum and to vary linearly with NI in between. The locational risk calculated with these globally scaled source and transport factors ranged between 0 and 0.4. Using the RRP results as reference, the 'global locational risk' was in better agreement with the average

DRP loads over the whole monitoring period (Fig. 4-8) than the original locational risk (Fig. 4-7). Since the catchments were similar with regard to their soil P status, the improvement resulted from the modified conversion of NI into the delivery risk.

4.4. Discussion

The performance of the three models indicates that a large amount of useful hydrological information can be extracted for making predictions on P export risks and CSAs from widely available data sources (soil map, geological map, topography). The results further indicate for our study area that runoff generation, and associated P export risks depend more on topography than on soil characteristics, when the information is solely extracted from conventional maps. Although neglecting topographic connectivity and using a rather crude binary soil classification by drainage capacity, the RRP model predicted spatial distributions of runoff risks that were in good (qualitative) agreement with local measurements of soil moisture, groundwater level and surface runoff (Hahn et al., in review). The DoRP predictions showed surprisingly close relationships with measured discharges at the catchment outlets. However, the DoRP model could not sufficiently differentiate between locations, because large areas fell into the same runoff category (STO2), while there was substantial variation in runoff risks within this category due to topography, which was accounted for by the RRP model and SCIMAP. The SCIMAP predictions were very similar to the RRP simulations, indicating that there aren't many areas with reduced topographic connectivity in the study catchments.

While the RRP model was found to be well suited to the identification of high-risk areas in our catchments, taking account of connectivity and differentiating between more soil types may be crucial in other types of catchments. This could be achieved most simply by combining predictions of the three models. The DoRP model can help to better distinguish between sites assigned to the same drainage class by the RRP model, as shown for the example of the measurement locations S1 and S4. Thus, in targeting mitigation measures to areas identified as CSAs using RRP, it may be worth checking for the runoff category assigned to these areas by the DoRP model, before priorities are determined.

SCIMAP, which accounts for topographic connectivity along flow pathways can be used to identify areas whose connectivity with the stream may be overestimated by the other two models due to the inherent assumption of unrestricted connectivity. In case of a DP zone, it is unlikely that the area is connected to a stream or lake by an artificial drainage system, which means that the risk of P export is less than predicted by the latter models. In STO1

and STO2 zones, it may be necessary to check for the presence of a drainage network before correcting the risk prediction.

4.4.1 Connectivity

Many studies highlight the importance of accounting for connectivity when identifying CSAs (Doody et al., 2012; Doppler et al., 2012; Frey et al., 2009; Lane et al., 2009; Srinivasan and McDowell, 2007). However, connectivity has been defined in different ways that are relevant for the interpretation. The Network Index NI used in SCIMAP assumes that the connectivity along a flow line breaks down if the topographic index values λ along a flow line have a local minimum. Given the definition of λ this implies that the connectivity is lost if a section of the flow path is steeper than the upslope part. Lane et al. (2009) illustrated the potential of the NI to generalize information about the hydrological connectivity between locations in areas where topography is the dominant factor. Another approach assumes that connectivity is only lost, if water cannot flow further downstream because it is retained in a sink area. While internal sink areas in catchments are often filled by default by conventional GIS software, detailed analysis have revealed that internal sinks may be essential elements of catchments. This may be caused by natural processes in landscapes like the pothole region in North America or may be caused by anthropogenic influence on topography in the Swiss Plateau (Doppler et al., 2012; Frey et al., 2009).

In summary, the two concepts assume different mechanisms behind the loss of connectivity. The first concept (NI) assumes that re-infiltration due to a increased gradient prevents surface runoff downhill. The second approach assumes the opposite in that ponding occurs because a topographic barrier prevents any flow downhill on the soil surface. Which process is more relevant for any catchment depends on the specific conditions. The steeper the terrain the less probable are formation of sinks. This was the reason why the NI has been used in our study area, which is steeper than other parts of the Swiss Plateau where sinks may be very relevant.

Due to its simplicity, the NI has a high potential to be widely applied especially within the scope of the WFD, as shown for Ireland by (Doody et al., 2012; Wall et al., 2011). This potential is still limited by insufficient knowledge about the relationship between the NI and the probability of a site to connect to the stream network of a catchment over time (Lane et al., 2009; Reaney et al., 2011). Here we related the NI to the runoff risk as predicted with the RRP model. These relationships contain information about the catchment responses during the monitoring period that can be used to refine the scaling of NI/connection-risk relationships used in SCIMAP.

The reasonable match between RRP and SCIMAP predictions of CSAs for larger events in our study catchments suggests that SCIMAP can be used as a screening tool for CSA delineation in catchments where CSAs are primarily determined by topography. This is of particular interest in regions where dynamic models cannot be applied due lack of discharge data. While SCIMAP was originally developed to predict relative risks for individual catchments, a modified version of SCIMAP can be used to compare P export risks among catchments and thus help to identify the most critical catchments within watersheds, given a homogeneous distribution of rainfall. However, the transformation of NI into a connection risk needs further refinement to appropriately describe the hydrological risk. If applicable, RRP simulations can be used for this purpose in addition to field data. The stepwise linear relationship with zero risk up to the 5% NI quantile and a maximum risk level with no further change at the 95% NI quantile, as proposed by (Reaney et al., 2011), was found to be appropriate for storm events, but not for ensembles of different events. Based on our results, we recommend a relationship with a linear increase from the 5% quantile up to the maximum NI value in the latter case.

4.4.2 Limitations of the model approaches

In contrast to the other two models, SCIMAP is not a dynamic model and thus cannot be used to predict how discharge and associated P losses vary between rainfall events of different magnitudes. However, it can be very useful to identify areas with a high potential for P losses in regions where topography governs hydrology. The DoRP model in contrast is advantageous where the drainage properties of soils are the dominant factor. The RRP model is less refined than the DoRP model with respect to differentiation between soils and does not account for topographic connectivity. However, combining the most basic of information on soil hydrology with the topographic information within a process-based framework seems to predict the relevant hydrological and DRP export processes in our study catchments well. The simplifications regarding the representation of the hydrologic processes in the RRP approach are an advantage in practical applications, but by necessity also come with limitations.

4.4.2.1 Hydrological drivers

The generation of fast flow, which includes all kinds of quickly responding runoff in the RRP model, is bound to λ and thus is more likely in wet areas. In reality, however, infiltration excess runoff can also contribute significantly to the total runoff and transport DRP and PP to a stream (Doppler et al., 2012; Srinivasan et al., 2002), depending on rainfall

patterns and soil properties. For certain high resolution soil maps it is possible to identify areas prone to HOF using the DoRP model (Schmocker-Fackel et al., 2007). Unfortunately, most soil maps do not contain sufficient information. In addition, one has to consider that relevant properties like the infiltration capacity of soils may strongly depend on management practices and hence vary in time. Srinivasan et al. (2002) for example reported that the occurrence of Infiltration Excess Runoff (IER) during field experiments was scattered, disjunct and transient, which makes the prediction of areas prone to IER difficult. IER may also be due to water repellent soil surfaces. While "repellency is common for many land-use types with permanent vegetation cover in humid temperate climates" (Doerr et al., 2006), we assume that it did not cause a lot of runoff that reached the stream network.

Another limitation of the approaches discussed here relates to the assumption that surface topography reflects the relevant gradients controlling water fluxes. If the topography of an impermeable layer differs significantly from surface topography runoff may occur on "unexpected" areas. Like the models evaluated by Srinivasan and McDowell (Srinivasan and McDowell, 2007), the models compared in our study do not enable users to "recognize areas where subsurface flows can potentially emerge to the surface as seeps and springs on steep hillsides" (Srinivasan and McDowell, 2007). Zheng et al, (2004) reported that particularly high P concentrations were associated with this type of runoff.

In principle, the RRP and DoRP models do not only account for surface but also for subsurface flow, which can also carry substantial amounts of P to a water body (Kleinman et al., 2011b). In practice, the difficulty is to account for artificial drainage systems, which can contribute substantially to DRP losses (Stamm et al., 1998; Stamm et al., 2002; Watson and Matthews, 2008). Drains can connect areas that appear disconnected on the basis of topographic analysis, and thus the lack of drainage data can be a major problem for CSA determination. To assess the potential role of IER and artificial drainage systems, it may be helpful to complement available ground information through field visits and interviews of local farmers, as suggested by Frey et al. (2011). The models discussed here can be very useful in guiding the collection of such information.

4.4.2.2 Sources and types of P

This study focused on the prediction of P losses in form of DRP, because DRP can immediately be taken up by algae (Dorioz et al., 2006; Sharpley, 1993; Sharpley et al., 1994) and thus represents the main risk factor for eutrophication (Kleinman et al., 2011b). However, it should be recognized that also particulate P (PP) can become bio-available, given specific physical-chemical dynamics (Dorioz et al., 2006). Particulate P losses can be

high, especially on arable land (Doody et al., 2012). There are several models that simulate sediment and PP losses (Krueger et al., 2012). SCIMAP can also be adjusted to predict CSAs for sediment (Reaney et al., 2011) and thus PP export. However, the RRP model was developed for grassland dominated catchments and solely simulates DRP losses. Phosphorus losses from vegetation (Kleinman et al., 2011b) and seasonal changes in P availability (Dorioz et al., 2006; Pote et al., 1999) were assumed to be negligible. Furthermore, freshly applied manure or other fertilizers can be a relevant source for P export (Withers et al., 2003). The RRP model is able to account for this source. However, as the application of manure can be easily controlled by appropriate management, we did not consider it for CSA delineation in this study.

4.5. Conclusion

The study demonstrates that a large amount of hydrological information needed for the prediction of P export risks and CSAs can be extracted from widely available data sources. The comparison of the predictions obtained with the three tools to each other and to the available experimental data indicates that the location and extent of CSAs within the study catchments was more dependent on topography than on variation in soil properties as they are represented in the DoRP model. SCIMAP predicted CSAs particularly well for large storm events. It may be especially useful for screening purposes, in particular in regions without discharge data. RRP simulations can be used to adapt the relationship between NI and connection risks used in SCIMAP to the particular characteristics of a catchment or region. The stepwise linear relationship with zero risk up to the 5% NI quantile and a maximum risk level with no further change at the95 % NI quantile, as proposed by (Reaney et al., 2011), was found to be appropriate for storm events, while we recommend a relationship with a linear increase from the 5% quantile up to the maximum NI value for a multitude of events. Two major problems in predicting P export risks and delineating CSAs in general are the difficulty to account for IER and the limited availability of data on tile drainage systems. To cope with this problem, we suggest that model predictions are complemented by ground information obtained from field visits and interviews of local farmers, as suggested by Frey et al. (2011). The models can be very useful in guiding the collection of such information.

4.6 Acknowledgements

The study war carried out within the framework of the COST Action 869, and was financially supported by the Swiss State Secretariat for Education and Research SER.

4.7 References

AGBA. 1993. Einzugsgebiet des Sempacher Sees. Übersichtskarte Luzern:

Beven, K.J., Kirkby, M.J., 1979. A physically based, variable contributing area model of basin hydrology. Hydrol. Sci. Bull. 24.

Bodenkarte Hochdorf 1983. Landeskarte der Schweiz 1:25000, Blatt 1130 (In German.) Zürich-Reckenholz: Eidg. Forschungsanstalt für landw. Pflanzenbau

Buda, A.R., Koopmans, G.F., Bryant, R.B., Chardon, W.J., 2012. Emerging technologies for removing nonpoint phosphorus from surface water and groundwater: introduction. J. Environ. Qual. 41, 621-627.

Carpenter, S.R., Caraco, N.F., Correll, D.L., Howarth, R.W., Sharpley, A.N., Smith, V.H., 1998. Nonpoint pollution of surface waters with phosphorus and nitrogen. Ecol. Appl. 8, 559-568.

Doerr, S.H., Shakesby, R.A., Dekker, L.W., Ritsema, C.J., 2006. Occurrence, prediction and hydrological effects of water repellency amongst major soil and land-use types in a humid temperate climate. Eur. J. Soil Sci. 57, 741-754.

Doody, D.G., Archbold, M., Foy, R.N., Flynn, R., 2012. Approaches to the implementation of the Water Framework Directive: Targeting mitigation measures at critical source areas of diffuse phosphorus in Irish catchments. J. Environ. Manage. 93, 225-234.

Doppler, T., Camenzuli, L., Hirzel, G., Krauss, M., Lück, A., Stamm, C., 2012. Spatial variability of herbicide mobilisation and transport at catchment scale: insights from a field experiment. Hydrol. Earth. Sys. Sc. 16, 1947-1967.

Dorioz, J.M., Wang, D., Poulenard, J., Trevisan, D., 2006. The effect of grass buffer strips on phosphorus dynamics - A critical review and synthesis as a basis for application in agricultural landscapes in France. Agr. Ecosyst. Environ. 117, 4-21.

Dubrovsky, N.M., Burow, K.R., Clark, G.M., Gronberg, J.M., P.A., H., Hitt, K.J., Mueller, D.K., Munn, M.D., Nolan, B.T., Puckett, L.J., Rupert, M.G., Short, T.M., Spahr, N.E., Sprague, L.A., Wilber, W.G. 2010. The quality of our Nation's waters—Nutrients in the Nation's streams and groundwater, 1994 - 2004, http://water.usgs.gov/nawqa/nutrients/pubs/circ1350.

Frey, M.P., Stamm, C., Schneider, M.K., Reichert, P., 2011. Using discharge data to reduce structural deficits in a hydrological model with a Bayesian inference approach and the implications for the prediction of critical source areas. Water Resour. Res. 47.

Frey, M.P., Schneider, M.K., Dietzel, A., Reichert, P., Stamm, C., 2009. Predicting critical source areas for diffuse herbicide losses to surface waters: Role of connectivity and boundary conditions. J. Hydrol. 365, 23-36.

Gburek, W.J., Sharpley, A.N., 1998. Hydrologic controls on phosphorus loss from upland agricultural watersheds. J. Environ. Qual. 27, 267-277.

Hahn, C., Prasuhn, V., Stamm, C., Schulin, R., 2012. Phosphorus losses in runoff from manured grassland of different soil P status at two rainfall intensities. Agr. Ecosyst. Environ. 153, 65-74.

Hahn, C., Prasuhn, V., Stamm, C., Lazzarotto, P., Schulin, R., in review. Prediction of dissolved reactive phosphorus losses from small agricultural catchments: calibration and validation of a parsimonious model. Hydrol. Earth. Sys. Sc.

Heathwaite, A.L., Reaney, S., Lane, S. 2007. Understanding spatial signals in catchments: linking critical areas, identifying connection and evaluating response Diffuse phosphorus loss: risk assessment, mitigation options and ecological effects in river basins. the 5th International Phosphorus Workshop (IPW5), Silkeborg, Denmark.

Heathwaite, L., Sharpley, A., Bechmann, M., 2003. The conceptual basis for a decision support framework to assess the risk of phosphorus loss at the field scale across Europe. J. Plant Nutr. Soil Sc. 166, 447-458.

Hering, D., Borja, A., Carstensen, J., Carvalho, L., Elliott, M., Feld, C.K., Heiskanen, A.-S., Johnson, R.K., Moe, J., Pont, D., Solheim, A.L., van de Bund, W., 2010. The European Water Framework Directive at the age of 10: A critical review of the achievements with recommendations for the future. Sci. Total Environ. 408, 4007-4019.

Herzog, P. 2005. Sanierung des Baldegger Sees, Auswertung der Zufluss-Untersuchungen 2000 bis 2004. (In German.) Luzern.

Kirkby, M., 1975. Hydrograph modelling strategies. In: Peel, R., et al. (Eds.), Processes in Physical and Human Geography. Heinemann, Lodon, pp. 69-90.

Kleinman, P.J.A., Sharpley, A.N., Saporito, L.S., Buda, A.R., Bryant, R.B., 2009. Application of manure to no-till soils: phosphorus losses by sub-surface and surface pathways. Nutr. Cycl. Agroecosys. 84, 215-227.

Kleinman, P.J.A., Sharpley, A.N., Buda, A.R., McDowell, R.W., Allen, A.L., 2011a. Soil controls of phosphorus in runoff: Management barriers and opportunities. Can. J. Soil Sci. 91, 329-338.

Kleinman, P.J.A., Allen, A.L., Needelman, B.A., Sharpley, A.N., Vadas, P.A., Saporito, L.S., Folmar, G.J., Bryant, R.B., 2007. Dynamics of phosphorus transfers from heavily manured Coastal Plain soils to drainage ditches. J. Soil Water Conserv. 62, 225-235.

Kleinman, P.J.A., Sharpley, A.N., McDowell, R.W., Flaten, D.N., Buda, A.R., Tao, L., Bergstrom, L., Zhu, Q., 2011b. Managing agricultural phosphorus for water quality protection: principles for progress. Plant Soil 349, 169-182.

Krueger, T., Quinton, J.N., Freer, J., Macleod, C.J.A., Bilotta, G.S., Brazier, R.E., Hawkins, J.M.B., Haygarth, P.M., 2012. Comparing empirical models for sediment and

phosphorus transfer from soils to water at field and catchment scale under data uncertainty. Eur. J. Soil Sci. 63, 211-223.

Lane, S.N., Reaney, S.M., Heathwaite, A.L., 2009. Representation of landscape hydrological connectivity using a topographically driven surface flow index. Water Resour. Res. 45.

Lane, S.N., Brookes, C.J., Kirkby, A.J., Holden, J., 2004. A network-indexbased version of TOPMODEL for use with high-resolution digital topographic data. Hydrol. Process. 18, 191-201.

Lane, S.N., Brookes, C.J., Heathwaite, A.L., Reaney, S., 2006. Surveillant science: Challenges for the management of rural environments emerging from the new generation diffuse pollution models. J. Agr. Econ. 57, 239-257.

Lazzarotto, P., 2005. Modeling phosphorus runoff at the catchment scale. Swiss Federal Institute of Technology (ETH), Zurich.

Lazzarotto, P., Stamm, C., Prasuhn, V., Fluhler, H., 2006. A parsimonious soil-type based rainfall-runoff model simultaneously tested in four small agricultural catchments. J. Hydrol. 321, 21-38.

Nash, J.E., Sutcliffe, J.V., 1970. River flow forecasting through conceptual models part I — A discussion of principles. J. Hydrol. 10, 282-290.

Pionke, H.B., Gburek, W.J., Sharpley, A.N., 2000. Critical source area controls on water quality in an agricultural watershed located in the Chesapeake Basin. Ecol. Eng. 14, 325-335.

Pionke, H.B., Gburek, W.J., Sharpley, A.N., Zollweg, J.A., 1997. Hydrological and chemical controls on phosphorus loss from catchments. In: Tunney H., et al. (Eds.), Phosphorus loss from soil to water, CAB International Press, Cambridge, pp. 225-242.

Pote, D.H., Daniel, T.C., Nichols, D.J., Sharpley, A.N., Moore, P.A., Miller, D.M., Edwards, D.R., 1999. Relationship between phosphorus levels in three ultisols and phosphorus concentrations in runoff. J. Environ. Qual. 28, 170-175.

Radcliffe, D.E., Freer, J., Schoumans, O., 2009. Diffuse phosphorus models in the united states and europe: Their usages, scales, and uncertainties. J. Environ. Qual. 38, 1956-1967.

Reaney, S.M., Lane, S.N., Heathwaite, A.L., Dugdale, L.J., 2011. Risk-based modelling of diffuse land use impacts from rural landscapes upon salmonid fry abundance. Ecol. Model. 222, 1016-1029.

Roberts, W.M., Stutter, M.I., Haygarth, P.M., 2012. Phosphorus Retention and Remobilization in Vegetated Buff er Strips: A Review. J. Environ. Qual. 41, 389-399.

Rodriguez, H.G., Popp, J., Maringanti, C., Chaubey, I., 2011. Selection and placement of best management practices used to reduce water quality degradation in Lincoln Lake watershed. Water Resour. Res. 47.

Scherrer, S., Naef, F., 2003. A decision scheme to indicate dominat hydrological flow processes on temperate grassland. Hydrol. Process. 17, 391-401.

Schmocker-Fackel, P., Naef, F., Scherrer, S., 2007. Identifying runoff processes on the plot and catchment scale. Hydrol. Earth. Sys. Sc. 11, 891-906.

Schoumans, O.F., Chardon, W.J., Bechmann, M., Gascuel-Odoux, C., Hofman, G., Kronvang, B., Litaor, M.I., Lo Porto, A., Newell-Price, P., Rubaek, G. 2011. Mitigation options for reducing nutrient emissions from agriculture. A study amongst European member states of Cost action 869. Alterra Wageningen UR, Wageningen.

Schoumans, O.F., Silgram, M., Groenendijk, P., Bouraoui, F., Andersen, H.E., Kronvang, B., Behrendt, H., Arheimer, B., Johnsson, H., Panagopoulos, Y., Mimikou, M., Lo Porto, A., Reisser, H., Le Gall, G., Barr, A., Anthony, S.G., 2009. Description of nine nutrient loss models: capabilities and suitability based on their characteristics. J. Environ. Monitor. 11, 506-514.

Schulte, R.P.O., Doody, D.G., Byrne, P., Cockerill, C., Carton, O.T., 2009. Lough Melvin: Developing cost-effective measures to prevent phosphorus enrichment of a unique aquatic habitat. Tearmann 7, 211-228.

Sharpley, A.N., 1993. Assessing phophorus bioavailability in agricultural soils and runoff. Fert. Res. 36, 259-272.

Sharpley, A.N., Chapra, S.C., Wedepohl, R., Sims, J.T., Daniel, T.C., Reddy, K.R., 1994. Managing agricultural phophorus for protection of surface waters - issues and options. J. Environ. Qual. 23, 437-451.

Srinivasan, M.S., McDowell, R.W., 2007. Hydrological approaches to the delineation of critical-source areas of runoff. New Zeal. J. Agr. Res. 50, 249-265.

Srinivasan, M.S., Gburek, W.J., Hamlett, J.M., 2002. Dynamics of stormflow generation - A hillslope-scale field study in east-central Pennsylvania, USA. Hydrol. Process. 16, 649-665.

Stamm, C., Flühler, H., Gächter, R., Leuenberger, J., Wunderli, H., 1998. Preferential transport of phosphorus in drained grassland soils. J. Environ. Qual. 27, 515-522.

Stamm, C., Sermet, R., Leuenberger, J., Wunderli, H., Wydler, H., Flühler, H., Gehre, M., 2002. Multiple tracing of fast solute transport in a drained grassland soil. Geoderma 109, 245-268.

Stutter, M.I., Chardon, W.J., Kronvang, B., 2012. Riparian Buffer Strips as a Multifunctional Management Tool in Agricultural Landscapes: Introduction. J. Environ. Qual. 41, 297-303.

Vadas, P.A., Kleinman, P.J.A., Sharpley, A.N., Turner, B.L., 2005. Relating soil phosphorus to dissolved phosphorus in runoff: A single extraction coefficient for water quality modeling. J. Environ. Qual. 34, 572-580.

Vadas, P.A., Srinivasan, M.S., Kleinman, P.J.A., Schmidt, J.P., Allen, A.L., 2007. Hydrology and groundwater nutrient concentrations in a ditch-drained agroecosystem. J. Soil Water Conserv. 62, 178-188.

Wall, D., Jordan, P., Melland, A.R., Mellander, P.E., Buckley, C., Reaney, S.M., Shortie, G., 2011. Using the nutrient transfer continuum concept to evaluate the European Union Nitrates Directive National Action Programme. Environ. Sci. Policy 14, 664-674.

Watson, C.J., Matthews, D.I., 2008. A 10-year study of phosphorus balances and the impact of grazed grassland on total P redistribution within the soil profile. Eur. J. Soil Sci. 59, 1171-1176.

Withers, P.J.A., Ulén, B., Stamm, C., Bechmann, M., 2003. Incidental phosphorus losses - can they be predicted? J. Plant Nutr. Soil Sc. 166, 459-468.

Zheng, F.L., Huang, C.H., Norton, L.D., 2004. Surface water quality - Effects of near-surface hydraulic gradients on nitrate and phosphorus losses in surface runoff. J. Environ. Qual. 33, 2174-2182.

4.8 Supplementary Information

Lippenrütibach catchment

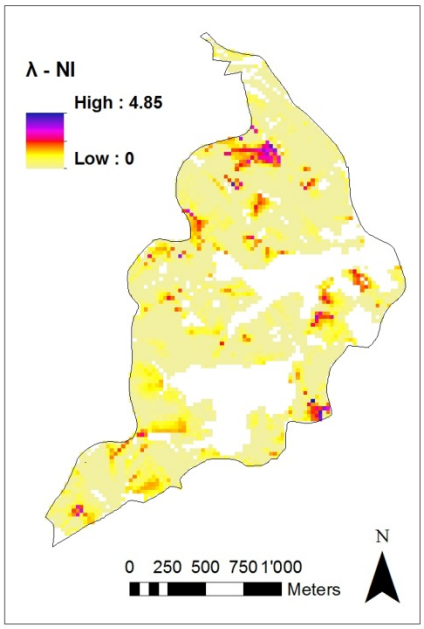

Stägbach catchment

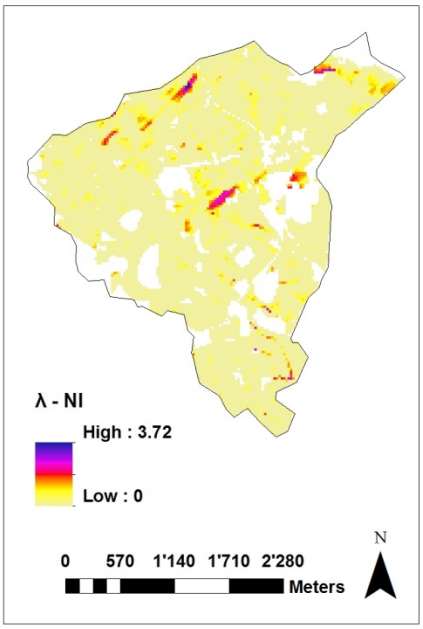

Figure 4-SI_1: Spatial distribution of the difference between Network Index (NI) and Topographic Index (λ) in the Lippenrütibach and the Stägbach catchment, indicating where connectivity might be a limiting factor for P loss into streams within the catchment.

5
Conclusion

The aim of this study was to assess and improve the predictive capabilities of the parsimonious Rainfall-Runoff-Phosphorus (RRP) model, in order to enable reliable predictions of critical source areas (CSA) for diffuse Phosphorus (P) losses from agricultural land on the basis of widely available data.

The artificial rainfall experiments carried out in 2008 on grassland plots located on the Swiss Plateau enabled us to enlarge the database of the RRP model and to assess its underlying concepts. We showed that dissolved reactive P (DRP) concentrations in runoff depended linearly on the water soluble P (WSP) concentrations in soil. Band application of manure led to elevated DRP losses but the influence of the soil P status was still obvious. This demonstrates that soil P is an important source for DRP losses. DRP concentrations in runoff decreased with increasing time between manure application and runoff generation. Runoff generation did not seem to be affected by manure application in our field experiments. These findings suggest that the mechanisms considered in the P sub-model are sufficient to estimate DRP losses and that it is a valid approach to treat soil and manure P as additive sources. We implemented the WSP-DRP relationship derived from the sprinkling experiments in the RRP model and thus substituted the estimated correlation previously built-in.

The good performance of the RRP model in the Stägbach catchment, which was not used for calibration, demonstrated the transferability of the model. The separate calibration of urban parameters enhanced model performance for the Stägbach catchment and the Lippenrütibach catchment. Data of the latter but from another period had been used for calibration. The model delivered reliable predictions of discharge and DRP loads at the catchment outlets. Spatial validation data collected in 2010 in the Stägbach catchment were in good agreement with spatial simulations, providing further support for the underlying concept of the RRP model. To address the main difficulty of parsimonious models, i.e. the high degree of simplification of field reality, we investigated how sensitive model predictions were to the rather arbitrary classification of soils into well-drained and poorly-drained soils. Model predictions proved to be sufficiently robust. This was probably due to

the simultaneous calibration of model parameters to four catchments. The results show that conventional soil maps can be used to assign drainage classes. The results support the CSA concept. In our case, more than 50% of the total DRP load originated from 10% of the agricultural area. According to the RRP model, soil P from past inputs - also called 'legacy P' - was the dominant source for DRP losses. The RRP model appears to be a suitable tool for CSA identification and thus could be used to direct mitigation options to the most critical areas.

Comparing spatial RRP model predictions with validation data and predictions of two other models, which either used more detailed soil data to identify Dominant Runoff Processes (DoRP model) or accounted for connectivity (Sensitive Catchment Integrated Modeling Analysis Platform SCIMAP) when deriving CSAs, demonstrated that mainly topography controlled the distribution of hydrological risk areas in our study catchments. It also showed that detailed soil and geological data can partly explain site differences that were not detected with the RRP model. Accounting for connectivity did not change CSAs predictions in our study areas substantially. Combining all three approaches would enable the use of all information present in available data and probably lead to even more reliable CSA delineation. This is especially important for catchments with highly diverse soils and a large fraction of unconnected areas. In our study catchments, where soils are generally of low permeability and often connected to stream via surface pathways or tile drains, the RRP model delivered good results.

Limitations & Outlook

Comparing spatial validation data with model predictions was crucial for the assessment of spatial model performance. The Overland-Flow-Detectors (OFDs) used in the field were very valuable measurement devices, although they do not say whether the runoff from a specific site indeed contributes to stream flow. Tracers are necessary to demonstrate that. Runoff-P measurements are so far restricted to stream and drainage flow measurements, and they cannot distinguish between the various P sources. Methods that enable such a differentiation are needed to further validate DRP predictions.

The RRP model was transferable from the calibration catchments to the test catchment. The latter catchment showed similar characteristics as the calibration catchments. However, based on the model structure the predictive capabilities are expected to be limited in regions with highly permeable soils, for dry conditions and for areas where Infiltration Excess Runoff (IER) dominates.

The RRP model does not explicitly distinguish between different kinds of fast flow runoff processes, but lumps all of them together and makes their occurrence dependent on the topographic index. As runoff generation is bound to wet areas, the model does not account for IER generation on dry soils. The spatial extent of hydrological risk areas might therefore be underestimated by the RRP model. Furthermore, the field experiments indicated that different WSP-DRP relationships may be needed for medium events and extreme rain bursts. Thus, in case of frequently occurring extreme rainfall events it would seem necessary to explicitly account for IER and the differences in the WSP-DRP relationship. However, even with input data like infiltration capacity, IER generating areas can be difficult to predict.

Regarding the applicability of the RRP model, we should point out that the need for soil P data limits the applicability of the P sub-model. In contrast, the hydrological sub-model requires only easily available input data and can therefore be widely applied to delineate hydrological risk areas. These predictions can easily be supplemented with results from the DoRP approach and SCIMAP. The good match between SCIMAP and RRP results might be especially interesting for local authorities who develop mitigation strategies and need easy screening tools.

The major problems in predicting P losses and CSAs in general are the challenge to account for IER, as well as the limited availability of data on artificial drainage networks and on soil-P. We therefore, like Frey et al. (2011), recommend to accompany model predictions with data obtained from field visits and to exchange knowledge with local farmers. The RRP model can be a very useful tool to design a collection scheme for the required information.

Overall, our field experiments and the RRP model results highlight the inherent risk that large soil P stocks bear for P losses. Closing the P cycle won't be enough to reduce P losses from agricultural land in the short run, due to the persistent risk of soil P stocks. Targeted mitigation measures are needed to reduce P losses from P enriched soils. Having proven to be a suitable tool for CSA identification in grassland dominated catchments on the Swiss Plateau the RRP model can guide the implementation of mitigation measures at critical sites. Such measures are no substitute, however, for balancing P inputs in agriculture against P outputs with cropping. Such balancing is a necessary prerequisite to avoid further aggravation of environmental pollution and wasting of the limited resource phosphorus.

5.1 References

Frey, M.P., Stamm, C., Schneider, M.K., Reichert, P., 2011. Using discharge data to reduce structural deficits in a hydrological model with a Bayesian inference approach and the implications for the prediction of critical source areas. Water Resour. Res. 47.

Acknowledgements

I want to thank everyone who contributed to this work in one way or another. Without the help of so many people especially during the field studies, this work would not have been possible.

First of all I want to thank Rainer Schulin, Volker Prasuhn and Christian Stamm for giving me the opportunity to work on this project, for their support and advice, for the guidance and the freedom they gave me, and for the fast feedback especially at the end of the project. I really appreciated that three research institutions were involved in the project and that the collaboration worked so well.

Many thanks go to Jean-Marcel Dorioz who agreed on a rather short-notice to read my thesis and to be my co-examiner. I am very grateful for that.

I want to thank

Isabelle Falconi-Bürgi and Franz Stadelmann from Canton Lucerne, Department agriculture and forest, for initiating the contact with the local farmers and their support during the project

Robert Lovas from Canton Lucerne, Department environment and energy, who kindly answered all the questions I had regarding the data that were available for the Stägbach catchment, and the placement of the ISCO sampler

the farmers, who allowed us to install measurements devices on their fields and kindly gave us access to their data, for their friendly cooperation. I am glad to have met so many friendly people

Trevor Page from the Centre for Sustainable Water Management (CSWM) in Lancaster for making my Short Term Scientific Mission at Lancaster University possible and for the interesting discussions about model structure and uncertainty analysis. I thank him, Phil Haygarth, Alona Armstrong (thanks for the bike!) and the whole CSWM group for making my stay at Lancaster very enjoyable

Dave Milledge from Durham University for the discussions, the fruitful cooperation and the visit to Durham University (many thanks to your girlfriend)

Patrick Lazzarotto for providing me a good start with the model and for being available for questions after such a long time

There are many people I would like to thank for their help during my field studies:

Erika Fässler, Monica Marchetti, Kerstin Hockmann & Thomas, Rainer Rees, Nazanin Roohani, Stephanie Roulier, Alexander Gogos, Chantal Le Marié, Anja Gramlich, Björn Studer, Bernd Felderer, Irene Wittmer, Tobias Doppler, Christian Stamm, Frank Liebisch, Else Bühnemann, Denise Frehner, Oliver Heckl, Federica Tamburini, Christine Bosshard, Christiane Vögeli-Albisser, Volker Prasuhn, Ernst Spiess for spending a day or more with me in the field, despite having enough own work to do and getting rewarded only with the view, if it was not raining. Thanks a lot!

René Saladin, Alain Valsangiacomo and the field group of ART for their help implementing the measurement devices in the field and for uninstalling them as well

Ivo Strahm and Luca Winiger for their help during the artificial rainfall experiments.

Claudia Amoroso for contacting the farmers and collecting soil-P data

René Flisch and Corinne Hörger for collecting water samples at times I couldn't do it

People from the eawag lab, for analyzing my water samples

Urs Zihlmann for the discussions and his help regarding the classification of soils

Hans Wunderli for his invaluable technical support during the field studies

Jörg Leuenberger for introducing me to the sprinkler device

Marlies Sommer for doing part of the soil analysis

Many thanks go to

Frank Liebisch for the good team work during our experiments in 2008, for introducing me to the lab in Eschikon, and most of all for the good company during those field days and for the great start in the PhD. Sharing the field work with you made it much more enjoyable.

Michael Evangelou for taking care of my soil samples in 2010, for your support, the discussions "über Gott und die Welt" and the cheering up.

and Tobias Doppler for the discussions, your help in the field, and most of all for the good company and for your visits in Lucerne.

I would like to thank the Group of Water Protection and Nutrient and Pollutant Flows as well as the Soil Protection Group and the field group at Agroscope Reckenholz-Tänikon for their help, the coffee breaks and the good time at ART. I am thankful to Walter Richner for

his support, to Peter Weisskopf for the discussions, and Chris Bosshard for the good time in the office, cake making and your visit in 2010.

I want to thank all the people from the soil protection group and the STEP group at ETH for the good time during my PhD, the lunch breaks, and the good company. I really enjoyed being part of the Soil Protection group and to share the office with Erika Fässler, Kajsa Knecht, Martin Tschan, Thomas Kuster, Nazanin Roohani, Susan Tandy, Gilbert Gradinger, and Michael Evangelou.

Finally, I would like to thank all the people who visited, helped and supported me in 2010. I am very thankful for that!

I am most thankful to Oliver Heckl for all the discussions and his encouragement, and to my family, Olli & his family for being there, helping me and supporting me whenever they can.

The project was carried out within the framework of the COST ACTION 869, and was financially supported by the Swiss State Secretariat for Education and Research SER.

Curriculum Vitae

Name:	Claudia Hahn
Date of Birth:	March 31st, 1982 (Dresden, Germany)
Nationality:	German

10.2007 – present	PhD student in the group of Water Protection at the Research Station Agroscope Reckenholz-Tänikon (ART), Zurich and in the Soil Protection Group, Institute of Terrestrial Ecosystems, ETH Zurich / Switzerland
10.2001 – 09.2007	Study of Geoecology at the Technical University of Mining and Technology, Freiberg / Germany
02.2004 – 02.2005	Study Abroad Program at the Australian National University (ANU), Canberra / Australia
09.2000 – 09.2001	Voluntary, ecological year in Diedorf / Germany
09.1992 – 06.2000	High School Johann Andreas Schubert Gymnasium, Dresden / Germany; Abitur (equals A-levels)